# Cornichon Proteins: Unexpected Roles in Plant Pathogen Infection, ER Morphology Maintenance and Pollen Development

Jianhui Li

Dissertation submitted to the faculty of the Virginia Polytechnic Institute and State University in partial fulfillment of the requirements for the degree of

Doctor of Philosophy
In
Plant Pathology, Physiology, and Weed Science

Xiaofeng Wang, Chair
John M. McDowell
Xiang-Jin Meng
Boris A. Vinatzer

April 24, 2017
Blacksburg, VA

Keywords: positive-strand RNA virus, cornichon proteins, protein trafficking, early secretory pathway, ER morphology, pollen development, bacterial infection

# Cornichon Proteins: Unexpected Roles in Plant Pathogen Infection, ER Morphology Maintenance and Pollen Development

Jianhui Li

## ABSTRACT

Cornichon (CNI) proteins are a conserved family of proteins among eukaryotes, from Erv14 in the yeast *Saccharomyces cerevisiae* to CNI homologs (CNIHs) in mammals and plants. Erv14 functions as a cargo receptor of coat protein complex II (COPII) for protein trafficking from the endoplasmic reticulum (ER) to the Golgi apparatus, en route to their final destinations. By interacting with specific cargo proteins, CNI proteins regulate key steps of embryo polarity in *Drosophila*, budding in yeast, and synaptic transmission in the mammalian brain. However, we have very limited understanding of plant CNIHs. Positive-strand RNA viruses assemble their viral replication complexes (VRCs) at specific host organelle membranes. With a better understanding of host factors involved in targeting viral replication proteins to the preferred organelles, we expect to block trafficking of viral replication proteins and thus, viral infection, by manipulating the required host proteins. *Brome mosaic virus* (BMV) is a model of positive-strand RNA viruses and its replication can be recapitulated in yeast. Importantly, BMV replication protein 1a is the only required viral protein to form VRCs at the perinuclear ER membrane in yeast. I demonstrate that Erv14 and COPII coat proteins are required for targeting BMV 1a to the perinuclear ER in yeast, suggesting a novel function of COPII vesicles in protein trafficking to the perinuclear ER membrane and in the BMV VRC formation. As for cellular functions, I show that plant CNIHs complement the defective distribution of BMV 1a in yeast mutant lacking Erv14. Taking advantage of *Arabidopsis thaliana* knockout mutants and knockdown of gene expression in *Nicotiana benthamina*, I also discover that CNIHs unexpectedly play crucial roles in pollen development, infection of a bacterial pathogen, and maintenance of ER tubules. I further confirm that CNI proteins are also required for maintaining ER tubules in yeast, suggesting a novel and conserved role in shaping ER morphology. Therefore, these findings indicate the functional diversity and redundancy of CNI proteins in key cellular processes and suggest a novel strategy to control plant pathogenic viruses and bacteria by manipulating plant CNIHs.

# Cornichon Proteins: Unexpected Roles in Plant Pathogen Infection, ER Morphology Maintenance and Pollen Development

Jianhui Li

## GENERAL AUDIENCE ABSTRACT

Many cellular proteins play important roles in plant development but unfortunately are hijacked by plant viral, bacterial, and/or fungal pathogens for their infections. Cornichon (CNI) proteins are a conserved family of proteins and a great example that is involved in both plant development and plant pathogen infection. CNI protein was first described in a *Drosophila* mutant. Only 3% of mutant cells survived, but showed abnormal phenotype in abdominal segmentation with a similar shape of "pickle" during embryo development. Later on, this family of proteins was well studied in yeast and mammals but rarely studied in plants. Erv14, one of CNI proteins in yeast, is a cargo receptor of coat protein complex II (COPII) vesicles that participate in cellular early secretory pathway. COPII vesicles serve as cellular carriers to recruit cargo proteins from the endoplasmic reticulum (ER) membrane and depart for the Golgi apparatus, en route to their final destinations for proper cellular processes. In this dissertation, I have discovered that Erv14 and COPII components are unexpectedly involved in targeting a replication protein of a plant RNA virus to the perinuclear ER membrane, instead of the Golgi apparatus, suggesting a novel function of COPII in targeting proteins to the perinuclear ER. Erv14 has never been shown as involved in viral infection and thus, my work has identified a new host protein required for viral infection. I have further explored the cellular functions of CNI proteins in plants, and found that plant CNI proteins play significant roles in maintaining cellular ER network, supporting normal pollen development, and bacterial pathogen infection. Therefore, plant CNI proteins function similarly as Erv14 to recruit various cargo proteins into COPII vesicles en route to their final destinations for proper cellular processes. These cellullar processes may include, but are not limited to: ER morphology maintenance, pollen development, and plant immune response to pathogen infection. Furthermore, it is possible to develop a novel strategy to make plants resistant to plant viruses and/or bacteria by manipulating plant CNIHs.

# Acknowledgements

First and foremost, I'm deeply grateful to my advisor Dr. Xiaofeng Wang for his constant guidance, insightful comments and suggestions, enormous help, and tremendous support during my PhD study and research. I thank him for providing me an excellent research environment and freedom to pursue my research of interest, and also for his strong recommendation during my postdoc application to continue academic trainings for my career development. It is a great honor for me to be his first PhD student. Without his guidance and persistent help this dissertation would not have been possible.

I would like to offer my special thanks to my committee members Drs John McDowell, Xiang-Jin Meng, and Boris Vinatzer for their constructive comments and suggestions during the committee meetings, critical review of my dissertation, and strong recommendations during my postdoc application to further my academic trainings.

I want to thank Ms. Haijie Liu for her technical assistance on bacterial growth analysis in Arabidopsis plants; Dr. Jiantao Zhang, Ms. Guijuan He and Mr. Zhenlu Zhang for their general assistance in my research; and undergraduate students Mr. Robert Postlethwaite, Mr. Sebastian Wellford, Mr. Richard Samuel Herron and Ms. Elizabeth Barton for their help in my research projects.

I am grateful to our lab collaborator Dr. Maya Schuldiner (Weizmann Institute of Science) for her critical suggestions during my research and providing yeast strains and plasmids; Dr. Randy Schekman (UC Berkeley), Dr. Charles Boone (University of Torronto) and Dr. Elizabeth Miller (MRC Laboratory of Molecular Biology) for providing yeast plasmids and mutants; Dr. Guillaume Pilot and Dr. Aiming Wang (Agriculture and Agri-Food Canada) for providing plant plasmids; Dr. Boris Vinatzer for providing a plant bacterial strain; Dr. Chengsong Zhao for his technical help on Arabidopsis plant crosses; Dr. Phoebe Williams and Dr. Shi Yu for their technical suggestions on agroinfiltration; and Arabidopsis Biological Resource Center (ABRC) for providing the T-DNA insertion mutant seeds of Arabidopsis.

At last, I would like to express my gratitude to my parents and my parents-in-law for their supports and understanding. My deepest appreciation goes to my wife Tingting Sun and my son Erick Li for their love, patience, supports, and encouragements during my study.

# Attribution

Several colleagues aided in the revising and research in the published manuscipt of Chapter 2 presented as part of this dissertation. Their contributions are described in the following.

**Xiaofeng Wang**, Deparment of Plant Pathology, Physiology, and Weed Science, Virginia Tech. Dr. Wang served as the advisor and committee chair of my research project. He assisted in revising and editing all the chapters in this dissertation. He coordinated the study, conceived and designed the experiments, wrote and revised the manuscript in Chapter 2.

**Maya Schuldiner**, Department of Molecular Genetics, Weizmann Institute of Sciences, Rehovot, Israel. Dr. Schuldiner designed the experiments and revised the manuscript.

**Shai Fuchs**, Department of Molecular Genetics, Weizmann Institute of Sciences. His present address is Department of Pediatric Endocrinology and Metabolism, The Hospital for Sick Children, Toronto, Ontario, Canada. Dr. Fuchs screened the yeast GFP library.

**Jiantao Zhang**, Deparment of Plant Pathology, Physiology, and Weed Science, Virginia Tech. His present address is Department of Pharmacology and Toxicology, The University of Arizona, Tucson, AZ. Dr. Zhang assisted in preparing yeast cells for electron microscopy.

**Sebastian Wellford**, Deparment of Plant Pathology, Physiology, and Weed Science, Virginia Tech. He was an undergraduate student in Dr. Wang's lab. He assisted in screening cellular ER proteins in yeast *sec24* ts mutant.

# Table of Contents

# List of Figures

# List of Tables

## List of Abbreviations

| | |
|---|---|
| (+)RNA: | positive-strand RNA |
| ACBP: | acyl-CoA binding protein |
| AGPs: | arabinogalactan proteins |
| AMPA: | α-amino-3-hydroxy-5-methyl-4-isoxazole propionic acid |
| Arf1: | ADP ribosylation factor 1 |
| ATL: | atlastin |
| BAK1: | brassinosteroid insensitive 1-associated receptor kinase 1 |
| BFA: | Brefeldin A |
| BiFC: | bimolecular fluorescence complementation |
| BIR1: | BAK1-interacting receptor-like kinase 1 |
| BMV: | *brome mosaic virus* |
| CFU: | colony-forming unit |
| CMV: | *cucumber mosaic virus* |
| CNI: | Cornichon |
| CNIHs: | Cornichon homologs |
| COPI: | coat protein complex I |
| COPII: | coat protein complex II |
| CP: | coat protein |
| CVB3: | Coxsackievirus B3 |
| DCV: | *Drosophila* C virus |
| DENV: | Dengue virus |
| dsRNA: | double-strand RNA |
| EM: | electron microscope |
| ER: | endoplasmic reticulum |
| ERES: | ER exit sites |
| EV11: | echovirus 11 |
| EV71: | enterovirus 71 |
| FASN: | fatty acid synthase |
| FHV: | Flock house virus |
| FMDV: | foot-and-mouth disease virus |
| FRAP: | fluorescence recovery after photobleaching |
| GCA: | Golgicide A |
| GEF: | guanine nucleotide exchange factor |

| | |
|---|---|
| GFP: | green fluorescent protein |
| GLRs: | glutamate receptor-like proteins |
| GO: | Gene Ontology |
| HCV: | hepatitis C virus |
| *Hpa*: | *Hyaloperonospora arabidopsidis* |
| HRFs: | host resistance factors |
| Hrp: | hypersensitive response and pathogenicity |
| HSFs: | host susceptibility factors |
| Hsp70: | heat shock protein 70 |
| hVAP-33: | human homologue of 33-kD vesicle-associated membrane protein-associated protein |
| iGluRs: | ionotropic glutamate receptors |
| Lnp: | Lunapark |
| $m^7G$: | 7-methylguanylate cap |
| mbSUS: | mating-based split ubiquitin system |
| mC: | mCherry |
| MVB: | multivesicular body |
| NMDA receptor: | N-methyl-D-aspartate receptor |
| NS: | nonstructural protein |
| OsSCAMP1: | rice secretory carrier membrane protein 1 |
| PC: | phosphatidylcholine |
| PE: | phosphatidylethanolamine |
| pgi | post galactose induction |
| *Pi*: | *Phytophthora infestans* |
| PI4P: | phosphatidylinositol-4 phosphate |
| PI4PIIIβ: | phosphatidylinositol-4 phosphate III kinase β |
| PLA: | proximity ligation assay |
| *Pst* DC3000: | *Pseudomonas syringae* pv. *tomato* DC3000 |
| RCNMV: | *Red clover necrotic mosaic virus* |
| RE: | recruitment element |
| RNAi: | RNA interference |
| RTNLB: | reticulon-like protein subfamily |
| RTNs: | reticulons |
| Sar1: | secretion-associated RAS super family 1 |

| | |
|---|---|
| Sey1: | synthetic enhancement of Yop1 |
| SFAs: | saturated fatty acids |
| SNARE: | soluble N-ethylmaleimide-sensitive factor attachment protein receptor |
| STP13: | sugar transporter 13 |
| SUS: | split ubiquitin system |
| SWEETs: | sugars will eventually be exported transporters |
| TBSV: | *tomato bushy stunt virus* |
| TEV: | *tobacco etch virus* |
| TMD: | transmembrane domain |
| TMV: | *tobacco mosaic virus* |
| TOM1: | tobamovirus multiplication 1 |
| ToMV: | *tomato mosaic virus* |
| TRV: | tobacco rattle virus |
| *ts*: | temperature sensitive |
| TuMV: | *turnip mosaic virus* |
| UFAs: | unsaturated fatty acids |
| UTR: | untranslated region |
| VIGS: | virus-induced gene silencing |
| VRC: | viral replication complex |
| WNV: | West Nile virus |
| wt: | wild type |

# Chapter 1 Introduction

Viruses are obligate intracellular infectious agents that are composed of proteins and nucleic acids in the form of nucleocapsids, and depend entirely on host cells to replicate their genomes and produce infectious progeny (Raoult and Forterre, 2008). There are seven classes of viruses based on the Baltimore classification system (Baltimore, 1971). Among seven viral classes, positive-strand RNA [(+)RNA] viruses are the largest one, occupying more than 30% of all virus genera. This class of viruses also include many important and emerging human, animal, and plant pathogens, such as Zika virus, hepatitis C virus (HCV), severe acute respiratory syndrome (SARS) coronavirus, foot-and-mouth disease virus (FMDV), *cucumber mosaic virus* (CMV), and *tobacco mosaic virus* (TMV). In particular, more than 60% of plant viruses are (+)RNA viruses. Moreover, 6 out of the top 10 plant viruses, based on their scientific and economic significance, are (+)RNA viruses (Scholthof et al., 2011). The genomic RNAs of (+)RNA viruses serve as messenger RNAs for viral protein translation and viral genomic replication.

All well-studied (+)RNA viruses assemble viral replication complex (VRC) in association with host organelle membranes. Since (+)RNA viruses usually encode only several proteins, they hijack cellular machinery to complete their infection cycles. Therefore, it is possible, in principle, to block or disrupt viral infection by manipulating host factors that are involved in the targeting and/or assembly of VRCs to the specific intracellular membranes. Furthermore, it is possible to extend the knowledge learned from one virus to other viruses within the same class because all (+)RNA viruses share similar strategies in viral replication.

## 1.1 *Brome mosaic virus*

*Brome mosaic virus* (BMV) belongs to the *Bromoviridae* family, and is a representative member of the alphavirus-like superfamily that includes many human, animal, and plant (+)RNA viruses. BMV has been extensively studied as a model of (+)RNA viruses for understanding viral replication mechanisms, virus-host interactions, and gene expression of (+)RNA viruses. BMV commonly infects *Bromus* grasses and cereal crops such as wheat and barley, and was first isolated from bromegrass (Lane, 1974). BMV has a tripartite linear RNA genome composed of RNA1, RNA2, and RNA3, with a 7-methylguanylate cap ($m^7G$) at the 5' end and a tRNA-like structure at the 3' end (Figure 1.1). The 3' untranslated region (UTR) of BMV RNAs are the central regulatory elements of the genome, which is involved in multiple processes during BMV infection such as translation, RNA recombination, and RNA encapsidation for virion assembly (Ahlquist et al., 1984; Ahlquist et al., 1981; Rao and Kao, 2015). Genomic RNA1 (3.2 kb) encodes BMV replication protein 1a (109kD). BMV 1a is involved in multiple viral replication processes (den Boon et al., 2001; Liu et al., 2009). Specifically, BMV 1a has a N-terminus methyltransferase domain for viral RNA capping (Ahola and Ahlquist, 1999; Kong et al., 1999) and a C-terminus NTPase/helicase-like domain for recruiting and translocating viral genomic RNAs into VRCs (Wang et al., 2005). Genomic RNA2 (2.9 kb) encodes $2a^{pol}$ (94 kD), which has a central RNA dependent RNA polymerase domain and a N-terminal domain that interacts with the NTPase/helicase-like domain of BMV 1a (Chen and Ahlquist, 2000; Kao and Ahlquist, 1992; O'Reilly et al., 1997). BMV 1a and $2a^{pol}$ are necessary and sufficient for BMV replication. Genomic RNA3 (2.1 kb) is dicistronic and encodes movement protein 3a (32 kD) and coat protein (CP, 20

kD). However, CP is translated from subgenomic RNA4 (sgRNA4, 0.9 kb), which is synthesized by using the negative-strand RNA3 as template via internal initiation during replication (Miller et al., 1985). BMV 3a and CP are responsible for systemic movement but not required for replication.

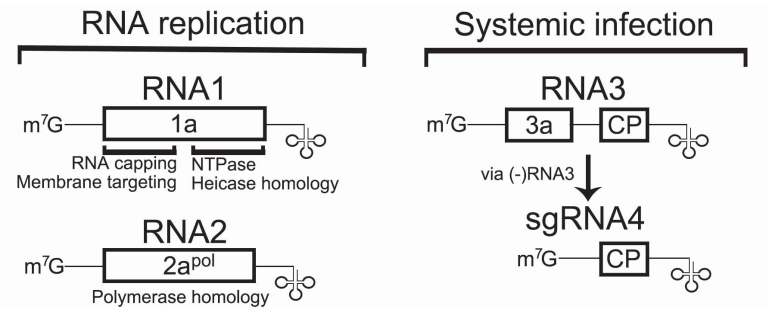


**Figure 1.1. BMV genome.**

BMV has three genomic RNAs: RNA1, RNA2, RNA3, and a subgenomic mRNA, RNA4 (sgRNA4). RNA4 is synthesized via negative-strand RNA3 during BMV replication. All BMV RNAs bear a 5' $m^7G$ and 3' tRNA-like structure (cloverleaf).

### 1.1.1 BMV-yeast system

BMV can replicate in a surrogate host, the yeast *Saccharomyces cerevisiae*. The engineered BMV-yeast system was established more than 20 years ago. Initially, the system was developed to express BMV 1a and $2a^{pol}$ from two individual high-copy-number plasmids under the control of a constitutive promoter, yeast alcohol dehydrogenase 1 (*ADH1*) promoter. Significantly, only coding sequences of BMV 1a and $2a^{pol}$ were used but not the 5' and 3' UTRs, which are essential for replication of RNA1 and RNA2, and thus, there is not replication of RNA1 and RNA2. Because CP is not required for replication and is only expressed after BMV replication, the coding sequence of CP was replaced with reporter genes to allow sensitive detection of viral replication. The reporter genes include

chloramphenicol acetyltransferase (CAT) which confers chloramphenicol resistance or orotidine 5'-phosphate decarboxylase (URA3) that supports uracil auxotrophic cell growth. When transcripts of RNA3 derivatives were transformed into yeast cells along with plasmids expressing BMV 1a and $2a^{pol}$, strong expression of CAT or URA3 were detected, indicating yeast cells have the capacity to support BMV replication (Janda and Ahlquist, 1993). To improve the assays detecting BMV RNA replication in yeast, a plasmid was developed to launch RNA3 or RNA3 derivatives. A self-cleaving ribozyme from hepatitis delta virus was inserted at or near 3' BMV UTR. Upon transcription, ribozyme cleaved itself and poly A tail off and thus, an authentic 3' end of RNA3 was produced (Ishikawa et al., 1997). This system was further improved to a two-plasmid system, in which one plasmid expresses 1a and $2a^{pol}$ from the bidirectional and galactose-inducible *GAL1-GAL10* promoter, and the other plasmid is for BMV RNA3 transcription under the control of a copper inducible promoter (*CUP1*) (Figure 1.2). With this tool, the BMV-yeast system is amenable to high-throughput transformation for genome-wide screening in yeast to study host factors that involved in BMV replication (Kushner et al., 2003). More importantly, BMV-directed genomic RNA replication, RNA4 transcription and selective RNA encapsidation of the engineered BMV-yeast system duplicate nearly all features of BMV replication in the plant cells (Ishikawa et al., 1997; Janda and Ahlquist, 1993; Restrepo-Hartwig and Ahlquist, 1999; Restrepo-Hartwig and Ahlquist, 1996; Schwartz et al., 2002).

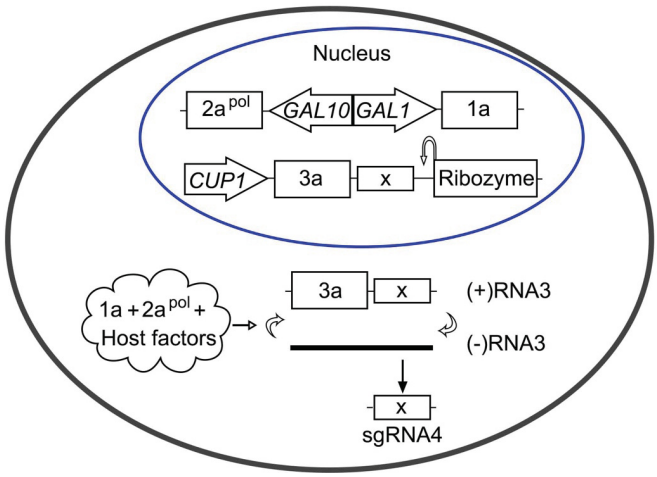


**Figure 1.2. The BMV-yeast system.**

The two plasmid-based BMV-yeast system was used to launch BMV replication in yeast. BMV 1a and $2a^{pol}$ are driven by *GAL1* and *GAL10* promoter respectively, while RNA3 or RNA3 derivatives with CP replaced with reporter genes, is driven by a copper inducible *CUP1* promoter. However, no copper was supplemented in the medium to maintain the minimum transcription of RNA3 or RNA3 derivatives. The 3' UTR of RNA3 or RNA3 derivatives is self-cleaved by a ribozyme. A 4-bp fragment is inserted in the CP coding sequence to abolish CP synthesis, and thus, no viral particles will be produced in this system. BMV 1a and $2a^{pol}$ together with host factors to produce (-)RNA3 and sgRNA4, and amplify (+)RNA3 by using (-)RNA3 as a template.

### 1.1.2 BMV-*Nicotiana benthamiana* system

The BMV-yeast system is an excellent model system for studying virus-host interactions at both molecular and genome-wide levels. However, some key features need to be confirmed in plants. BMV does not replicate and infect efficiently in the model plant *Arabidopsis thaliana* (Fujisaki et al., 2003) or most other dicots. However, *Nicotiana benthamiana* can support BMV replication and is thus a valuable tool. An *Agrobacterium tumefaciens*-based transient expression system to launch BMV infection has been developed. Specifically, full length cDNA copies of each individual BMV genomic RNA were cloned into a Ti plasmid between the CaMV 35S promoter and the ribozyme of hepatitis delta virus (Figure 1.3).

BMV RNA transcripts are produced when Ti plasmid-harboring agrobacteria are infiltrated into leaf tissues of *N. benthamiana* by agroinfiltration. BMV replication can be detected at about 2 days post viral inoculation in the infiltrated leaves (Annamalai and Rao, 2005; Diaz et al., 2015; Gopinath et al., 2005).

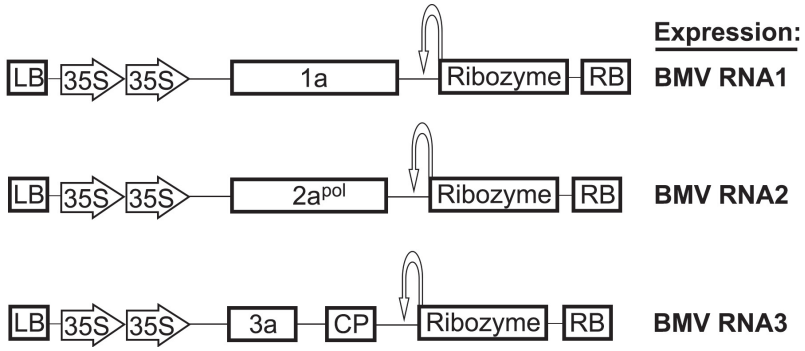


**Figure 1.3. BMV-*N. benthamiana* system.**

Three individual Ti plasmids that are used to express BMV genomic RNAs are shown. Full length cDNAs of BMV genomic RNAs are cloned into the Ti plasmid between the 35S promoter and ribozyme. Ti plasmid is transformed into leaf epidermal cell by agroinfiltration. Three authentic BMV genomic RNAs are present in a plant cell to support viral replication and viral particle production.

In addition to supporting BMV replication, an added advantage of using *N. benthamiana* is that virus-induced gene silencing (VIGS) technique has been well established for reverse genetics in *N. benthamiana* (Senthil-Kumar and Mysore, 2014). VIGS has been well used to trigger the degradation of host corresponding mRNAs in addition to viral genome, and causes specific gene knockdown effects in the *N. benthamiana* plant (Velásquez et al., 2009). VIGS has also been used to identify and/or confirm host genes that are required for viral infection of a specific virus (Caplan et al., 2009; Wang et al., 2009; Xu et al., 2014). If a yeast gene is identified as critical for BMV replication in yeast, the homologous plant gene will be identified and its expression will be knocked down by VIGS. BMV replication will then be tested in the VIGS-treated plant leaf tissues. Because *N. benthamiana* also serves as a

universal host for many plant viruses (Goodin et al., 2008), we are able to test several diverse plant (+)RNA viruses in the VIGS-treated plants to determine whether the target gene is widely involved in replication of multiple (+)RNA viruses (Diaz et al., 2015).

### 1.1.3 The formation of BMV replication complexes

BMV induces the formation of spherular VRCs (spherules herein) by invaginating the outer perinuclear endoplasmic reticulum (ER) membrane into the ER lumen (Schwartz et al., 2002). These spherules are about 60-80 nm in diameter and have a neck (about 10 nm in diameter) that connects the interior of spherules to the cytoplasm of host cell for importing and exporting genetic materials and other essential materials during viral replication. More importantly, it is BMV 1a that is responsible to induce the formation of spherules (Sullivan and Ahlquist, 1999). The amphipathic alpha-helix of BMV 1a, termed helix A, inserts into lipid bilayer membranes and is required for the perinuclear ER membrane association of BMV 1a (Liu et al., 2009). In addition to inducing membrane rearrangement, BMV 1a recruits $2a^{pol}$ into spherules through 1a-$2a^{pol}$ interaction, and directs viral RNA templates to the viral spherules by recognizing the cis-acting element presented only in viral genomic RNAs termed RE (recruitment element) (Figure 1.4) (Chen and Ahlquist, 2000; den Boon et al., 2001; Krol et al., 1999; Restrepo-Hartwig and Ahlquist, 1999; Restrepo-Hartwig and Ahlquist, 1996; Schwartz et al., 2002; Sullivan and Ahlquist, 1999). In addition, the formation of spherules requires many host factors in yeast cells (Diaz and Wang, 2014; Kushner et al., 2003)

In summary, the BMV-yeast system enables us to use yeast genetic and genomic tools to

identify host factors and cellular processes that are required for or involved in BMV replication. The BMV-*N. benthamiana* system enables us to verify some of key findings obtained from yeast and test the broad involvement of the host proteins in other plant (+)RNA viruses.

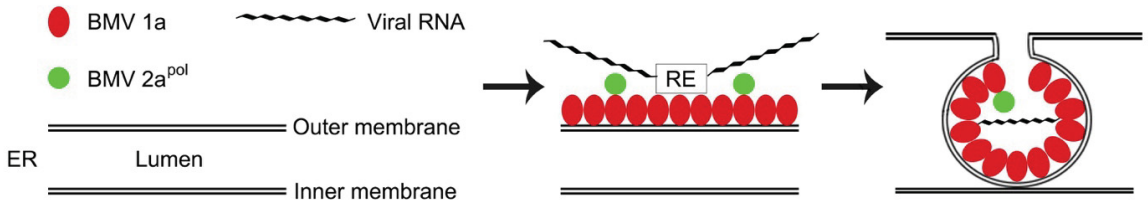


**Figure 1.4. BMV-induced spherule formation.**

BMV 1a targets to the perinuclear ER membrane to initiate spherule formation. BMV 1a interacts with itself and host factors to induce negative membrane curvature by invaginating the outer perinuclear ER membrane into the ER lumen, recruits BMV $2a^{pol}$ to the spherules by 1a-$2a^{pol}$ interaction, and recruits viral genomic RNAs to the spherules by recognizing the RE cis-element.

## 1.2 Host factors involved in (+)RNA virus replication

With very limited coding capacity, (+)RNA viruses rely entirely on host factors to complete their infection cycles, including viral entry, replication, assembly, and release. (+)RNA viruses have the ability to use limited viral proteins to dynamically and actively interact with a large number of host factors for viral replication and infection (Hyodo and Okuno, 2016). Therefore, identification and characterization of host factors that are involved in (+)RNA virus replication will enable us to develop antiviral strategies to disrupt viral replication, while maintaining normal cellular function or minimizing the off-target effects on host cells. Below, I review host factors involved in replication of various (+)RNA viruses, and in particular, those that are required for or involved in VRC formation.

### 1.2.1 Genome-wide screening of host factors involved in viral infection

Genome-wide approaches comprise powerful means to identify host factors involved in (+)RNA virus replication. Many different groups of host genes have been identified using genome-scale screenings. The RNA interference (RNAi) based genome-wide screening approach has been performed for animal viruses such as Dengue virus (DENV), West Nile virus (WNV), and HCV (Krishnan et al., 2008; Sessions et al., 2009; Tai et al., 2009). For example, 116 candidate host genes of *Drosophila melanogaster* have been identified that are required for DENV2 propagation by using 22,632 double-strand RNA (dsRNA) to knock down gene expression. Among these, 82 have human homologs and 42 of the human homologous genes have been previously identified to be involved in DENV2 propagation, These data validate the genome-wide approach and suggest that DENV2 propagation requires host factors conserved between dipteran and human hosts (Sessions et al., 2009). These screening results are consistent with current concept that viruses remodel cellular membrane during replication (Nagy et al., 2016). As for WNV infection, 305 human proteins, including 283 host susceptibility factors (HSFs) and 22 host resistance factors (HRFs), have been identified. Moreover, all of the 305 host factors that involved in WNV infection have been further checked for roles in DENV2 infection. About 102 HSFs and all 22 HRFs are involved in both DENV2 and WNV infections, suggesting that flaviviruses have both virus specific and shared interaction strategies in different host cells. The 102 HSFs are primarily involved in seven cellular processes: cell adhesion, cell cycle, signal transduction, transport, developmental processes, cell proliferation, and intracellular protein trafficking (Krishnan et

al., 2008). For HCV, 96 human genes have been identified as required for HCV replication by using 21,094 small interfering RNAs (siRNAs) that cover the entire human NCBI RefSeq transcript database. Gene Ontology (GO) biological process analysis of the 96 human genes showed that most of them are involved in Golgi vesicle binding, vesicle organization and biogenesis, membrane sorting and trafficking, suggesting that HCV mainly depends on lipid and membrane-related processes for VRC assembly (Tai et al., 2009). It should be emphasized that host genes identified from genome-wide screening could serve as useful resources for further characterization and for developing antiviral therapies, although the roles of most genes in viral infection and propagation have not been well characterized. This should be a major area of emphasis in the future.

The genome-wide screening approach that exploits yeast genetic and genomic tools has been directed to identify plant genes involved in the replication of (+)RNA viruses such as BMV and *tomato bushy stunt virus* (TBSV). About 100 non-essential yeast genes (Kushner et al., 2003) and 24 essential yeast genes (Gancarz et al., 2011), whose loss or repression either stimulated or inhibited BMV replication significantly, have been identified. These genes are mainly involved in lipid synthesis or metabolic pathways, ribosome biosynthesis, cell cycle regulation, ubiquitin pathway and protein homeostasis, RNA and protein modification pathways, and other cellular processes (Gancarz et al., 2011; Kushner et al., 2003).

TBSV belongs to the *Tombusviridae* family and has been well studied in yeast and plants. About 96 non-essential host genes and 30 essential genes are involved in TBSV replication (Jiang et al., 2006; Panavas et al., 2005). The identified host genes are mainly involved in the

RNA transcription, metabolism of nucleic acids, lipids, proteins, and other compounds and in protein targeting and/or transport, as well as many other cellular processes. In a comparison of host genes that involved in BMV and TBSV replication, most of the host genes are specific to a given virus with only a small number of genes that involved in both BMV and TBSV replication (Jiang et al., 2006; Panavas et al., 2005). One possible reason is that they replicate in different organelle membranes: BMV at perinuclear ER and TBSV at peroxisomal membrane. However, both viruses require similar pathways, such as lipid synthesis (Xu and Nagy, 2015; Zhang et al., 2016) or ESCRT (endosomal sorting complex required for transport) (Barajas et al., 2009; Diaz et al., 2015).

### 1.2.2 Host factors are involved in targeting viral replication proteins to specific intracellular membranes

All (+)RNA viruses replicate in a close relationship with host intracellular membranes and furthermore, targeting of viral proteins to specific subcellular sites plays a vital role in viral infection cycle. For instance, TBSV replication protein p33 transiently interacted with host Pex19, a transporter protein, for targeting to the peroxisomal membranes. Retargeting Pex19 to mitochondria caused redistribution of p33 to the mitochondria but inhibited TBSV replication, suggesting that Pex19 is most likely to recognize the peroxisomal localization signal motif of p33 and functions as a cellular carrier for transporting p33 to the peroxisomal membranes (Pathak et al., 2008). In addition, an *Arabidopsis* protein tobamovirus multiplication 1 (TOM1) is required for TMV replication. TOM1 has multiple transmembrane domains, interacts with the helicase domain of TMV replication proteins, and

serves as a membrane anchor for targeting viral replication proteins to the membranes to assemble VRCs (Yamanaka et al., 2000).

Similar to TOM1, the human homolog of 33-kD vesicle-associated membrane protein-associated protein (hVAP-33), which is a soluble N-ethylmaleimide-sensitive factor attachment protein receptor (SNARE)-like protein, serves as an anchor for HCV VRCs. HCV replication proteins nonstructural protein 5A (NS5A) and NS5B interacted with hVAP-33 (Tu et al., 1999). Furthermore, inhibition of hVAP-33 expression relocalized NS5B from detergent-resistant to detergent-sensitive membranes and inhibited HCV replication, suggesting that hVAP-33 might serve as a membrane anchor for HCV targeting to the detergent-resistant membranes to assemble VRCs (Gao et al., 2004). These examples demonstrate how host factors can play crucial roles in the targeting of viral proteins and VRCs of (+)RNA viruses to the specific intracellular membranes during viral replication.

Nevertheless, some (+)RNA viruses do not rely strictly on particular organelle membranes for viral replication, and have the capability of seeking alternative intracellular membranes for efficient viral replication. For example, Flock house virus (FHV), an alphanodavirus virus, replicates in outer mitochondria membrane-bound spherules. The replication protein, protein A, is the only viral protein that is required for FHV targeting to the outer mitochondrial membrane for VRC assembly and viral replication. Replacing the mitochondrion-targeting sequence of protein A with an ER-targeting sequence retargeted protein A and viral replication to the ER membrane. Surprisingly, FHV achieved a better replication in ER membrane than that in mitochondria, suggesting that FHV is flexible in its

VRC microenvironment requirement (Miller et al., 2003).

### 1.2.3 Membrane-shaping protein and viral replication

Many (+)RNA viruses require membrane-shaping proteins to build and maintain the membrane architecture of functional VRCs. The ER membrane-shaping reticulons (RTNs), which induce and stabilize the highly curved ER tubular membrane (Voeltz et al., 2006), play important roles in VRC assembly and function of BMV and human picornaviruses (Diaz and Ahlquist, 2012). BMV 1a interacted with and relocalized RTNs from peripheral ER membrane to the interior of spherules at the perinuclear ER membrane (Diaz et al., 2010). Deleting one or two *RTN* genes in yeast resulted in smaller spherules that did not fully support BMV replication. However, no spherules were formed when all three *RTN* genes were deleted, indicating that RTNs are required for initiating and/or maintaining BMV spherules (Diaz et al., 2010). Not surprisingly, human HsRTN3 interacted with 2C proteins of picornaviruses, such as poliovirus, Coxsackievirus A16, and enterovirus 71 (EV71). Knockdown of *HsRTN3* by RNAi inhibited EV71 replication whereas ectopic expression of non-degradable HsRTN3 in *RTN3* knockdown cells rescued EV71 replication, suggesting that RTN3 plays a crucial role in EV71 replication and infection (Tang et al., 2007). Therefore, membrane-shaping proteins are important host factors to induce and maintain the membrane structure of functional VRCs that are essential to (+)RNA virus replication.

### 1.2.4 Lipids and viral replication

Because all well-studied (+)RNA viruses rearrange host intracellular membranes to build

functional VRCs and lipids are the major component of cellular membranes, it seems clear that lipids play important roles in viral replication. Lipids contribute to the recruitment of viral proteins to the viral replication sites and the assembly of VRCs (Konan and Sanchez-Felipe, 2014; Shulla and Randall, 2016; Stapleford and Miller, 2010). For instance, a single nucleic acid alteration in the *OLE1* gene, which encodes Δ9 fatty acid desaturase converting saturated fatty acids (SFAs) to unsaturated fatty acids (UFAs), inhibited BMV replication by more than 20-fold. It was further shown that UFAs were locally depleted from BMV spherule-associated membranes but not host cellular membranes. This is consistent with the fact that BMV replication is more sensitive to the reduced UFAs as compared with host growth, suggesting the important role of lipid composition in BMV replication (Lee and Ahlquist, 2003; Lee et al., 2001). Another example is *ACB1* encoded acyl-CoA binding protein (ACBP), which also plays a critical role in BMV replication via lipid synthesis. ACBP binds to long-chain fatty acyl-CoA and is involved in maintaining lipid homeostasis by regulating general lipid synthesis (Neess et al., 2015). Deletion of *ACB1* inhibited BMV replication by reducing the size but increasing the number of spherules, suggesting that the interactions between BMV 1a and lipids play important roles in VRC assembly and function (Zhang et al., 2012a).

Furthermore, Cho2, a cellular phospholipid synthesis enzyme converting phosphatidylethanolamine (PE) to phosphatidylcholine (PC), was relocalized to VRCs by a specific interaction with BMV 1a (Zhang et al., 2016). The relocalization of Cho2 was correlated with the enriched-PC level at BMV VRCs, suggesting that BMV promotes PC

synthesis at the viral replication sites by recruiting Cho2. VRC-enriched PC content is apparently a conserved feature among a group of (+)RNA viruses because the enhanced PC levels are also associated with VRCs of HCV and poliovirus. It needs to note that BMV, HCV and poliovirus are very different from each other and belong to the alphavirus-like superfamily, flavivirus-like superfamily, and picornavirus-like superfamily, respectively. Intriguingly, it might be possible to develop a broad-spectrum antiviral strategy by disrupting PC synthesis at the viral replication sites, while leaving the host's general PC synthesis capacity intact (Zhang et al., 2016).

On the other hand, TBSV promotes a PE-enriched microenvironment in its VRCs. Deleting *CHO2* gene increased PE level and thus, increased TBSV replication dramatically. On the contrary, depletion of PE in yeast by deleting PE synthesis genes such as *PSD1*, *PSD2* and *DPL1*, inhibited TBSV replication. PE levels increased in yeast and plants upon TBSV replication, and furthermore, PE was enriched at the viral replication sites of TBSV (Xu and Nagy, 2015). Moreover, TBSV replication protein p33 interacted with the small GTPase Rab5, a key regulator of the early endosomal biogenesis, and most likely to recruit the endosomal lipids, especially PE, to the peroxisome-localized VRCs (Xu and Nagy, 2016).

Similar to BMV in redistributing host lipid synthesis enzyme to viral replication sites, DENV redistributed fatty acid synthase (FASN) to the viral replication sites by a specific interaction between viral replication protein NS3 and FASN. Moreover, NS3 stimulated the enzymatic activities of FASN to support DENV replication, suggesting that DENV coopts and increases cellular fatty acid synthesis for building VRCs (Heaton et al., 2010). In

contrast, HCV infection increased FASN protein levels and thus, fatty acid production in host cells (Nasheri et al., 2013). It is also likely that HCV viral replication protein NS4B activated sterol regulatory element-binding protein, a master transcription factor regulating the transcription of FASN and a group of lipid synthesis enzymes (Park et al., 2009). It is clear that fatty acids play important roles in replication of various viruses and therefore, targeting fatty acid biosynthetic pathway could be an efficient way to control viral infection.

## 1.3 Host early secretory pathway and viral replication

Host vesicle secretion and endocytic pathways are actively involved in plant immune responses triggered by pathogenic microbes. Plants not only secrete antimicrobial molecules through protein trafficking pathways, but also perceive microbe-associated patterns by endocytic trafficking pathways (Frey and Robatzek, 2009). In contrast, invasive pathogens can suppress immune responses by hijacking cellular components of secretory pathways (Frey and Robatzek, 2009). The cellular early secretory pathways, mainly composed of coat protein complex II (COPII) and coat protein complex I (COPI), play important roles in various infection stages for producing infectious progeny, especially the biogenesis of (+)RNA virus-induced VRC formation and function.

### 1.3.1 Cellular coat protein complex II and viral replication

COPII is mainly involved in protein trafficking from the ER to the Golgi apparatus. Yeast COPII vesicle is composed of Sar1 GTPase, inner shell Sec23/24, and outer shell Sec13/31, with the five components assembled sequentially. Sec12, a guanine nucleotide exchange

factor (GEF), resides in the ER membrane and loads GTP to Sar1 to activate Sar1. The resulting Sar1-GTP exposes its N-terminal amphipathic alpha-helix and inserts into the lipid bilayer of ER membrane to initiate COPII vesicle assembly. Specifically, Sar1-GTP interacts with Sec23 to recruit the inner shell Sec23/24 and form the pre-budding complex comprising Sar1-Sec23/24. Then Sec23 interacts with Sec31 to recruit the outer shell Sec13/31 to form a spherical cage-like outer coat layer on the nascent vesicles and thus, the COPII vesicle is generated (Figure 1.5) (Gomez-Navarro and Miller, 2016). Sec24 serves as the principle cargo recruiter by binding to the sorting signals present in cargo proteins to direct cargo proteins into ER membrane-bound COPII vesicles (D'Arcangelo et al., 2013; Gomez-Navarro and Miller, 2016; Lord et al., 2013; Matsuoka et al., 2001). COPII interacts with cargo proteins and cargo receptors (such as Erv14) that facilitate cargo protein incorporation into the ER-derived COPII vesicles for cargo protein trafficking to their destined localizations (Kuehn et al., 1998).

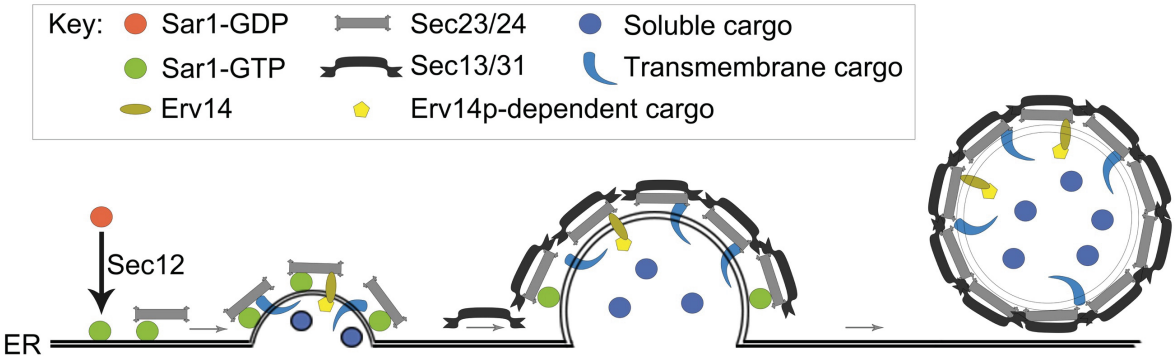


**Figure 1.5. Formation of COPII vesicle on ER membrane by sequential recruitment of COPII coats.**

Sec12 is a GEF that activates Sar1 to initiate the assembly of COPII vesicles at the ER membrane, Sar1 interacts with Sec23 to recruit the inner shell of COPII vesicles Sec23/24 to form the pre-budding complex Sar1-Sec23/24, then Sec23 interacts with Sec31 to assemble the cage-like outer coat layer of COPII vesicles Sec13/31 on the nascent vesicles. This figure is adapted from (Venditti et al.,

2014).

The COPII pathway plays important roles in supporting the completion of viral infection cycles, such as viral protein trafficking and VRC assembly, of several (+)RNA viruses. For instance, *turnip mosaic virus* (TuMV), a plant (+)RNA virus that belongs to the *Potyviridae* family, requires COPII pathway for its infection. The formation of TuMV VRCs was dependent on COPII through the physical interaction between TuMV viral protein $6K_2$ and COPII coat protein Sec24a, suggesting that TuMV might coopt cellular ER export machinery for the biogenesis and trafficking of VRCs (Jiang et al., 2015). Poliovirus rearranges ER and Golgi membranes to form double-membrane VRCs. Immunofluorescence labeling indicated that poliovirus nonstructural proteins 2B and 2BC colocalized with COPII coat proteins Sec13 and Sec31, indicating that poliovirus might coopt cellular COPII budding mechanism for the formation of VRCs during viral replication (Rust et al., 2001).

### 1.3.2 Cellular coat protein complex I and viral replication

COPI vesicles are primarily involved in recycling membrane and ER-resident proteins from the Golgi to the ER. COPI vesicles are generated on the Golgi or ER-Golgi intermediate compartment membranes by the small GTPase ADP ribosylation factor 1 (Arf1) to initiate the formation of a heptameric protein complex that composed of a trimeric complex composed of Sec33 (α-COP), Sec27 (β′-COP), Sec28 (ε-COP), and a tetrameric complex composed of Sec21 (γ-COP), Ret2 (δ-COP), Ret3 (ζ-COP), Sec26 (β-COP). The assembly of COPI vesicles requires the binding of Arf1 to the membrane via a short amphipathic helix at the N-terminus and the subsequent recruitment of heptameric protein complex, which then

recruits cargo proteins into the COPI vesicles for trafficking (Gomez-Navarro and Miller, 2016).

COPI has diverse roles in many stages of viral infection such as viral entry, replication, and intracellular transport of viral proteins (Thompson and Brown, 2012). For instance, EV71, a member of the *Picornaviridae* family, requires COPI but not COPII for its replication. EV71 viral protein 2C interacted with the ζ-COP subunit and directed COPI components to the VRCs. Inhibition of COPI activity with pharmacological inhibitors of Arf1, such as Brefeldin A (BFA) and Golgicide A (GCA), inhibited EV71 replication (Wang et al., 2012). Similar to EV71, *Drosophila* C virus (DCV) replication requires COPI-associated genes for DCV entry into the host cells and generating VRCs for viral replication (Cherry et al., 2006). In addition, VRCs of another picornavirus, echovirus 11 (EV11), were associated with COPI subunit β-COP. Treatment of BFA inhibited EV11 replication, suggesting that the formation of EV11 VRCs is dependent on COPI components (Gazina et al., 2002). Similarly, inhibition of Arf1 activity by BFA or GCA treatment reduced viral RNA levels as well as the accumulation of infectious particles in HCV-infected cells and the extracellular medium, suggesting that Arf1 is involved in the regulation of HCV replication and production of infectious viral particles (Matto et al., 2011). One major effector protein of Arf1 is phosphatidylinositol-4 phosphate III kinase β (PI4PIIIβ), which produces phosphatidylinositol-4 phosphate (PI4P) from phosphatidylinositol. It was further found that Arf1 colocalizaed with PI4PIIIβ during HCV infection, suggesting that Arf1 plays an important role in HCV replication through the regulation of PI4P synthesis (Zhang et al.,

2012b).

### 1.3.3 Interplay among COPI, COPII and viral replication

Many plant, animal and human (+)RNA viruses interfere with or take advantage of both COPI and COPII to support their replication. For instance, *Red clover necrotic mosaic virus* (RCNMV), a plant (+)RNA virus that belongs to the *Tombusviridae* family, remodels ER membrane to assemble large punctate structures that host VRCs. RCNMV hijacks the COPI component Arf1 and the COPII coat Sar1. RCNMV replication protein p17 interacted with Arf1 within the virus-induced large punctate structures of the ER membrane, while BFA treatment or expression of a dominant negative mutant of *Arf1* or *Sar1* inhibited RCNMV replication, suggesting that RCNMV replication is dependent on both pathways (Hyodo et al., 2013). Furthermore, RCNMV p17 inhibited the trafficking of secretory pathway marker proteins such as rice secretory carrier membrane protein 1 (OsSCAMP1) and *Arabidopsis* LRR84A (AtLRR84A), a member of leucine-rich repeat receptor-like kinase protein family, to the plasma membrane. Normally, OsSCAMP1 and AtLRR84A are transported to the plasma membrane through the ER-Golgi-trans Golgi network pathway. However, RCNMV infection caused ER retention of OsSCAMP1 and AtLRR84A, suggesting that RCNMV can actively subvert cellular secretory pathway to favor viral replication (Hyodo et al., 2014). Similarly, another plant (+)RNA virus *tobacco etch virus* (TEV), which belongs to the *Potyviridae* family, also relies on COPI and COPII to assemble VRC during viral replication. The TEV protein $6K_2$ localized to the ER exit sites (ERES) to induce VRC assembly, while disruption of COPII or COPI activity by dominant negative mutants of *Sar1* and *Arf1*

prevented the localization of $6K_2$ to the ERES and inhibited TEV infection (Wei and Wang, 2008).

Several (+)RNA viruses infecting mammals also subvert cellular early secretory pathways to support the biogenesis of VRC formation and viral proliferation. For instance, FMDV is a picornavirus and requires pre-Golgi membranes of the early secretory pathway for viral infection. Disruption of COPII vesicles by siRNA-mediated Sar1 depletion or expression of a dominant negative *Sar1* mutant inhibited FDMV infection. On the other hand, disruption of COPI vesicles by BFA treatment or expression of a dominant negative *Arf1* mutant enhanced FDMV infection (Midgley et al., 2013). Moreover, piconavirus Coxsackievirus B3 (CVB3) is recruited PI4PIIIβ to its VRCs. It has been shown that CVB3 replication protein 3A selectively recruited PI4PIIIβ, which is the effector protein of Arf1, to the viral replication sites for creating a PI4P-enriched microenvironment to initiate VRC assembly. Furthermore, the CVB3 viral protein $3D^{pol}$ specifically and preferentially bound to PI4P, and thus the resulting PI4P-enriched microenvironments further recruited $3D^{pol}$ to the VRCs for viral RNA synthesis. In addition, dominant negative *Sar1* mutant inhibited CVB3 replication significantly, indicating the importance of COPII in poliovirus infection. The results suggest that (+)RNA viruses can exploit specific cellular elements to generate VRCs and favor viral replication (Hsu et al., 2010).

## 1.4 Objectives

All well-studied (+)RNA viruses exploit host specific organelle membranes to create favorable microenvironments that support VRC assembly and viral RNA synthesis. However,

it is not clear how viral replication proteins are targeted to their destination organelles. More specifically, what properties of viral replication proteins are the determinant and what host pathway(s) are involved in the trafficking of such viral replication proteins. Targeting viral replication proteins to their preferred organelle membranes to initiate VRC formation is one of the initial steps of viral replication. A better understanding of this process will provide not only new information on viral replication but also identify new host targets for developing new strategies to control viral infection.

The BMV-yeast system is well-established to examine viral replication mechanisms and virus-host interactions of (+)RNA viruses. My research project aimed to understand how host factors are involved in BMV 1a targeting to the perinuclear ER membrane and in BMV replication. By taking advantage of the versatile yeast genetic and genomic tools, I started my research project by identifying yeast deletion mutants that could disrupt BMV 1a targeting to the perinuclear ER membrane. The plant homologs of many yeast genes are clearly identifiable in *N. benthamiana* and *A. thaliana*. Thus, I extended my BMV-yeast studies to explore the cellular functions of plant homologs and their roles in infection by plant (+)RNA viruses and other plant pathogens. Finally, I expect to identify the conserved features of host factors in yeast and plants to provide a proof of concept for the development of a novel strategy to interrupt plant pathogen infections.

## 1.5 References

**Ahlquist, P., Dasgupta, R. and Kaesberg, P.** (1984). Nucleotide sequence of the brome mosaic virus genome and its implications for viral replication. *J Mol Biol* **172**, 369-383.

**Ahlquist, P., Luckow, V. and Kaesberg, P.** (1981). Complete nucleotide sequence of brome mosaic virus RNA3. *J Mol Biol* **153**, 23-38.

**Ahola, T. and Ahlquist, P.** (1999). Putative RNA capping activities encoded by brome mosaic virus: methylation and covalent binding of guanylate by replicase protein 1a. *J Virol* **73**, 10061-10069.

**Annamalai, P. and Rao, A. L. N.** (2005). Replication-independent expression of genome components and capsid protein of brome mosaic virus in planta: A functional role for viral replicase in RNA packaging. *Virology* **338**, 96-111.

**Baltimore, D.** (1971). Expression of animal virus genomes. *Bacteriol Rev* **35**, 235-241.

**Barajas, D., Jiang, Y. and Nagy, P. D.** (2009). A unique role for the host ESCRT proteins in replication of tomato bushy stunt virus. *PLoS Pathog* **5**, e1000705.

**Caplan, J. L., Zhu, X., Mamillapalli, P., Marathe, R., Anandalakshmi, R. and Dinesh-Kumar, S. P.** (2009). Induced ER-chaperones regulate a novel receptor-like kinase to mediate a viral innate immune response. *Cell Host Microbe* **6**, 457-469.

**Chen, J. and Ahlquist, P.** (2000). Brome mosaic virus polymerase-like protein 2a is directed to the endoplasmic reticulum by helicase-like viral protein 1a. *J Virol* **74**, 4310-4318.

**Cherry, S., Kunte, A., Wang, H., Coyne, C., Rawson, R. B. and Perrimon, N.** (2006). COPI activity coupled with fatty acid biosynthesis is required for viral replication. *PLoS Pathog* **2**, e102.

**D'Arcangelo, J. G., Stahmer, K. R. and Miller, E. A.** (2013). Vesicle-mediated export from the ER: COPII coat function and regulation. *Biochim Biophys Acta* **1833**, 2464-2472.

**den Boon, J. A., Chen, J. and Ahlquist, P.** (2001). Identification of sequences in brome mosaic virus replicase protein 1a that mediate association with endoplasmic reticulum membranes. *J Virol* **75**, 12370-12381.

**Diaz, A. and Ahlquist, P.** (2012). Role of host reticulon proteins in rearranging membranes for positive-strand RNA virus replication. *Curr Opin Microbiol* **15**, 519-524.

**Diaz, A. and Wang, X.** (2014). Bromovirus-induced remodeling of host membranes during viral RNA replication. *Curr Opin Virol* **9**, 104-110.

**Diaz, A., Wang, X. and Ahlquist, P.** (2010). Membrane-shaping host reticulon proteins play

crucial roles in viral RNA replication compartment formation and function. *Proc Natl Acad Sci USA* **107**, 16291-16296.

**Diaz, A., Zhang, J., Ollwerther, A., Wang, X. and Ahlquist, P.** (2015). Host ESCRT proteins are required for bromovirus RNA replication compartment assembly and function. *PLoS Pathog* **11**, e1004742.

**Frey, N. F. d. and Robatzek, S.** (2009). Trafficking vesicles: pro or contra pathogens? *Curr Opin Plant Biol* **12**, 437-443.

**Fujisaki, K., Hagihara, F., Kaido, M., Mise, K. and Okuno, T.** (2003). Complete nucleotide sequence of spring beauty latent virus, a bromovirus infectious to Arabidopsis thaliana. *Arch Virol* **148**, 165-175.

**Gancarz, B. L., Hao, L., He, Q., Newton, M. A. and Ahlquist, P.** (2011). Systematic identification of novel, essential host genes affecting bromovirus RNA replication. *PLoS ONE* **6**, e23988.

**Gao, L., Aizaki, H., He, J.-W. and Lai, M. M. C.** (2004). Interactions between viral nonstructural proteins and host protein hVAP-33 mediate the formation of hepatitis C virus RNA replication complex on lipid raft. *J Virol* **78**, 3480-3488.

**Gazina, E. V., Mackenzie, J. M., Gorrell, R. J. and Anderson, D. A.** (2002). Differential requirements for COPI coats in formation of replication complexes among three genera of Picornaviridae. *J Virol* **76**, 11113-11122.

**Gomez-Navarro, N. and Miller, E. A.** (2016). COP-coated vesicles. *Curr Biol* **26**, R54-R57.

**Goodin, M. M., Zaitlin, D., Naidu, R. A. and Lommel, S. A.** (2008). Nicotiana benthamiana: Its history and future as a model for plant–pathogen interactions. *Mol Plant Microbe In* **21**, 1015-1026.

**Gopinath, K., Dragnea, B. and Kao, C.** (2005). Interaction between brome mosaic virus proteins and RNAs: effects on RNA replication, protein expression, and RNA stability. *J Virol* **79**, 14222-14234.

**Heaton, N. S., Perera, R., Berger, K. L., Khadka, S., LaCount, D. J., Kuhn, R. J. and Randall, G.** (2010). Dengue virus nonstructural protein 3 redistributes fatty acid synthase to sites of viral replication and increases cellular fatty acid synthesis. *Proc Natl Acad Sci USA* **107**, 17345-17350.

**Hsu, N.-Y., Ilnytska, O., Belov, G., Santiana, M., Chen, Y.-H., Takvorian, P. M., Pau, C., van der Schaar, H., Kaushik-Basu, N., Balla, T. et al.** (2010). Viral reorganization of the secretory pathway generates distinct organelles for RNA replication. *Cell* **141**, 799-811.

**Hyodo, K., Kaido, M. and Okuno, T.** (2014). Traffic jam on the cellular secretory pathway generated by a replication protein from a plant RNA virus. *Plant Signal Behav* **9**, e28644.

**Hyodo, K., Mine, A., Taniguchi, T., Kaido, M., Mise, K., Taniguchi, H. and Okuno, T.** (2013). ADP ribosylation factor 1 plays an essential role in the replication of a plant RNA virus. *J Virol* **87**, 163-176.

**Hyodo, K. and Okuno, T.** (2016). Pathogenesis mediated by proviral host factors involved in translation and replication of plant positive-strand RNA viruses. *Curr Opin Virol* **17**, 11-18.

**Ishikawa, M., Janda, M., Krol, M. A. and Ahlquist, P.** (1997). In vivo DNA expression of functional brome mosaic virus RNA replicons in *Saccharomyces cerevisiae*. *J Virol* **71**, 7781-7790.

**Janda, M. and Ahlquist, P.** (1993). RNA-dependent replication, transcription, and persistence of brome mosaic virus RNA replicons in *S. cerevisiae*. *Cell* **72**, 961-970.

**Jiang, J., Patarroyo, C., Garcia Cabanillas, D., Zheng, H. and Laliberté, J.-F.** (2015). The vesicle-forming 6K2 protein of turnip mosaic virus interacts with the COPII coatomer Sec24a for viral systemic infection. *J Virol* **89**, 6695-6710.

**Jiang, Y., Serviene, E., Gal, J., Panavas, T. and Nagy, P. D.** (2006). Identification of essential host factors affecting tombusvirus RNA replication based on the yeast tet promoters hughes collection. *J Virol* **80**, 7394-7404.

**Kao, C. C. and Ahlquist, P.** (1992). Identification of the domains required for direct interaction of the helicase-like and polymerase-like RNA replication proteins of brome mosaic virus. *J Virol* **66**, 7293-7302.

**Konan, K. V. and Sanchez-Felipe, L.** (2014). Lipids and RNA virus replication. *Curr Opin Virol* **9**, 45-52.

**Kong, F., Sivakumaran, K. and Kao, C.** (1999). The N-terminal half of the brome mosaic virus 1a protein has RNA capping-associated activities: specificity for GTP and s-adenosylmethionine. *Virology* **259**, 200-210.

**Krishnan, M. N., Ng, A., Sukumaran, B., Gilfoy, F. D., Uchil, P. D., Sultana, H., Brass, A. L., Adametz, R., Tsui, M., Qian, F. et al.** (2008). RNA interference screen for human genes associated with West Nile virus infection. *Nature* **455**, 242-245.

**Krol, M. A., Olson, N. H., Tate, J., Johnson, J. E., Baker, T. S. and Ahlquist, P.** (1999). RNA-controlled polymorphism in the in vivo assembly of 180-subunit and 120-subunit virions from a single capsid protein. *Proc Natl Acad Sci USA* **96**, 13650-13655.

**Kuehn, M. J., Herrmann, J. M. and Schekman, R.** (1998). COPII-cargo interactions direct protein sorting into ER-derived transport vesicles. *Nature* **391**, 187-190.

**Kushner, D. B., Lindenbach, B. D., Grdzelishvili, V. Z., Noueiry, A. O., Paul, S. M. and Ahlquist, P.** (2003). Systematic, genome-wide identification of host genes affecting replication of a positive-strand RNA virus. *Proc Natl Acad Sci USA* **100**, 15764-15769.

**Lane, L. C.** (1974). The Bromoviruses. In *Adv Virus Res*, vol. Volume 19 (eds F. B. B. K. M. Max A. Lauffer and M. S. Kenneth), pp. 151-220: Academic Press.

**Lee, W.-M. and Ahlquist, P.** (2003). Membrane synthesis, specific lipid requirements, and localized lipid composition changes associated with a positive-strand RNA virus RNA replication protein. *J Virol* **77**, 12819-12828.

**Lee, W.-M., Ishikawa, M. and Ahlquist, P.** (2001). Mutation of host Δ9 fatty acid desaturase inhibits brome mosaic virus RNA replication between template recognition and RNA synthesis. *J Virol* **75**, 2097-2106.

**Liu, L., Westler, W. M., Den Boon, J. A., Wang, X., Diaz, A., Steinberg, H. A. and Ahlquist, P.** (2009). An amphipathic α-helix controls multiple roles of brome mosaic virus protein 1a in RNA replication complex assembly and function. *PLoS Pathog* **5**, e1000351.

**Lord, C., Ferro-Novick, S. and Miller, E. A.** (2013). The highly conserved COPII coat complex sorts cargo from the endoplasmic reticulum and targets it to the golgi. *Cold SH Perspect Biol* **5**, a013367.

**Matsuoka, K., Schekman, R., Orci, L. and Heuser, J. E.** (2001). Surface structure of the COPII-coated vesicle. *Proc Natl Acad Sci USA* **98**, 13705-13709.

**Matto, M., Sklan, E. H., David, N., Melamed-Book, N., Casanova, J. E., Glenn, J. S. and Aroeti, B.** (2011). Role for ADP ribosylation factor 1 in the regulation of hepatitis C virus replication. *J Virol* **85**, 946-956.

**Midgley, R., Moffat, K., Berryman, S., Hawes, P., Simpson, J., Fullen, D., Stephens, D. J., Burman, A. and Jackson, T.** (2013). A role for endoplasmic reticulum exit sites in foot-and-mouth disease virus infection. *J Gen Virol* **94**, 2636-2646.

**Miller, D. J., Schwartz, M. D., Dye, B. T. and Ahlquist, P.** (2003). Engineered retargeting of viral RNA replication complexes to an alternative intracellular membrane. *J Virol* **77**, 12193-12202.

**Miller, W. A., Dreher, T. W. and Hall, T. C.** (1985). Synthesis of brome mosaic virus subgenomic RNA in vitro by internal initiation on (-)-sense genomic RNA. *Nature* **313**, 68-70.

**Nagy, P. D., Strating, J. R. P. M. and van Kuppeveld, F. J. M.** (2016). Building viral replication organelles: close encounters of the membrane types. *PLoS Pathog* **12**, e1005912.

**Nasheri, N., Joyce, M., Rouleau, Y., Yang, P., Yao, S., Tyrrell, D. L. and Pezacki,**

**John P.** (2013). Modulation of fatty acid synthase enzyme activity and expression during hepatitis C vrus replication. *Chem Biol* **20**, 570-582.

**Neess, D., Bek, S., Engelsby, H., Gallego, S. F. and Færgeman, N. J.** (2015). Long-chain acyl-CoA esters in metabolism and signaling: Role of acyl-CoA binding proteins. *Prog Lipid Res* **59**, 1-25.

**O'Reilly, E. K., Paul, J. D. and Kao, C. C.** (1997). Analysis of the interaction of viral RNA replication proteins by using the yeast two-hybrid assay. *J Virol* **71**, 7526-32.

**Panavas, T., Serviene, E., Brasher, J. and Nagy, P. D.** (2005). Yeast genome-wide screen reveals dissimilar sets of host genes affecting replication of RNA viruses. *Proc Natl Acad Sci USA* **102**, 7326-7331.

**Park, C.-Y., Jun, H.-J., Wakita, T., Cheong, J. H. and Hwang, S. B.** (2009). Hepatitis C virus nonstructural 4B protein modulates sterol regulatory element-binding protein signaling via the AKT pathway. *J Biol Chem* **284**, 9237-9246.

**Pathak, K. B., Sasvari, Z. and Nagy, P. D.** (2008). The host Pex19p plays a role in peroxisomal localization of tombusvirus replication proteins. *Virology* **379**, 294-305.

**Rao, A. L. N. and Kao, C. C.** (2015). The brome mosaic virus 3′ untranslated sequence regulates RNA replication, recombination, and virion assembly. *Virus Res* **206**, 46-52.

**Raoult, D. and Forterre, P.** (2008). Redefining viruses: lessons from Mimivirus. *Nat Rev Micro* **6**, 315-319.

**Restrepo-Hartwig, M. and Ahlquist, P.** (1999). Brome mosaic virus RNA replication proteins 1a and 2a colocalize and 1a independently localizes on the yeast endoplasmic reticulum. *J Virol* **73**, 10303-10309.

**Restrepo-Hartwig, M. A. and Ahlquist, P.** (1996). Brome mosaic virus helicase- and polymerase-like proteins colocalize on the endoplasmic reticulum at sites of viral RNA synthesis. *J Virol* **70**, 8908-16.

**Rust, R. C., Landmann, L., Gosert, R., Tang, B. L., Hong, W., Hauri, H.-P., Egger, D. and Bienz, K.** (2001). Cellular COPII proteins are involved in production of the vesicles that form the poliovirus replication complex. *J Virol* **75**, 9808-9818.

**Scholthof, K.-B. G., Adkins, S., Czosnek, H., Palukaitis, P., Jacquot, E., Hohn, T., Hohn, B., Saunders, K., Candresse, T., Ahlquist, P. et al.** (2011). Top 10 plant viruses in molecular plant pathology. *Mol Plant Pathol* **12**, 938-954.

**Schwartz, M., Chen, J., Janda, M., Sullivan, M., den Boon, J. and Ahlquist, P.** (2002). A positive-strand RNA virus replication complex parallels form and function of retrovirus capsids. *Mol*

*Cell* **9**, 505-514.

**Senthil-Kumar, M. and Mysore, K. S.** (2014). Tobacco rattle virus–based virus-induced gene silencing in Nicotiana benthamiana. *Nat Protoc* **9**, 1549-1562.

**Sessions, O. M., Barrows, N. J., Souza-Neto, J. A., Robinson, T. J., Hershey, C. L., Rodgers, M. A., Ramirez, J. L., Dimopoulos, G., Yang, P. L., Pearson, J. L. et al.** (2009). Discovery of insect and human dengue virus host factors. *Nature* **458**, 1047-1050.

**Shulla, A. and Randall, G.** (2016). (+) RNA virus replication compartments: a safe home for (most) viral replication. *Curr Opin Microbiol* **32**, 82-88.

**Stapleford, K. A. and Miller, D. J.** (2010). Role of cellular lipids in positive-sense RNA virus replication complex assembly and function. *Viruses* **2**, 1055-1068.

**Sullivan, M. L. and Ahlquist, P.** (1999). A brome mosaic virus intergenic RNA3 replication signal functions with viral replication protein 1a to dramatically stabilize RNA in vivo. *J Virol* **73**, 2622-2632.

**Tai, A. W., Benita, Y., Peng, L. F., Kim, S.-S., Sakamoto, N., Xavier, R. J. and Chung, R. T.** (2009). A functional genomic screen identifies cellular cofactors of hepatitis C virus replication. *Cell Host Microbe* **5**, 298-307.

**Tang, W.-F., Yang, S.-Y., Wu, B.-W., Jheng, J.-R., Chen, Y.-L., Shih, C.-H., Lin, K.-H., Lai, H.-C., Tang, P. and Horng, J.-T.** (2007). Reticulon 3 binds the 2C protein of enterovirus 71 and is required for viral replication. *J Biol Chem* **282**, 5888-5898.

**Thompson, J. A. and Brown, J. C.** (2012). Role of coatomer protein I in virus replication. *J Virol Antivir Res* **1**, 10.4172/2324-8955.1000102.

**Tu, H., Gao, L., Shi, S. T., Taylor, D. R., Yang, T., Mircheff, A. K., Wen, Y., Gorbalenya, A. E., Hwang, S. B. and Lai, M. M. C.** (1999). Hepatitis C virus RNA polymerase and NS5A complex with a SNARE-like protein. *Virology* **263**, 30-41.

**Velásquez, A. C., Chakravarthy, S. and Martin, G. B.** (2009). Virus-induced gene silencing (VIGS) in Nicotiana benthamiana and tomato. *J Vis Exp*, 1292.

**Venditti, R., Wilson, C. and De Matteis, M. A.** (2014). Exiting the ER: what we know and what we don't. *Trends Cell Biol* **24**, 9-18.

**Voeltz, G. K., Prinz, W. A., Shibata, Y., Rist, J. M. and Rapoport, T. A.** (2006). A class of membrane proteins shaping the tubular endoplasmic reticulum. *Cell* **124**, 573-586.

**Wang, J., Wu, Z. and Jin, Q.** (2012). COPI Is Required for Enterovirus 71 Replication. *PLoS ONE* **7**, e38035.

**Wang, R. Y.-L., Stork, J. and Nagy, P. D.** (2009). A key role for heat shock protein 70 in

the localization and insertion of replication proteins to intracellular membranes. *J Virol* **83**, 3276-3287.

**Wang, X., Lee, W.-M., Watanabe, T., Schwartz, M., Janda, M. and Ahlquist, P.** (2005). Brome mosaic virus 1a nucleoside triphosphatase/helicase domain plays crucial roles in recruiting RNA replication templates. *J Virol* **79**, 13747-13758.

**Wei, T. and Wang, A.** (2008). Biogenesis of cytoplasmic membranous vesicles for plant potyvirus replication occurs at endoplasmic reticulum exit sites in a COPI- and COPII-dependent manner. *J Virol* **82**, 12252-12264.

**Xu, K., Lin, J.-Y. and Nagy, P. D.** (2014). The Hop-like stress-induced protein 1 cochaperone is a novel cell-intrinsic restriction factor for mitochondrial tombusvirus replication. *J Virol* **88**, 9361-9378.

**Xu, K. and Nagy, P. D.** (2015). RNA virus replication depends on enrichment of phosphatidylethanolamine at replication sites in subcellular membranes. *Proc Natl Acad Sci USA* **112**, E1782-E1791.

**Xu, K. and Nagy, P. D.** (2016). Enrichment of phosphatidylethanolamine in viral replication compartments via co-opting the endosomal Rab5 small GTPase by a positive-strand RNA virus. *PLoS Biol* **14**, e2000128.

**Yamanaka, T., Ohta, T., Takahashi, M., Meshi, T., Schmidt, R., Dean, C., Naito, S. and Ishikawa, M.** (2000). TOM1, an Arabidopsis gene required for efficient multiplication of a tobamovirus, encodes a putative transmembrane protein. *Proc Natl Acad Sci USA* **97**, 10107-10112.

**Zhang, J., Diaz, A., Mao, L., Ahlquist, P. and Wang, X.** (2012a). Host acyl coenzyme A binding protein regulates replication complex assembly and activity of a positive-strand RNA virus. *J Virol* **86**, 5110-5121.

**Zhang, J., Zhang, Z., Chukkapalli, V., Nchoutmboube, J. A., Li, J., Randall, G., Belov, G. A. and Wang, X.** (2016). Positive-strand RNA viruses stimulate host phosphatidylcholine synthesis at viral replication sites. *Proc Natl Acad Sci USA* **113**, E1064-E1073.

**Zhang, L., Hong, Z., Lin, W., Shao, R.-X., Goto, K., Hsu, V. W. and Chung, R. T.** (2012b). ARF1 and GBF1 generate a PI4P-enriched environment supportive of hepatitis C virus replication. *PLoS ONE* **7**, e32135.

# Chapter 2 An unrecognized function for COPII components in recruiting the viral replication protein BMV 1a to the perinuclear ER

This chapter has been published in the Journal of Cell Science, and is reproduced/adapted with permission from the Journal of Cell Science. The full citation detail is: Jianhui Li, Shai Fuchs, Jiantao Zhang, Sebastian Wellford, Maya Schuldiner and Xiaofeng Wang (2016). An unrecognized function for COPII components in recruiting the viral replication protein BMV 1a to the perinuclear ER. *J Cell Sci* 129, 3597-3608 (https://doi.org/10.1242/jcs.190082).

## 2.1 Abstract

Positive-strand RNA viruses invariably assemble their viral replication complexes (VRCs) by remodeling host intracellular membranes. How viral replication proteins are targeted to specific organelle membranes to initiate VRC assembly remains elusive. Brome mosaic virus (BMV), whose replication can be recapitulated in *Saccharomyces cerevisiae*, assembles its VRCs by invaginating the outer perinuclear endoplasmic reticulum (ER) membrane. Remarkably, BMV replication protein 1a (BMV 1a) is the only viral protein required for such membrane remodeling. We show that ER-vesicle protein of 14 kD (Erv14), a cargo receptor of coat protein complex II (COPII), interacts with BMV 1a. Moreover, the perinuclear ER localization of BMV 1a is disrupted in cells lacking *ERV14* or expressing dysfunctional COPII coat components (Sec13, Sec24, or Sec31). The requirement of Erv14 for the localization of BMV 1a is bypassed by addition of a Sec24-recognizable sorting signal to BMV 1a or by overexpressing Sec24, suggesting a coordinated effort by both Erv14 and Sec24 for the proper localization of BMV 1a. The COPII pathway is well known for being

involved in protein secretion; our data suggest that a subset of COPII coat proteins have an unrecognized role in targeting proteins to the perinuclear ER membrane.

## 2.2 Introduction

Positive-strand RNA [(+)RNA] viruses include many important human, animal, and plant pathogens. All well-studied (+)RNA viruses assemble their viral replication complexes (VRCs) by remodeling host intracellular membranes, and different viruses target particular organelle membranes to initiate VRC assembly. For instance, hepatitis C virus, brome mosaic virus (BMV), and tobacco mosaic virus replicate in association with endoplasmic reticulum (ER) membranes. In contrast, Flock House virus and carnation Italian ringspot virus replicate in mitochondria, while tomato bushy stunt virus replicates in peroxisomes (den Boon et al., 2010; Laliberté and Sanfaçon, 2010; Paul and Bartenschlager, 2013; Romero-Brey and Bartenschlager, 2014). However, the mechanisms by which viruses target their replication proteins to particular membranes for VRC assembly are not well documented.

BMV belongs to the plant virus family *Bromoviridae* and is a productive model for dissecting virus-host interactions and viral replication mechanisms of (+)RNA viruses (Diaz and Wang, 2014; Wang and Ahlquist, 2008). BMV genomic replication can be reconstituted in the yeast *Saccharomyces cerevisiae*, duplicating nearly all features of BMV replication in its natural plant hosts (Janda and Ahlquist, 1993; Restrepo-Hartwig and Ahlquist, 1996; Schwartz et al., 2002; Wang and Ahlquist, 2008). BMV has a tripartite RNA genome and a sub-genomic mRNA, RNA4. BMV encodes two replication proteins, BMV 1a and $2a^{pol}$, which are necessary and sufficient for genomic replication in plants and yeast. BMV $2a^{pol}$

contains a central RNA-dependent RNA polymerase (RdRp) domain and serves as a replicase. BMV 1a contains an N-terminal RNA capping domain (Ahola and Ahlquist, 1999; Kong et al., 1999) and a C-terminal NTPase or helicase-like domain (Wang et al., 2005). In yeast, expression of 1a and $2a^{pol}$, along with other host factors, supports the replication of BMV genomic RNAs. BMV VRCs are formed by invaginating the outer perinuclear ER membrane into the ER lumen, giving rise to spherular compartments that are 60 to 80 nm in diameter with a neck-like opening of ~10 nm that connects the VRC interior to the cytoplasm (Schwartz et al., 2002). The expression of BMV 1a alone in yeast induces the formation of spherules, which are morphologically indistinguishable from VRCs. When co-expressed, BMV $2a^{pol}$ and genomic RNA are recruited by BMV 1a into the interior of spherules, which then become VRCs (Martelli and Russo, 1985; Schwartz et al., 2002). An amphipathic α-helix within BMV 1a, helix A (amino acids 392-407), is required for its perinuclear ER membrane association in yeast and for BMV infection in plants (Liu et al., 2009). The formation of BMV 1a-induced spherules also requires host proteins (Diaz and Wang, 2014). Well-studied examples include reticulons (RTNs) and sucrose nonfermenting7 (Snf7), which are recruited by BMV 1a via protein-protein interactions and are required for spherule formation in yeast (Diaz et al., 2010; Diaz et al., 2015). However, the mechanism by which BMV 1a is targeted to the perinuclear ER membrane is still unknown.

Coat protein complex II (COPII) is the cellular machinery responsible for anterograde protein trafficking from the ER to the Golgi. The core components of COPII include the GTPase Sar1, which initiates vesicle formation, an inner shell complex comprising Sec23 and

Sec24, and an outer shell complex comprising Sec13 and Sec31 (Brandizzi and Barlowe, 2014; D'Arcangelo et al., 2013; Lord et al., 2013). Sec24 serves as the principle cargo recruiter by recognizing sorting signals present in cargos and recruiting them into vesicles. However, many cargos do not have Sec24-binding motifs and, therefore, require a cargo receptor to facilitate their incorporation into vesicles (Belden and Barlowe, 2001; Herzig et al., 2012; Kuehn et al., 1998; Miller et al., 2003; Mossessova et al., 2003; Pagant et al., 2015). As a typical cargo receptor, ER-vesicle protein of 14 kD (Erv14) binds to both its client cargos and Sec24 to facilitate cargo incorporation into vesicles for ER exit (Herzig et al., 2012; Pagant et al., 2015; Powers and Barlowe, 2002). It has only recently been shown that COPII coat components have additional functions such as contributing to the biogenesis of autophagosomes (Davis and Ferro-Novick, 2015; Ge et al., 2014; Wang et al., 2014).

Here, we report that perinuclear ER membrane association of BMV 1a requires Erv14, which interacts and colocalizes with BMV 1a. Deletion of *ERV14* disrupts proper distribution of BMV 1a, leads to the formation of BMV spherules that are less abundant in number but larger in size, and significantly inhibits BMV RNA replication. We further demonstrate that the ability of Erv14 to bind to cargos and to COPII vesicles is required for the perinuclear ER localization of BMV 1a. In addition, three COPII coat proteins, Sec13, Sec24, and Sec31, are also required for proper BMV 1a distribution. Our data, therefore, suggest an unrecognized function for COPII components in targeting a viral replication protein to the perinuclear ER membrane, in sharp contrast to their canonical role in cargo exit from ER membranes.

## 2.3 Results

### 2.3.1 A high-content screen identifies host factors involved in BMV 1a localization

To identify host factors that colocalize with BMV 1a and might, therefore, have a role in its recruitment to the perinuclear ER, we screened a yeast GFP (green fluorescent protein)-tagged library (Huh et al., 2003). The mCherry-tagged version of BMV 1a (BMV 1a-mC) used for the screen localized primarily at the perinuclear ER membrane (Figure 2.1A, upper panels), similar to BMV 1a without a tag (Wang et al., 2005). Using automated mating approaches (Cohen and Schuldiner, 2011), we then integrated BMV 1a-mC into the GFP-tagged library and imaged all resulting strains using a high-throughput microscopy platform (Breker et al., 2013).

Table 2.1 lists the 17 candidate hits identified in the screen. Among them, choline-requiring 2 (Cho2) has been shown to be enriched at the perinuclear ER and to colocalize with BMV 1a during BMV replication (Zhang et al., 2016), validating our approach. Three hits (Ncw2, Cwp2, and Fit2) were discarded as they were mislocalized due to the GFP tag at the C-terminus. Interestingly, two of the hits were enzymes involved in ergosterol synthesis, Erg3 and Erg24 (Mo and Bard, 2005). Remarkably, eight of the hits were nuclear pore complex (NPC) proteins (Pom33, Ndc1, Nup2, Nup85, Nup100, Nup145, Nup157, and Nup159), suggesting that spherules form near NPCs. Two additional hits were Kre1 and Gpi11, both important for cell wall formation (Boone et al., 1991; Taron et al., 2000). The final hit, Erv14, posed a conundrum. As a cargo receptor, Erv14 is known to facilitate ER exit of more than 20 cargo proteins that are membrane proteins with a long transmembrane

domain (TMD) (Herzig et al., 2012; Pagant et al., 2015; Powers and Barlowe, 2002). However, in contrast to the role of Erv14 in facilitating client cargos for ER exit, BMV 1a remains in ER membranes without evidence suggesting its exit from the ER (Schwartz et al., 2002).

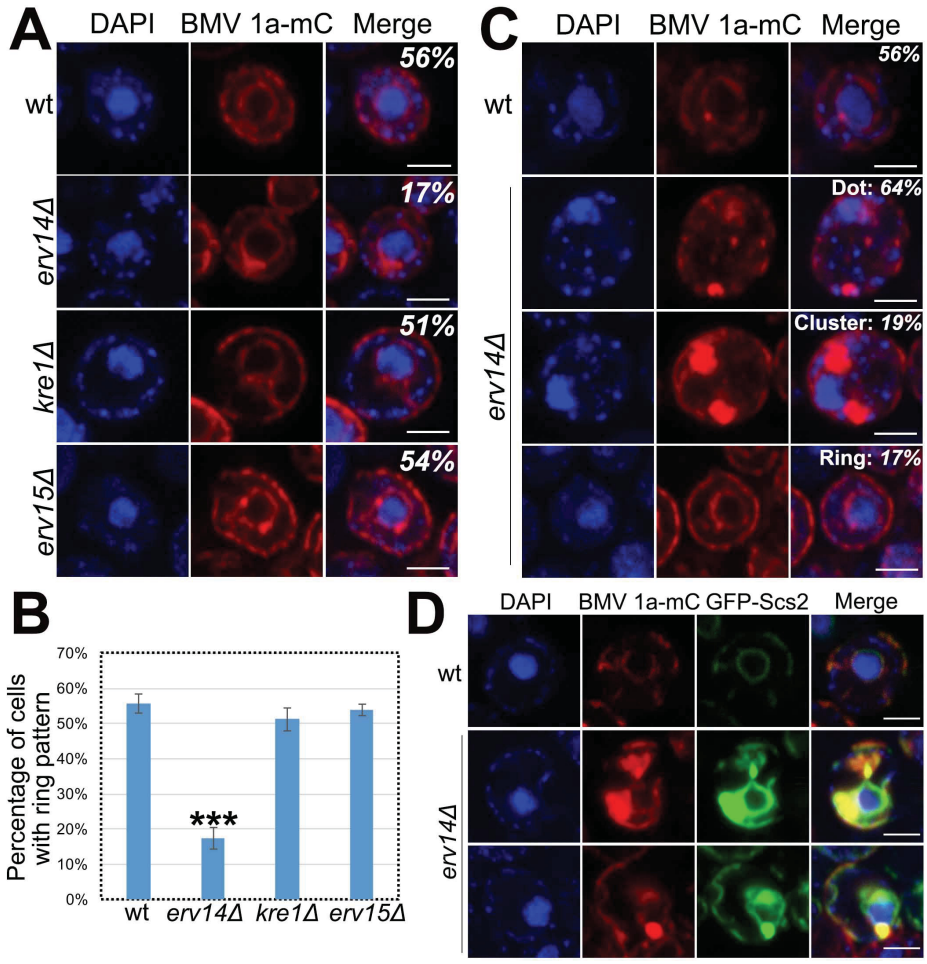


**Figure 2.1. Host Erv14 is required for the perinuclear ER localization of BMV 1a-mC in yeast.** **(A)** Confocal microscopy images of BMV 1a-mC in wild-type (wt) or selected deletion mutant cells. The ring localization pattern, which indicates the localization of BMV 1a at the perinuclear ER membrane, was the most common (>50% cell population) in wt (n=723), *kre1Δ* (n=459), and *erv15Δ* (n=760) cells with BMV 1a-mC signal. The percentage of cells with the ring pattern is shown. **(B)** Percentage of cells with the BMV 1a-mC ring pattern in the wt, *erv14Δ*, *kre1Δ*, and *erv15Δ* cells analyzed in A. Results are mean±s.d. ***$P$<0.001 (ANOVA single factor analysis of percentage of the deletion mutant cells with BMV 1a-mC ring localization rate as compared to that in wt). **(C)** BMV 1a-mC distribution in wt (n=723) and *erv14Δ* (n=1255) cells. The percentage of cells with a ring, dot,

or cluster localization pattern is shown. **(D)** Dot and cluster structures colocalize with the ER membrane marker GFP-Scs2 in *erv14Δ* cells. Nuclei were stained with DAPI (blue). Scale bars: 2 μm.

**Table 2.1. The hit list of yeast GFP-tagged library screening**

| Open reading frame | Gene Name | Essential gene |
|---|---|---|
| YGR157W | *CHO2* | No |
| YLR194C | *NCW2* | No |
| YKL096W-A | *CWP2* | No |
| YOR382W | *FIT2* | No |
| YLR056W | *ERG3* | No |
| YNL280C | *ERG24* | No |
| YLR335W | *NUP2* | No |
| YJR042W | *NUP85* | Yes |
| YKL068W | *NUP100* | No |
| YGL092W | *NUP145* | Yes |
| YER105C | *NUP157* | No |
| YIL115C | *NUP159* | Yes |
| YLL023C | *POM33* | No |
| YML031W | *NDC1* | Yes |
| YNL322C | *KRE1* | No |
| YDR302W | *GPI11* | Yes |
| YGL054C | *ERV14* | No |

### 2.3.2 Deleting *ERV14* disrupts perinuclear ER localization of BMV 1a

To assess whether any of the candidate proteins has a role in determining the localization of BMV 1a, we checked the localization of BMV 1a-mC by performing epifluorescence and confocal fluorescence microscopy in yeast strains lacking the individual candidate genes for those that are non-essential (Table 2.1). A ring localization pattern indicating perinuclear ER distribution of BMV 1a-mC was observed in ~50 to 56% of the wild-type (wt) cell population showing the mCherry signal. A similar pattern was found in many deletion mutants, as illustrated for Kre1 (Figure 2.1A). Surprisingly, the ring pattern was only observed in 17% of *ERV14* deletion (*erv14Δ*) cells, a statistically significant reduction ($P<0.001$, Figure 2.1B).

*ERV14* has a paralog, *ERV15*, whose deletion did not affect localization of BMV 1a (Figure 2.1A, B).

Three major localization patterns of BMV 1a-mC were observed in *erv14Δ* cells: ~64% of cells had punctate dots and ~19% of cells had clusters, whereas only ~17% of cells had a ring structure (Figure 2.1C). It should be noted that the percentage of each pattern varied among experiments, however, in all cases the percentage of cells with a ring pattern was significantly less than those with cluster and dot patterns. These differences might be related to the growing stage at which cells were harvested, BMV 1a-mC expression levels and/or minor differences in growth conditions, among others. To eliminate the possibility that the altered distribution was due to the addition of the mCherry tag to BMV 1a, we repeated the experiments using a Histidine6-tagged version of BMV 1a (BMV 1a-His6). About 70% of wt cells expressing BMV 1a-His6 had a ring structure in the perinuclear ER (Figure 2.2). Similar to with BMV 1a-mC, in *erv14Δ* cells BMV 1a-His6 was predominantly found as dots (65%) with only 3% as clusters (Figure 2.2). About 32% of *erv14Δ* cells had the ring structure, a statistically significant reduction ($P<0.001$).

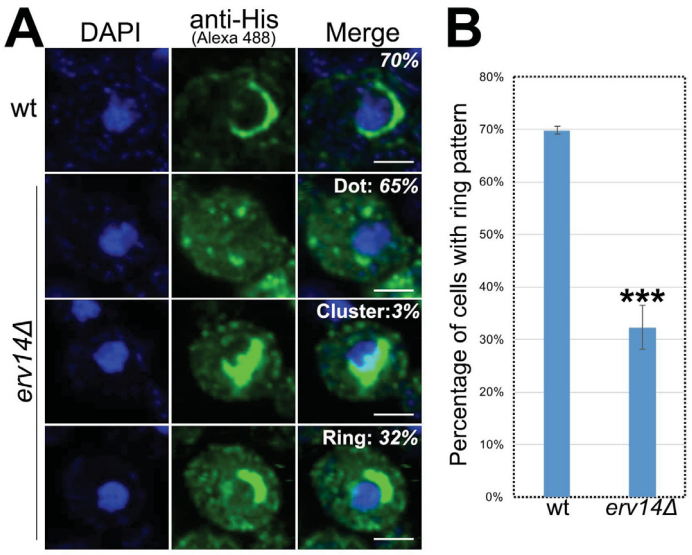


**Figure 2.2. Erv14 is required for the perinuclear ER localization of BMV 1a-His6 in yeast.**

**(A)** Immunofluorescence (IF) images of BMV 1a-His6 distribution in wt (n=947) and *erv14Δ* (n=1,115) cells. BMV 1a-His6 was detected by using an anti-His mAb and anti-mouse secondary antibody conjugated to Alexa Fluor 488. Percentage of cells with each specific localization pattern is shown. The nucleus was stained with DAPI (blue). Scale bars: 2 μm. **(B)** Percentage of cells with the ring pattern of BMV 1a-His6 in wt and *erv14Δ* cells. ANOVA single factor analysis of BMV 1a-His6 ring pattern rate in *erv14Δ* compared to that in wt, ***$P<0.001$ and error bars represent the standard deviation.

To determine the nature of the dot and cluster structures, we co-expressed BMV 1a-mC with ER, Golgi, and inclusion bodies markers. The dot and cluster structures did not colocalize with the Golgi marker plasma membrane ATPase related 1 (Pmr1) (Antebi and Fink, 1992) in *erv14Δ* cells (Figure 2.3, n=100). However, the inclusion body marker von Hippel-Lindau (VHL) protein (Kaganovich et al., 2008) colocalized with a fraction of clusters or dots in 44 out of 100 *erv14Δ* cells (Figure 2.3). In contrast, the ER membrane marker suppressor of choline sensitivity 2 (Scs2) (Manford et al., 2012) associated with the majority of disrupted BMV 1a-mC structures in most *erv14Δ* cells (97 out of 100 counted cells, Figure 2.1D). It should be noted that BMV 1a-mC colocalized with Scs2 primarily in

the perinuclear ER membrane in wt cells (Figure 2.1D, upper panels). These data suggest that deleting *ERV14* might not affect the ER membrane association of BMV 1a but rather its enrichment to the perinuclear ER membrane.

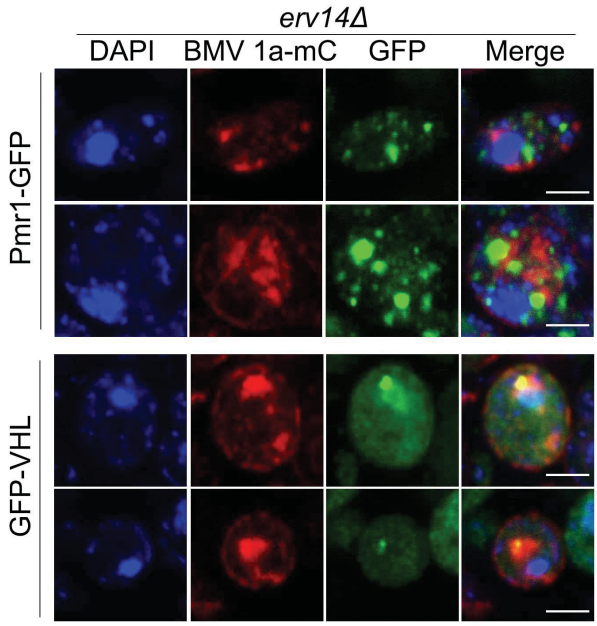


**Figure 2.3. Disrupted BMV 1a-mC structures partially colocalize with an inclusion body marker but not with a Golgi marker in *erv14*Δ cells.**

Confocal images of *erv14Δ* cells co-expressing BMV 1a-mC and a Golgi marker Pmr1-GFP or an inclusion body marker GFP-VHL. The disrupted BMV 1a-mC structures did not colocalize with Pmr1-GFP but, instead, partially colocalized with GFP-VHL in *erv14*Δ cells. Note: GFP-VHL colocalizing with some but not all disrupted structures in each cell counted as colocalization. The nucleus was stained with DAPI (blue). Scale bars: 2 μm.

### 2.3.3 Deleting *ERV14* affects spherule formation and genomic replication of BMV

We next examined the effects of deleting *ERV14* on BMV spherule formation and genomic replication, both of which normally occur on perinuclear ER membranes (Schwartz et al., 2002). Expression of BMV 1a in yeast induces the formation of spherules by invaginating the outer perinuclear ER membrane into the ER lumen. No spherules were found in wt and *erv14Δ* cells in the absence of BMV 1a as assessed with transmission

electron microscopy (Figure 2.4A). Agreeing well with prior results (Zhang et al., 2012; Zhang et al., 2016), in wt cells there were 7.2 ± 1.6 spherules per cell section with an average diameter of 74.3 ± 24.8 nm (mean ± s.d.; n=122). In *erv14Δ* cells, the average number of spherules per cell section decreased to 3.0 ± 1.3 (n=67). Intriguingly, we observed two spherule populations in *erv14Δ* cells, the first group had an average diameter similar to that in wt cells while the diameter of the second group was larger than that of wt spherules, resulting an average size of 95.2 ± 36.1 nm, a 28% increase over those of wt (Figure 2.4B).

We next measured BMV genomic RNA replication in *erv14Δ* cells expressing BMV 1a, $2a^{pol}$, and a genomic RNA3 transcript, all of which were expressed from plasmids. Deleting *ERV14* reduced BMV RNA replication by ~threefold (Figure 2.4C) based on the accumulation of positive-strand RNA4 and negative-strand RNA3 molecules, which are only produced during BMV replication. Accumulation of BMV 1a was not significantly affected by deleting *ERV14* (Figure 2.4D), eliminating the possibility that the decrease in spherule numbers and genomic replication was due to effects on BMV 1a expression and/or stability.

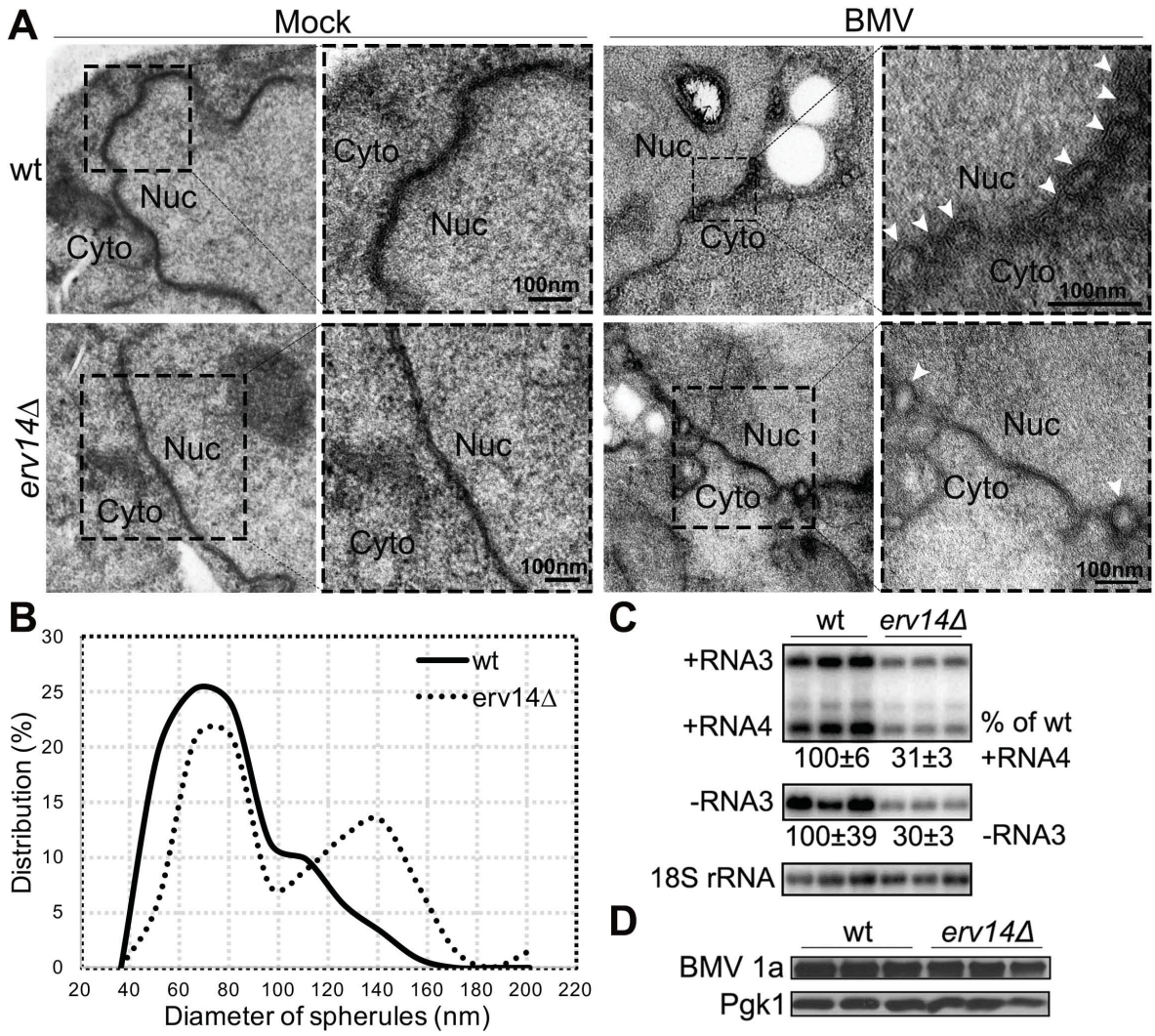


**Figure 2.4. Deleting *ERV14* affects the morphology of BMV spherules and inhibits BMV RNA replication.**

**(A)** Electron micrographs of wt and *erv14*Δ cells in the absence (Mock) or presence of BMV replication (BMV). Nuc: nucleus; Cyto: cytoplasm. Arrowheads point out spherules. **(B)** Distribution of spherule sizes in both wt and *erv14Δ* cells. Two groups of spherules with different sizes were observed in *erv14Δ* cells: the diameter of the first population was similar to that in wt cells while the diameter of the second population was larger. Sixty-seven spherules were examined. **(C)** BMV RNA replication was inhibited in *erv14Δ* cells. BMV positive- or negative-strand RNA was detected by $^{32}$P-labeled BMV strand-specific probes. 18S rRNA was detected using an 18S rRNA specific probe to serve as a loading control. The value given are mean±s.d. for three experiments. **(D)** Accumulated BMV 1a levels in wt and *erv14Δ* cells. Anti-BMV 1a antiserum was used to detect BMV 1a. Pgk1 served as a loading control. A representative blot is shown.

### 2.3.4 The perinuclear ER localization of BMV 1a-mC requires the canonical function of Erv14

We hypothesized that Erv14 might simply serve as an attachment factor for BMV 1a given that Erv14 is primarily detected at the perinuclear ER membrane (Pagant et al., 2015). Alternatively, or additionally, Erv14 might be required to facilitate the distribution of BMV 1a through its association with COPII vesicles. To verify which of the above possibilities was correct, we checked the localizations of BMV 1a-mC in *erv14Δ* cells co-expressing one of two Erv14 mutants that retain the perinuclear ER localization but block the ability of Erv14 to bridge cargos to COPII vesicles (Pagant et al., 2015). With three predicted TMDs, Erv14 contains an N-terminal cytoplasmic domain, an ER lumen loop, a cytoplasmic loop and a C-terminal ER lumen tail (Figure 2.5A) (Pagant et al., 2015; Powers and Barlowe, 2002). Mutations in the second TMD at amino acids 62 and 63 ($Erv14^{62\text{-}63A}$) block Erv14 from binding to its client cargos whereas mutations in the cytoplasmic loop at amino acids 97-101 ($Erv14^{97\text{-}101A}$) prevent Erv14 from binding to Sec24, and thus, COPII vesicles (Pagant et al., 2015; Powers and Barlowe, 2002) (Figure 2.5A). As such, cargos are retained at the ER and are not transported to their final destinations. The two *Erv14* mutants were expressed under control of the endogenous promoter from a low-copy-number plasmid. In *erv14Δ* cells with an empty vector, BMV 1a-mC displayed a ring localization pattern in ~23% of cells (Figure 2.5B). Expressing wt Erv14 increased the number of cells with a normal distribution to 63%, close to a threefold increase. However, neither of the Erv14 mutants complemented the defective distribution of BMV 1a-mC as the percentage of cells with a ring pattern was close

to that in cells expressing an empty plasmid (Figure 2.5B). The inability of Erv14 mutants to restore the localization of BMV 1a-mC was not due to its instability, as both accumulated to similar levels as the wt protein (Figure 2.5C) (Pagant et al., 2015). These data suggest that the canonical function of Erv14 in the COPII pathway is required for the perinuclear ER localization of BMV 1a.

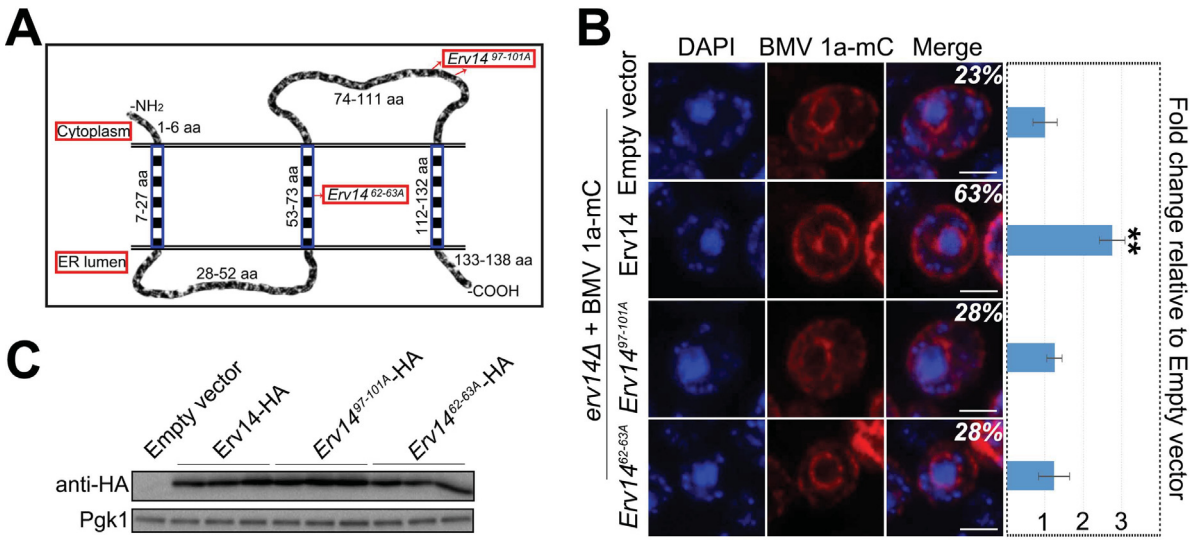


**Figure 2.5. BMV 1a perinuclear ER localization requires the ability of Erv14 to bind to cargos and COPII vesicles.**

**(A)** Illustration of the predicted Erv14 structure. The red arrows indicate mutation at amino acids 62-63 and 97-101, which block binding of Erv14 to its client cargo and to Sec24, respectively. **(B)** The percentage of *erv14Δ* cells displaying the ring pattern when BMV 1a-mC was co-expressed with an empty vector (n=717), or with plasmids expressing HA-tagged Erv14 (n=682), $Erv14^{97\text{-}101A}$ (n=683) or $Erv14^{62\text{-}63A}$ (n=549). Representative images of the BMV 1a-mC ring pattern are shown. Results are mean±s.d. $^{**}P<0.01$ (ANOVA single factor analysis as in Figure 2.1). Scale bars: 2 μm. **(C)** Accumulated Erv14, $Erv14^{97\text{-}101A}$ or $Erv14^{62\text{-}63A}$ levels in *erv14Δ* cells. Total proteins from equal numbers of cells were separated by SDS-PAGE. Erv14 proteins were expressed under the control of *ERV14* promoter from a centrameric plasmid and were detected using an anti-HA pAb in western blotting. Pgk1 served as a loading control. A representative blot is shown.

### 2.3.5 BMV 1a interacts with Erv14

To test whether Erv14 binds to BMV 1a and thus, whether the effect of *ERV14* deletion on the localization of BMV 1a was direct, we co-expressed a HA-tagged version of Erv14 (Erv14-HA) with BMV 1a-mC in *erv14Δ* cells. Erv14-HA colocalized with BMV 1a-mC at the perinuclear ER in 47% of cells, a twofold increase over those with an empty vector (16%) (Figure 2.6A). Interestingly, BMV 1a-mC dots were predominant when Erv14-HA failed to associate with the perinuclear ER (Figure 2.6A). Although the reason for why Erv14 fails to localize to the perinuclear ER is unclear, this tight dependence again suggests a direct relationship between the two proteins.

To demonstrate that BMV 1a interacts with Erv14, we first used a mating-based split ubiquitin system (mbSUS), which detects protein-protein interactions in their native environment (Obrdlik et al., 2004). We used BMV 1a self-interaction as a positive control, as it is known to self-interact (O'Reilly et al., 1997) and form oligomers (Diaz et al., 2012). Indeed, when BMV 1a was used as bait, it interacted with itself but not with two other proteins, acyl-CoA binding 1 (Acb1) and acetyl-coA carboxylase 1 (Acc1) (Figure 2.6B). Moreover, when Erv14 served as bait, it did not interact with Acb1 and Acc1. Erv14 and BMV 1a interacted regardless of which protein was used as a bait or prey (Figure 2.6B). In addition, we found that Erv14 interacted with itself (Figure 2.6B). However, the biological significance of the self-interaction of Erv14 to its cellular function and the distribution of BMV 1a is currently unknown.

To verify the BMV 1a-Erv14 interaction, we next performed an *in situ* proximity ligation

assay (PLA), which we recently used to confirm the interaction between BMV 1a and the host protein Cho2 (Zhang et al., 2016). In PLA, a monoclonal antibody (mAb) and a polyclonal antibody (pAb) that recognize each component of the protein pair is incubated with fixed spheroplasts (yeast cells without cell wall). If the two proteins are close together (<30 nm), a fluorescent dye will be deposited after performing PLA (Soderberg et al., 2006). Positive PLA signals surrounding the nucleus were detected in cells expressing the pair of BMV 1a-His6 and BMV 1a-HA, which served as a positive control (Figure 2.6D). The pair of BMV 1a-His6 and dolichol phosphate mannose synthase1 (Dpm1) was included as a negative control. No PLA signal was detected when cells were incubated with anti-BMV 1a antiserum and an anti-Dpm1 mAb (to detect endogenously expressed Dpm1), even though both proteins colocalized at the perinuclear ER membrane (Figure 2.6C). In addition, PLA signals were never identified in cells expressing only Erv14-HA (Figure 2.6D). In cells co-expressing BMV 1a-His6 and Erv14-HA, PLA dots were observed near the nucleus when an anti-His mAb and an anti-HA pAb were used, suggesting an interaction between BMV 1a and Erv14.

We also performed a co-immunoprecipitation assay to confirm the interaction. Given that the interaction of Erv14 with its cargos, for example axial 2 bud site selection (Axl2), is transient (Powers and Barlowe, 2002), we crosslinked samples with 1% formaldehyde and used plasmid-borne Dpm1-HA to control for non-specific crosslinking in the co-immunoprecipitation (Zhang et al., 2016). BMV 1a-His6 consistently pulled down Erv14-HA when an anti-His antibody was used in the co-immunoprecipitation assay in both wt and

*erv14Δ* cells (Figure 2.6E). By contrast, Dpm1-HA was not pulled down under the same conditions (Figure 2.6E), verifying a specific interaction between BMV 1a and Erv14. However, we did not detect BMV 1a-His6 after crosslinking and pulling down Erv14-HA.

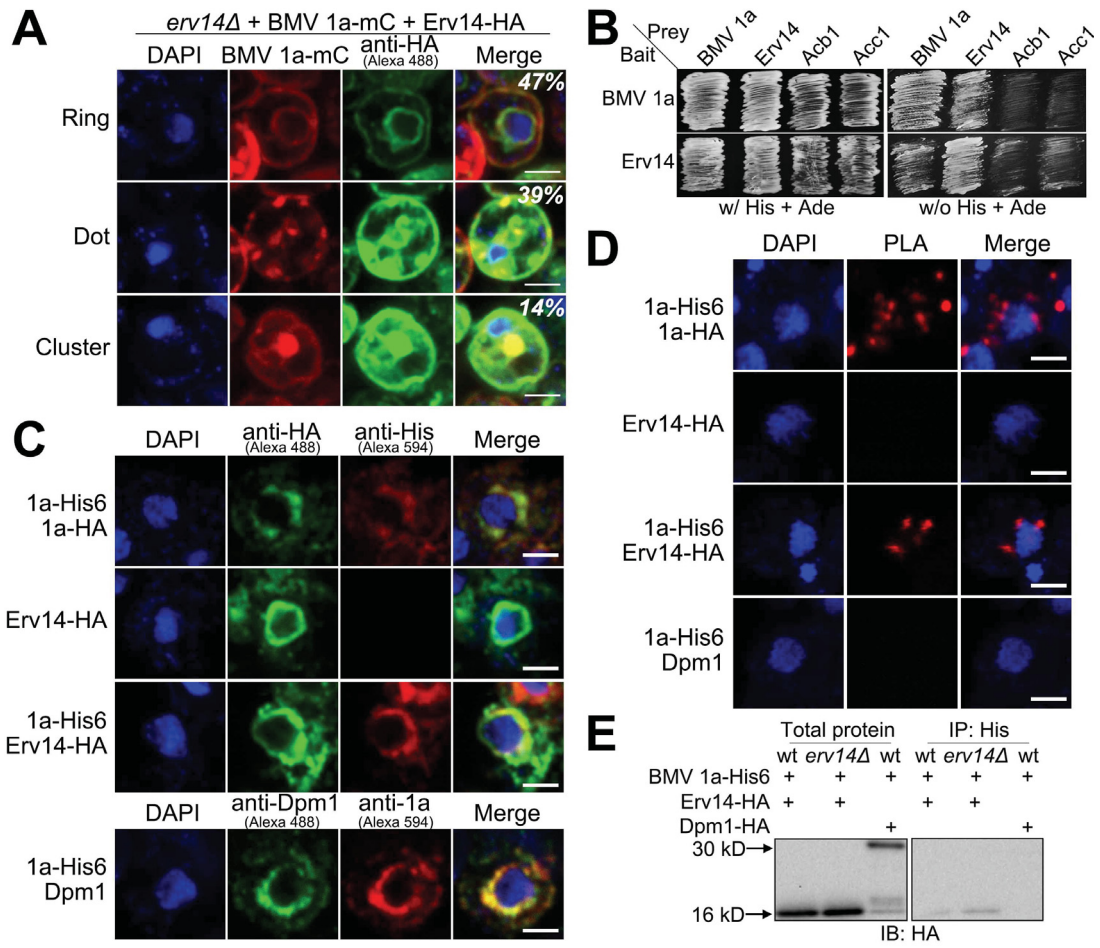


**Figure 2.6. BMV 1a interacts with Erv14.**

**(A)** Images of *erv14Δ* cells expressing BMV 1a-mC and Erv14-HA. The percentage of cells displaying the various BMV 1a-mC localization patterns is shown (n=1062). Erv14-HA was detected by using an anti-HA pAb and immunofluorescence microscopy. **(B)** The interaction between BMV 1a and Erv14 as assayed in the mating-based split ubiquitin system (mbSUS). BMV 1a self-interaction served as a positive control, the pairs of BMV 1a and Acb1 or Acc1 served as negative controls. Diploid cells expressing a pair of target genes were grown on medium supplemented with (w/) or without (w/o) histidine (His) and adenine (Ade). **(C)** Immunofluorescence images of wt cells co-expressing BMV 1a-His6 and BMV 1a-HA (top), or *erv14*Δ cells expressing Erv14-HA only (second row), or BMV 1a-His6 and Erv14-HA (third and fourth rows). BMV 1a-HA, Erv14-HA and BMV 1a-His6 were detected by using an anti-HA pAb or an anti-His mAb as primary antibodies. In the fourth

row, BMV 1a-His6 and endogenous Dpm1 were detected using anti-BMV 1a antiserum and an anti-Dpm1 mAb, respectively. **(D)** Proximity ligation assay (PLA) signal (red) was detected using the same primary antibody combinations as in C: anti-His mAb and anti-HA pAb in cells co-expressing BMV 1a-His6 and BMV 1a-HA (positive control), or BMV 1a-His6 and Erv14-HA. Erv14-HA only or the pair of BMV 1a-His6 and Dpm1 served as negative controls. **(E)** Erv14-HA co-immunoprecipitates with BMV 1a-His6. Cells expressing BMV 1a-His6 and Erv14-HA or Dpm1-HA were lysed, subjected to immunoprecipitation with an anti-His (IP: His) mAb, separated by SDS-PAGE and subjected to western blotting with an anti-HA pAb (IB: HA). Dpm1-HA served as a negative control. Representative results are shown. Scale bars: 2 μm.

### 2.3.6 BMV 1a-mC behaves like an Erv14-dependent cargo

The role of Erv14 as a cargo receptor is to help recruit cargo that weakly binds to Sec24 on its own or cannot bind directly at all. Cargos with either a DxE (x as any amino acid) or LASLE sorting signal can bind directly to Sec24 (Mossessova et al., 2003; Votsmeier and Gallwitz, 2001). It has been shown that the addition of DLE motif to mating pheromone-induced death 2 (Mid2), an Erv14-dependent cargo, facilitated Mid2-DLE ER exit in *erv14Δ* cells (Herzig et al., 2012). If the role of Erv14 in BMV 1a localization is mediated through COPII vesicles, its deletion should be bypassed by the addition of a sorting signal at the C-terminus of BMV 1a-mC. We, therefore, added either DLE or LASLE (Figure 2.7A) to BMV 1a-mC. We also included an 8-amino acid linker (GDGAGLIN) between BMV 1a-mC and the sorting signal to increase the accessibility of DLE or LASLE by Sec24. Addition of either DLE or LASLE significantly increased the localization of BMV 1a-mC at the perinuclear ER membrane, increasing the percentage of *erv14Δ* cells with a ring structure from 15% to 32% or 42%, respectively (Figure 2.7B). Inclusion of the linker, however, did not have a significant effect (Figure 2.7A, B).

Given that receptor-dependent cargos have been shown to weakly bind Sec24, the failed ER exit of cargos can be rescued by overexpressing Sec24 in cells lacking the cargo receptor. For example, overexpression of Sec24 promotes ER exit of yeast oligomycin resistance 1 (Yor1), an Erv14-dependent cargo, in *erv14Δ* cells (Pagant et al., 2015). We found that in ~44% of *erv14Δ* cells, BMV 1a-mC properly localized to the perinuclear ER when Sec24 was overexpressed, in sharp contrast to ~15% of cells expressing an empty vector (Figure 2.7C). This result supports a role for Sec24 in targeting BMV 1a to the perinuclear ER along with Erv14.

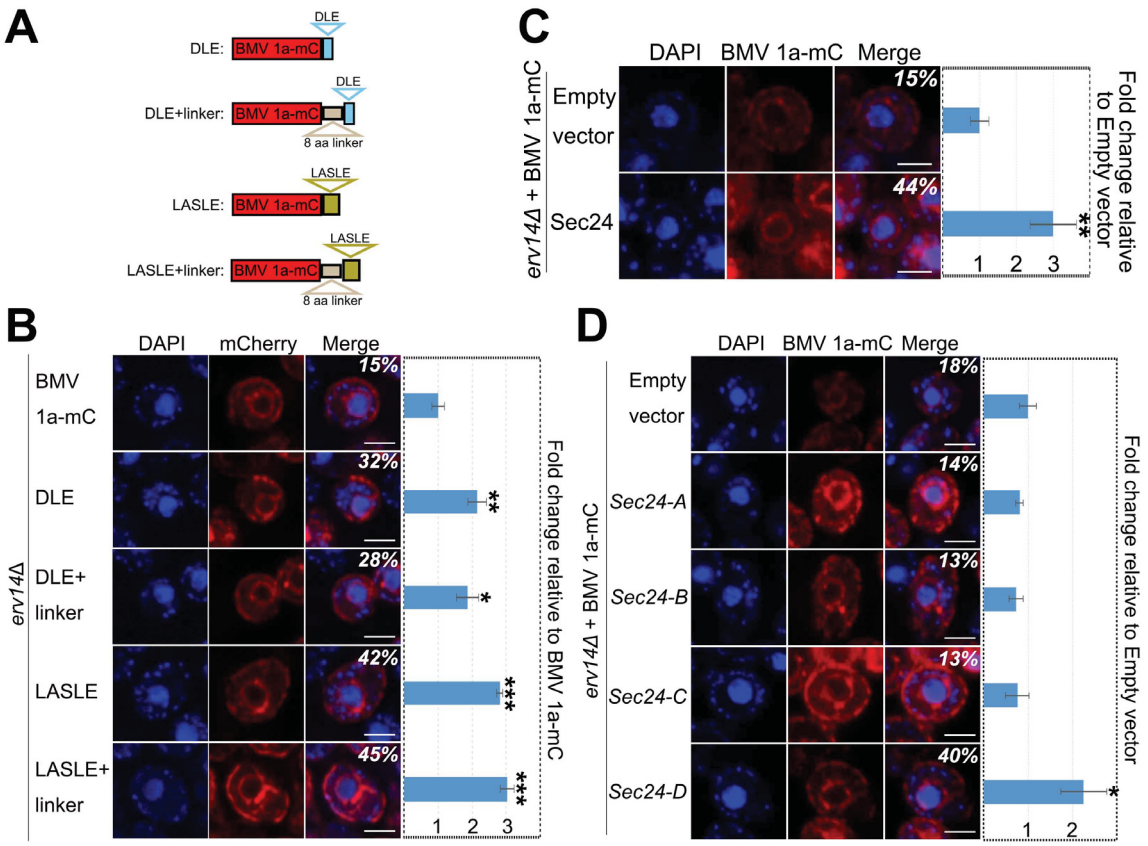


**Figure 2.7. Sec24 is involved in targeting BMV 1a-mC to the perinuclear ER membrane.**

**(A)** Diagram of various BMV 1a-mC derivatives fused to a DLE or LASLE sorting signal. An 8-amino-acid linker (GDGAGLIN) was inserted between BMV 1a-mC and DLE or LASLE in two vectors. **(B-D)** Percentage of cells showing the ring pattern in *erv14*Δ cells expressing BMV 1a-mC (n=1119), BMV 1a-mC-DLE (n=1152), -DLE+linker (n=988), -LASLE (n=1059), or -LASLE+linker

(n=962) in **(B)**, empty vector (n=1229) or wt Sec24 (n=1400) in **(C)**, empty vector (n=1810), *Sec24-A* (n=1521), *Sec24-B* (n=1558), *Sec24-C* (n=1945), or *Sec24-D* (n=2093) in **(D)**. Representative images of cells expressing with a ring pattern are shown. Results are mean±s.d. **P*<0.05, ***P*<0.01, ****P*<0.001. (ANOVA single factor analysis as in Figure 2.1). Scale bars: 2 μm.

Sec24 has four binding sites that enable it to recognize various sorting signals present in different groups of cargos (Miller et al., 2003; Pagant et al., 2015). The A site recognizes the sorting signal YNNSNPF of Sed5; the B site binds to the sorting signal DxE or LASLE; the C site binds to Sec22; and the D site binds to Erv14 (Mossessova et al., 2003; Pagant et al., 2015). To examine which binding site(s) might play a crucial role in the perinuclear ER localization of BMV 1a, we overexpressed Sec24 with mutations in each site, denoted *Sec24-A*, *Sec24-B*, *Sec24-C* or *Sec24-D*. Overexpression of the *Sec24-D* mutant largely reversed the defective localization BMV 1a-mC in *erv14Δ* cells (Figure 2.7D). It should be noted that this result does not suggest that the D site is not important for BMV 1a distribution, rather, it is consistent with the fact that the Sec24 D site binds to Erv14 (Pagant et al., 2015). However, overexpressing the *Sec24-A*, *Sec24-B* or *Sec24-C* mutant did not improve BMV 1a-mC distribution in *erv14Δ* cells, suggesting that all three binding sites play an important role in the localization of BMV 1a and might be responsible for its proper localization in the 17% of *erv14Δ* cells with the ring pattern (Figure 2.1).

### 2.3.7 COPII coat proteins are required for the perinuclear ER localization of BMV 1a-mC

Given that both Erv14 and Sec24 were involved in the perinuclear ER association of BMV 1a-mC, we wondered whether other COPII coat subunits were also involved in

maintaining the normal distribution of BMV 1a. To this end, we checked BMV 1a-mC distribution in COPII temperature-sensitive (*ts*) strains of the four COPII coat subunits: *sec23-1*, *sec24*, *sec13-1*, and *sec31-1*. We also tested a *ts* mutant of Sec12, which activates and recruits Sar1 to the ER to initiate the COPII vesicle assembly (D'Arcangelo et al., 2013; Lord et al., 2013). BMV 1a-mC was expressed in all *ts* mutants under both permissive (23°C) and restrictive temperatures (30°C and 37°C) and its distribution was determined. Surprisingly, BMV 1a-mC was localized correctly at the perinuclear ER in *sec12-4* and *sec23-1,* even after the strains were incubated at non-permissive temperatures for 2 hours (Figure 2.8 for 37°C). To verify that these mutations completely blocked the function of these proteins (as would be expected due to their lethality at the restrictive temperature), we monitored ER exit of cell division cycle 50 (Cdc50), an Erv14-dependent cargo (Herzig et al., 2012; Pagant et al., 2015). Although Cdc50-HA localized to the Golgi at 23°C in *sec23-1* cells, it was retained in ER membranes at 37°C (Figure 2.9), indicating an inhibition of ER exit in the *sec23-1* mutant and confirming that Sec23 is not required for proper BMV 1a localization. Strikingly, BMV 1a-mC was mislocalized in more than 95% of *sec24* and *sec13-1* mutant cells at 37°C for 2 h (Figure 2.8). The distributions of BMV 1a-mC in these mutants, however, were different. In *sec24* cells there was one or two punctate dots, whereas larger aggregates were detected in *sec13-1* cells (Figure 2.8A). In addition, in the *sec31-1* mutant, less than 30% of cells had a ring pattern ($P<0.01$, Figure 2.8B). Collectively, these results suggest that Sec13, Sec24, and Sec31 are required for the proper localization of BMV 1a-mC.

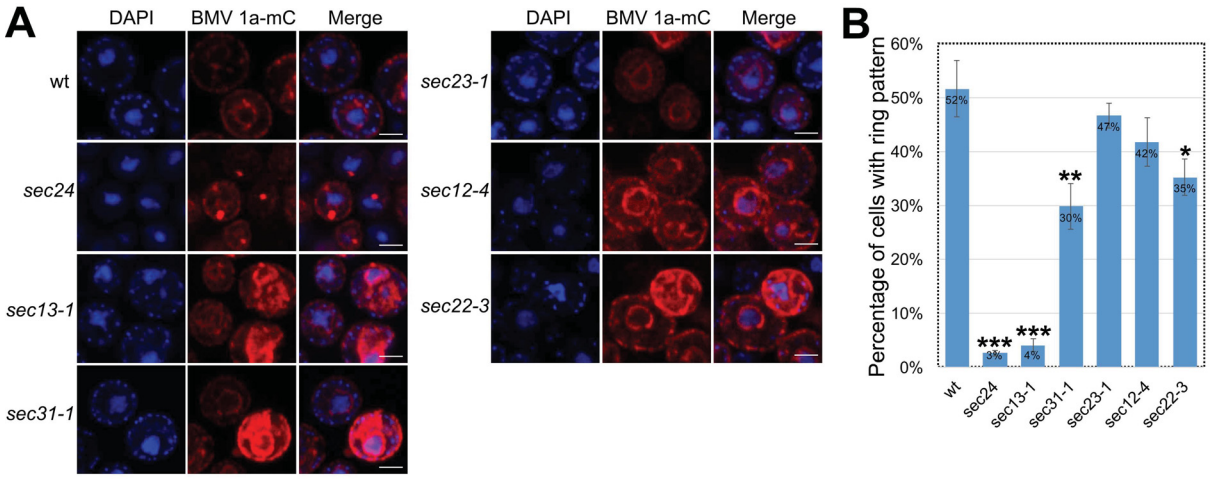


**Figure 2.8. Localization of BMV 1a-mC in mutants with dysfunctional COPII components.**

**(A)** Distribution of BMV 1a-mC in wt and COPII temperature-sensitive mutants after incubating cells at 37°C for 2 h. Representative images of the major localization patterns for BMV 1a-mC are shown. Scale bars: 2 μm. **(B)** Percentage of cells with a ring pattern in wt and each mutant at 37°C for 2 h. Total valid number of cells analyzed for each strain: wt (n=746), *sec24* (n=919), *sec13-1* (n=1163), *sec31-1* (n=776), *sec23-1* (n=713), *sec12-4* (n=965) and *sec22-3* (n=842). Results are mean±s.d. **P*<0.05, ***P*<0.01, ****P*<0.001 (ANOVA single factor analysis as in Figure 2.1).

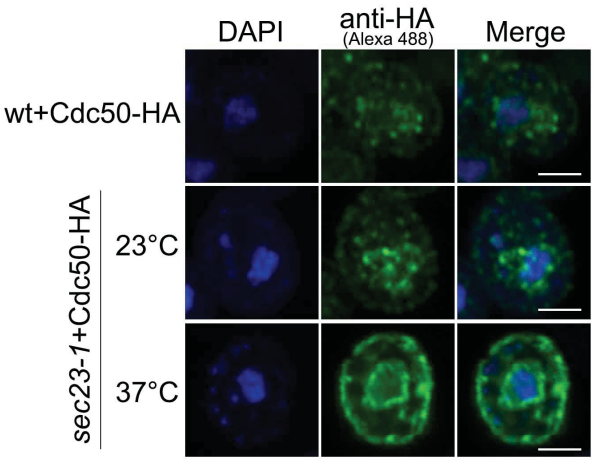


**Figure 2.9. ER exit of Erv14-dependent cargo Cdc50 is blocked in *sec23-1* cells at non-permissive temperature.**

IF images of HA-tagged Cdc50 (green) in wt or *sec23-1* cells. Erv14-dependent cargo Cdc50-HA was detected using an anti-HA pAb and anti-rabbit secondary antibody conjugated to Alexa Fluor 488. Cdc50-HA was localized at the perinuclear ER membrane in *sec23-1 ts* mutant at 37°C, but localized at the Golgi at both 23°C and 37°C in wt and at 23°C in *sec23-1* cells. The nucleus was stained with DAPI (blue). Scale bars: 2 μm.

Given that the C site in Sec24 binds to Sec22 and overexpressing *Sec24-C* failed to rescue the mis-localization phenotype for BMV 1a-mC in *erv14Δ* cells (Figure 2.7D), Sec22 could also be involved in regulating the distribution of BMV 1a (Figure 2.7D). Agreeing well with the result from the *Sec24-C* mutant, the ring pattern was observed in 35% of *sec22-3* cells when they were cultured at 37°C for 2 h, a significant reduction ($P<0.05$) from the 52% seen in wt cells.

### 2.3.8 The plant homologs of *ERV14*, Cornichons, complements the loss of Erv14 in yeast

Erv14 belongs to a conserved protein family called Cornichons (CNIs). CNIs are functionally conserved among eukaryotes, from yeast to *Drosophila* to mammals (Brandizzi and Barlowe, 2013; Dancourt and Barlowe, 2010). We first examined whether any plant CNIs could functionally complement the defective localization of BMV 1a-mC in *erv14Δ* cells. There are five CNI genes in *Arabidopsis thaliana*, referred to as CNI homologs (*AtCNIH*s): AT4G12090 (*AtCNIH1*), AT1G12340 (*AtCNIH2*), AT1G12390 (*AtCNIH3*), AT1G62880 (*AtCNIH4*), and AT3G12180 (*AtCNIH5*) (Rosas-Santiago et al., 2015). Each AtCNIH was expressed from a low-copy-number plasmid under the control of the *ERV14* endogenous promoter to achieve similar protein levels as the endogenous Erv14. BMV 1a-mC was then expressed along with each AtCNIH in *erv14Δ* cells. We found that yeast expressing *AtCNIH1*, *AtCNIH4,* and At*CNIH5* had similar percentage of cells with a ring pattern to those expressing wt Erv14 (Figure 2.10). In contrast, cells expressing *AtCNIH2* and *AtCNIH3* did not increase the percentage of cells with a ring pattern compared to the empty

plasmid (Figure 2.10). We concluded that AtCNIH1, AtCNIH4 and AtCNIH5 are functionally equivalent to Erv14 in yeast and suggest that they might contribute to BMV replication in plants.

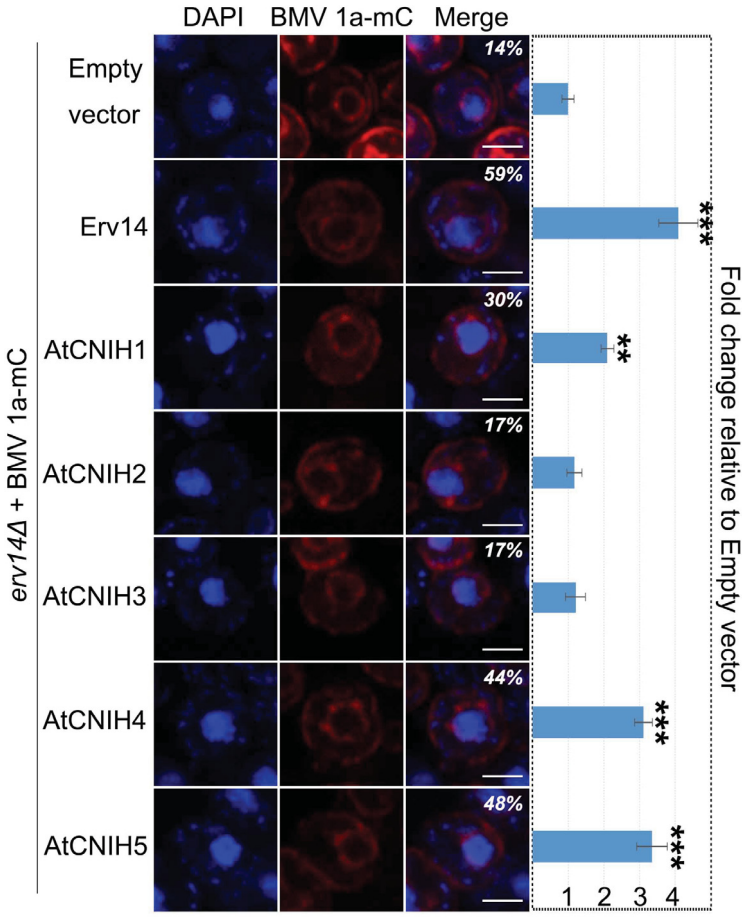


**Figure 2.10. Plant CNIs, homologs of Erv14, functionally complement the loss of Erv14 in yeast.** Percentage of cells showing a ring pattern in *erv14Δ* cells co-expressing BMV1a-mC with an empty vector (n=842), Erv14 (n=1122), AtCNIH1 (n=1023), AtCNIH2 (n=814), AtCNIH3 (n=1252), AtCNIH4 (n=1168) or AtCNIH5 (n=965). Representative images are shown. Results are mean±s.d. $^{**}P<0.01$, $^{***}P<0.001$. (ANOVA single factor analysis as in Figure 2.1). Scale bars: 2 μm.

## 2.4 Discussion

All well-studied (+)RNA viruses target their replication proteins to organelle membranes or specific membrane microdomains to initiate VRC formation. Understanding the mechanisms by which viral proteins are targeted to particular organelle membranes will

identify potential targets during the early steps of viral replication and offer insights into the development of novel antiviral strategies for virus control in humans, animals, and crops.

Previous studies have demonstrated that host factors are crucial to intracellular membrane association of viral replication proteins in plants. Tomato mosaic virus (ToMV) encodes two replication proteins, the 130K helicase-like protein and the 180K replicase. Although both proteins do not have TMDs, a pool of these proteins is associated with host membranes in VRCs (Hagiwara et al., 2003; Ishibashi et al., 2012). The host integral membrane proteins tobamovirus multiplication 1 (TOM1) and TOM3 interact with ToMV replication proteins and serve as membrane anchors for ToMV VRCs (Ishikawa et al., 1993; Yamanaka et al., 2002; Yamanaka et al., 2000). Mutating both TOM1 and TOM3 completely inhibits ToMV infection (Yamanaka et al., 2002). By contrast, the viral protein 6 kDa protein 2 ($6K_2$) of tobacco etch virus (TEV) and turnip mosaic virus (TuMV) is responsible for initiating the assembly of $6K_2$-induced vesicles ($6K_2$-vesicles). These vesicles serve as VRCs, exit ER membranes and eventually assemble into large granule structures at chloroplasts in addition to playing a possible role in cell-to-cell movement (Cheng et al., 2015; Cotton et al., 2009; Jiang et al., 2015; Wei and Wang, 2008; Wei et al., 2010). Out of the three *Arabidopsis* Sec24 isoforms (Sec24a, b, and c) (Marti et al., 2010), $6K_2$ interacts with Sec24a to assemble $6K_2$-vesicles at ER exit sites (ERES). Indeed, the systemic spread of TuMV is reduced in a Sec24a-defective *Arabidopsis* mutant (Jiang et al., 2015), and a dominant negative Sar1 mutant (H74L) blocks the formation of $6K_2$ vesicles and virus spread (Wei and Wang, 2008). Coxsackievirus B3 (CVB3), a picornavirus, also assembles its VRCs at ERES and a

dominant negative Sar1 mutant (T39N) inhibited CVB3 replication by ~50% (Hsu et al., 2010) These data collectively indicate the importance of COPII vesicles in VRC formation for viruses in the picornavirus-like superfamily, which include CVB3, TEV, and TuMV.

We report here that the perinuclear ER membrane association of BMV 1a is facilitated by the presence and canonical function of the cargo receptor Erv14 (Figures. 2.1 and 2.5). In support of Erv14 acting as a canonical cargo receptor for BMV 1a is the fact that they physically interact (Figure 2.6), that the ability of Erv14 to bind cargo and to bind Sec24 is required for proper distribution of BMV 1a-mC (Figure 2.5), and that the requirement of Erv14 for distribution of BMV 1a was bypassed by addition of a Sec24-recognizable sorting signal to BMV 1a-mC or by overexpressing Sec24 (Figure 2.7).

Our findings were surprising because BMV 1a is not a typical Erv14-dependent cargo as it lacks a long TMD. BMV 1a associates with ER membranes through an amphipathic α-helix (Liu et al., 2009). In contrast to the cargos that depend on COPII vesicles for ER exit, BMV 1a remains at the perinuclear ER and resides in the interior of spherules as a shell (Schwartz et al., 2002). BMV 1a is also not a typical Sec24-dependent cargo. For instance, overexpression of Sec24, *Sec24-A*, *Sec24-C*, or *Sec24-D* mutants, but not the *Sec24-B* mutant, support the exit of Yor1 from the ER in the absence of Erv14, as Yor1 has a sorting signal that weakly interacts with the Sec24 B site. However, with regards to perinuclear localization of BMV 1a, mutations in the Sec24 A, B, or C site inhibited the ability of Sec24 to compensate for the absence of *ERV14*, suggesting that BMV 1a might bind to multiple sites within Sec24. Given that a mutated version of Sec24 (the *sec24 ts* mutant) altered BMV

1a-mC localization from the perinuclear ER membrane to dotted structures in 97% of cells, it indicates that Sec24 plays an active role in targeting BMV 1a to the perinuclear ER (Figure 2.8).

How are Erv14 and Sec24 involved in the perinuclear ER association of BMV 1a? As Erv14 primarily localizes at the perinuclear ER membrane, one possibility is that BMV 1a is distributed to the perinuclear ER through its interaction with Erv14 (Figure 2.6). However, it should be noted that the interaction between BMV 1a and Erv14 is either weak or transient because we could only pull them down together when cells were treated with formaldehyde to cross link protein complexes (Figure 2.6E). In addition, we cannot totally rule out the possibility that BMV 1a interacts with Erv14 through a protein that binds both and serves as a bridge. Similar to other Erv14-depenent client cargos, BMV 1a requires both Erv14 and Sec24 for its targeting. One possibility is that Erv14 and Sec24 recycle BMV 1a from peripheral tubular ER to the perinuclear regions. In support of this notion is the finding that a large pool of BMV 1a-mC dot and cluster structures colocalized with an ER marker in *erv14Δ* cells (Figure 2.1D). This is also consistent with the fact that BMV 1a redistributes host reticulons from peripheral ER to the perinuclear ER through a direct interaction between BMV 1a and reticulons (Diaz et al., 2010). It is therefore possible that BMV 1a encounters reticulons at the peripheral ER tubules and redirects them to the perinuclear ER. It is also possible that BMV 1a remains at the perinuclear ER by interfering with the function of COPII vesicles for targeting itself out of the ER. However, our results are not consistent with this possibility, as the dot and cluster structures observed in *erv14Δ* cells colocalize with an

ER marker (Figure 2.1D) but not a Golgi marker (Figure 2.3). Moreover, we cannot rule out the possibility that Erv14 and Sec24 might recruit BMV 1a into COPII vesicles to enrich and facilitate the self-interaction of BMV 1a. Several host proteins, including reticulons, Snf7 and Cho2, are recruited to spherules by BMV 1a and are required for the formation of functional VRCs (Diaz et al., 2010; Diaz et al., 2015; Zhang et al., 2016). Given that spherule diameter increased, whereas the number of spherules per cell decreased, in *erv14Δ* cells (Figure 2.4), it is also likely that Erv14 and/or Sec24 participates in forming or stabilizing spherules through their connection with BMV 1a. However, this awaits further evidence.

Although Sec13 is necessary for the proper localization of BMV 1a-mC, the possible role of Sec13 is less clear. As a NPC component, Sec13 is additionally localized to perinuclear ER membranes, besides residing in ERES. It should also be noted that eight hits in our screen are NPC components (Table 2.1). It is, therefore, possible that Erv14, Sec24 and Sec13 could target or maintain BMV 1a at the perinuclear ER by delivering BMV 1a to NPCs to initiate spherule formation.

Erv14 belongs to the conserved CNI family. CNIs have been well-studied in *Drosophila* and mammalian cells (Dancourt and Barlowe, 2010). CNI was first identified in *Drosophila* and is required for the transport of Gurken (Grk), a transforming growth factor α (TGFα), from the ER to the oocyte surface (Roth et al., 1995). Among four CNI homologs (CNIHs) in mammals, CNIH2 and CNIH3 function as α-amino-3-hydroxy-5-methyl-4-isoxazole-propionic acid (AMPA) receptors for glutamatergic neurotransmission in the central nervous system (Herring et al., 2013; Jackson and Nicoll, 2009; Schwenk et al., 2009). CNIH4

interacts with both G-protein-coupled receptors (GPCRs) and Sec23 and Sec24 and, thus, acts as a cargo receptor for recruiting GPCRs into COPII vesicles and transporting them to the cell surface (Sauvageau et al., 2014). Additionally, human CNIs functionally complement the loss of Erv14 in yeast (Castro et al., 2007). However, plant CNIs have not been well-studied. Recently, a specific rice CNI has been identified as a possible cargo receptor for the sodium transporter O*s*HKT1;3 to the Golgi (Rosas-Santiago et al., 2015). Among five CNI members in *Arabidopsis*, we showed that AtCNIH1, AtCNIH4 and AtCNIH5 are functionally equivalent to Erv14 in yeast (Figure 2.10). The roles that AtCNIHs play in BMV replication in plants, however, are under further investigation.

In conclusion, we identified the cargo receptor Erv14 as a new host factor required for targeting BMV replication protein 1a to the perinuclear ER membrane, for VRC formation and genomic RNA replication. Our data are consistent with a working model that Erv14, through a direct interaction with BMV 1a, targets BMV 1a from ER membranes to, or maintains BMV 1a at, the perinuclear ER membrane, along with COPII coat components Sec24, Sec13 and Sec31. Although COPII vesicles are known for their role in anterograde protein transport from the ER to the Golgi and biogenesis of autophagosomes, our data suggest a new role for Erv14, Sec24, Sec13 and Sec31 in targeting or maintaining protein(s) at the perinuclear ER membrane.

## 2.5 Materials and methods

### 2.5.1 High-throughput yeast GFP-tagged library screening

Plasmid pB1YT3-mC, which expresses BMV 1a-mCherry, was transformed into an synthetic genetic array (SGA) compatible yeast strain (YMS140) and introduced into the yeast GFP-tagged library (Huh et al., 2003) using automated mating approaches (Cohen and Schuldiner, 2011; Herzig et al., 2012). The strains were imaged using a high-content screening platform (Breker et al., 2013) and the localization of all the GFP-tagged host proteins and BMV 1a-mC was analyzed by eye for colocalization.

### 2.5.2 Yeast strains and cell growth

Yeast strain YPH500 and its various single gene deletion derivatives were used in all experiments, unless specified otherwise. Temperature sensitive strains *sec12-4*, *sec13-1*, *sec22-3*, *sec23-1*, *sec31-1* and *sec24* were based on X2180-1A (Novick et al., 1980) or BY4741 (Li et al., 2011). All yeast cells were grown at 30°C, with the exception of *ts* strains, which were grown overnight at 23°C and sub-cultured for 2 h at 30°C or 37°C. All yeast cells were grown in defined synthetic medium containing 2% galactose as a carbon source. Leucine, uracil, histidine, or combinations thereof were omitted to maintain plasmid selection. Cells were grown in galactose medium for two passages (36 to 48 h) and harvested when the optical density at 600 nm ($OD_{600}$) was between 0.4 and 1.0.

### 2.5.3 Plasmids and plasmid construction

His6-, mCherry- or HA-tagged versions of BMV 1a were expressed from pB1YT3-cH6, -mC, or -HA, respectively. BMV 1a and $2a^{pol}$ were expressed from pB12VG1 (Kushner et al., 2003) whereas BMV RNA3 was transcribed from pB3VG128-H (Zhang et al., 2012) to launch BMV replication in yeast cells. pB1YT3-mC was used as the vector to add the COPII recognizable sorting signal DLE or LASLE (Mossessova et al., 2003; Votsmeier and Gallwitz, 2001) to the C-terminus of BMV 1a-mC by overlapping PCR. For some constructs, a linker (GDGAGLIN) was added in between BMV 1a-mC and the sorting signal. GFP-tagged Scs2 served as an ER membrane marker, GFP-tagged Pmr1 served as a Golgi marker, and GFP-tagged VHL served as an inclusion body marker. HA-tagged Erv14 mutants or *Arabidopsis* CNIHs (AtCNIHs) were expressed under the control of the *ERV14* endogenous promoter from a low-copy-number plasmid. For the mbSUS assay, target genes were either cloned into the bait vector pMetYCgate or the prey vectors pNXgate33-3HA or pXNgate21-3HA (Obrdlik et al., 2004).

### 2.5.4 Immunofluorescence confocal microscopy and proximity ligation assay

Two $OD_{600}$ units of yeast cells were harvested and fixed with 4% (v/v) formaldehyde, and the cell wall was removed by lyticase at 30°C for 1 h and permeabilized with 0.1% Triton X-100 for 15 min at room temperature. Spheroplasts were incubated with primary anti-HA pAb (Invitrogen, Cat. no. 71-5500, Lot no. 1544744A), anti-1a antiserum (Restrepo-Hartwig and Ahlquist, 1996), anti-His mAb (GeneScript, Cat. no. A00186, Lot no. 12L000548), or anti-Dpm1 mAb (Invitrogen, Cat. no. A6429, Lot no. 425998) at a 1:100 dilution overnight at

4°C, followed by a secondary antibody at 1:100 dilution for 1h at 37°C. The secondary antibodies were anti-rabbit IgG conjugated to Alexa Fluor 488 or Alexa Fluor 594 (Jackson ImmunoResearch, Cat. no. 711-545-152, Lot no. 116141 or 711-585-152, Lot no. 113078, respectively) or anti-mouse IgG conjugated to Alexa Fluor 594 or Alexa Fluor 488 (Life Technologies, Cat. no. A11020, Lot no. 1606260 or A11001, Lot no. 1397999, respectively) at 1:100 dilution. The nucleus was stained with DAPI for 10 min and samples were observed using a Zeiss LSM Scanning 880 microscope or a Zeiss epifluorescence microscope (Observer.Z1) at the Fralin microscopy facility at Virginia Tech.

PLA was performed following the standard procedure (Duolink, Sigma). Briefly, yeast spheroplasts were incubated with anti-His mAb and anti-HA pAb or anti-Dpm1 mAb and anti-1a antiserum at 1:100 dilutions overnight at 4°C, followed by a 1 h incubation at 37°C with antibodies conjugated to oligonucleotides (PLA probe Minus and Plus). After a 30-min ligation reaction and 100-min amplification reaction at 37°C, samples were stained with DAPI and observed using a Zeiss LSM Scanning 880 microscope.

### 2.5.5 Electron microscopy

Fixation, dehydration and embedding of yeast cells were performed as previously described (Zhang et al., 2012). Images were obtained using a JEOL JEM 1400 transmission electron microscope located at the Virginia-Maryland College of Veterinary Medicine, Virginia Tech.

### 2.5.6 RNA extraction and Northern blotting

Total RNA was extracted from yeast cells that were harvested at $OD_{600}$ values of 0.4 to 1.0 by a hot phenol approach (Kohrer and Domdey, 1991). Northern blotting was performed as previously described (Zhang et al., 2012). Briefly, equal amounts of total RNA were separated by agarose-formaldehyde electrophoresis and transferred to Nytran membranes. BMV positive- and negative-strand RNAs were detected using $P^{32}$-labeled probes specific to BMV RNAs. To eliminate loading variations, an 18S rRNA specific probe was used to normalize the signals. Radioactive signals were scanned by using a Typhoon FLA 7000 phosphoimager and the intensity of radioactive signals were quantified by using ImageQuant TL (GE healthcare).

### 2.5.7 Protein extraction and western blotting

Total proteins were extracted and western blotting was performed as described previously (Zhang et al., 2012). Briefly, two $OD_{600}$ units of yeast cells were harvested, broken in yeast lysis buffer (50 mM Tris-HCl pH 8.0, 10 mM $MgCl_2$, 1 mM EGTA, 2 mM EDTA pH 8, 20% Glycerol, and 15 mM KCl) containing a protein inhibitor mix (Sigma-Aldrich) at a 1:200 dilution using a bead beater. SDS lysis buffer (2% SDS, 90 mM Hepes, pH 7.5, 30 mM DTT) and loading buffer was added to the mixture and boiled for 5 min, the cell debris was removed and equal volumes of total protein extracts were loaded onto a 10% (v/v) SDS-PAGE gel, followed by the transfer of proteins to a polyvinylidene difluoride (PVDF) membrane. The membranes were incubated in anti-BMV 1a antiserum (1:10,000 dilution), anti-HA pAb (1:3000 dilution), or anti-Pgk1 mAb (1:10,000 dilution, Invitrogen, Cat. no.

459250, Lot no. C0240) primary antibodies, followed by anti-rabbit-IgG or anti-mouse-IgG secondary antibodies conjugated to horseradish peroxidase (HRP) (Thermo Scientific, Cat no. 32460, Lot no. LH148799 or 32430, Lot no. LK152904) at 1:10,000 dilution. The membranes were incubated in Supersignal West Femto substrate (Thermo Scientific) and the protein signals were detecting using X-ray film or a Bio-Rad ChemiDoc imager.

### 2.5.8 Chemical cross-linking and co-immunoprecipitation assay

Ten $OD_{600}$ units of yeast cells were harvested, resuspended in 5 ml of growth media containing 1% formaldehyde, incubated at 30°C for 10 min and quenched at 30°C for 10 min by adding glycine at a final concentration of 0.125 M. The co-immunoprecipitation assay was performed as previously described (Diaz et al., 2010). Briefly, crosslinked cells were lysed in RIPA buffer (50 mM Tris at pH 8.0, 1% Nonidet P-40, 0.1% SDS, 150 mM NaCl, 0.5% sodium deoxycholate, 5 mM EDTA, 10 mM NaF, 10 mM NaPPi, and protease inhibitor mix) by glass beads in a bead beater for 2 min and further incubated in RIPA buffer at 4°C for 2 h. Cell debris was removed and the supernatant was mixed with Protein-A-sepharose beads (GE healthcare) and anti-His mAb overnight at 4°C. Beads were washed three times with RIPA buffer, re-suspended in 1 x SDS loading buffer, and incubated at 50°C for 20 min to release the proteins. Samples were boiled for 10 min before loading onto a 10% (v/v) SDS-PAGE gel, followed by western blotting to detect target proteins using anti-HA pAb.

### 2.5.9 Statistical analysis of BMV 1a localization pattern

The percentage of cells with ring, dot and cluster localization patterns of BMV 1a was

calculated based on the total number of cells that had a visible nucleus as well as a BMV 1a-mC signal. The numbers of cells counted for each assay are shown in the figure legends. Each experiment was repeated at least three times and the percentages shown in the figures represent the average of all the experiments. The formula for calculating the percentage of cells with the ring localization is as following: number of cells with the ring pattern/(number of cells with ring+number of cells with dot+number of cells with cluster). A similar formula was used to calculate percentages of cells with dot or cluster patterns. ANOVA single factor analysis was used to test percentage of cells with BMV 1a-mC ring localization pattern in comparison to that in negative control. Error bar represents the standard deviation.

## 2.6 References

**Ahola, T. and Ahlquist, P.** (1999). Putative RNA capping activities encoded by brome mosaic virus: methylation and covalent binding of guanylate by replicase protein 1a. *J Virol* **73**, 10061-10069.

**Antebi, A. and Fink, G. R.** (1992). The yeast Ca(2+)-ATPase homologue, PMR1, is required for normal Golgi function and localizes in a novel Golgi-like distribution. *Mol Biol Cell* **3**, 633-654.

**Belden, W. J. and Barlowe, C.** (2001). Role of Erv29p in collecting soluble secretory proteins into ER-derived transport vesicles. *Science* **294**, 1528-1531.

**Boone, C., Sdicu, A., Laroche, M. and Bussey, H.** (1991). Isolation from Candida albicans of a functional homolog of the Saccharomyces cerevisiae KRE1 gene, which is involved in cell wall beta-glucan synthesis. *J Bacteriol* **173**, 6859-6864.

**Brandizzi, F. and Barlowe, C.** (2013). Organization of the ER-Golgi interface for membrane traffic control. *Nat Rev Mol Cell Biol* **14**, 382-392.

**Brandizzi, F. and Barlowe, C.** (2014). ER-Golgi transport: authors' response. *Nat Rev Mol Cell Biol* **15**, 1-1.

**Breker, M., Gymrek, M. and Schuldiner, M.** (2013). A novel single-cell screening platform reveals proteome plasticity during yeast stress responses. *J Cell Biol* **200**, 839-850.

**Castro, C. P., Piscopo, D., Nakagawa, T. and Derynck, R.** (2007). Cornichon regulates transport and secretion of TGFα-related proteins in metazoan cells. *J Cell Sci* **120**, 2454-2466.

**Cheng, X., Deng, P., Cui, H. and Wang, A.** (2015). Visualizing double-stranded RNA distribution and dynamics in living cells by dsRNA binding-dependent fluorescence complementation. *Virology* **485**, 439-451.

**Cohen, Y. and Schuldiner, M.** (2011). Advanced methods for high-throughput microscopy screening of genetically modified yeast libraries. In *Netw Biol*, vol. 781 (eds G. Cagney and A. Emili), pp. 127-159: Humana Press.

**Cotton, S., Grangeon, R., Thivierge, K., Mathieu, I., Ide, C., Wei, T., Wang, A. and Laliberté, J.-F.** (2009). Turnip mosaic virus RNA replication complex vesicles are mobile, align with microfilaments, and are each derived genome. *J Virol* **83**, 10460-10471.

**D'Arcangelo, J. G., Stahmer, K. R. and Miller, E. A.** (2013). Vesicle-mediated export from the ER: COPII coat function and regulation. *Biochim Biophys Acta* **1833**, 2464-2472.

**Dancourt, J. and Barlowe, C.** (2010). Protein sorting receptors in the early secretory pathway. *Annu Rev Biochem* **79**, 777-802.

**Davis, S. and Ferro-Novick, S.** (2015). Ypt1 and COPII vesicles act in autophagosome biogenesis and the early secretory pathway. *Biochem Soc T* **43**, 92-96.

**den Boon, J. A., Diaz, A. and Ahlquist, P.** (2010). Cytoplasmic viral replication complexes. *Cell Host Microbe* **8**, 77-85.

**Diaz, A., Gallei, A. and Ahlquist, P.** (2012). Bromovirus RNA replication compartment formation requires concerted action of 1a's self-interacting RNA capping and helicase domains. *J Virol* **86**, 821-834.

**Diaz, A. and Wang, X.** (2014). Bromovirus-induced remodeling of host membranes during viral RNA replication. *Curr Opin Virol* **9**, 104-110.

**Diaz, A., Wang, X. and Ahlquist, P.** (2010). Membrane-shaping host reticulon proteins play crucial roles in viral RNA replication compartment formation and function. *Proc Natl Acad Sci USA* **107**, 16291-16296.

**Diaz, A., Zhang, J., Ollwerther, A., Wang, X. and Ahlquist, P.** (2015). Host ESCRT proteins are required for bromovirus RNA replication compartment assembly and function. *PLoS Pathog* **11**, e1004742.

**Ge, L., Zhang, M. and Schekman, R.** (2014). Phosphatidylinositol 3-kinase and COPII generate LC3 lipidation vesicles from the ER-Golgi intermediate compartment. *eLife* **3**, e04135.

**Hagiwara, Y., Komoda, K., Yamanaka, T., Tamai, A., Meshi, T., Funada, R., Tsuchiya, T., Naito, S. and Ishikawa, M.** (2003). Subcellular localization of host and viral proteins associated with tobamovirus RNA replication. *Embo J* **22**, 344-353.

**Herring, Bruce E., Shi, Y., Suh, Young H., Zheng, C.-Y., Blankenship, Sabine M., Roche, Katherine W. and Nicoll, Roger A.** (2013). Cornichon proteins determine the subunit composition of synaptic AMPA receptors. *Neuron* **77**, 1083-1096.

**Herzig, Y., Sharpe, H. J., Elbaz, Y., Munro, S. and Schuldiner, M.** (2012). A systematic approach to pair secretory cargo receptors with their cargo suggests a mechanism for cargo selection by Erv14. *PLoS Biol* **10**, e1001329.

**Hsu, N.-Y., Ilnytska, O., Belov, G., Santiana, M., Chen, Y.-H., Takvorian, P. M., Pau, C., van der Schaar, H., Kaushik-Basu, N., Balla, T. et al.** (2010). Viral reorganization of the secretory pathway generates distinct organelles for RNA replication. *Cell* **141**, 799-811.

**Huh, W.-K., Falvo, J. V., Gerke, L. C., Carroll, A. S., Howson, R. W., Weissman, J. S. and O'Shea, E. K.** (2003). Global analysis of protein localization in budding yeast. *Nature* **425**, 686-691.

**Ishibashi, K., Miyashita, S., Katoh, E. and Ishikawa, M.** (2012). Host membrane proteins involved in the replication of tobamovirus RNA. *Curr Opin Virol* **2**, 699-704.

**Ishikawa, M., Naito, S. and Ohno, T.** (1993). Effects of the tom1 mutation of Arabidopsis thaliana on the multiplication of tobacco mosaic virus RNA in protoplasts. *J Virol* **67**, 5328-5338.

**Jackson, A. C. and Nicoll, R. A.** (2009). Neuroscience: AMPA receptors get 'pickled'. *Nature* **458**, 585-586.

**Janda, M. and Ahlquist, P.** (1993). RNA-dependent replication, transcription, and persistence of brome mosaic virus RNA replicons in *S. cerevisiae*. *Cell* **72**, 961-970.

**Jiang, J., Patarroyo, C., Garcia Cabanillas, D., Zheng, H. and Laliberté, J.-F.** (2015). The vesicle-forming 6K2 protein of turnip mosaic virus interacts with the COPII coatomer Sec24a for viral systemic infection. *J Virol* **89**, 6695-6710.

**Kaganovich, D., Kopito, R. and Frydman, J.** (2008). Misfolded proteins partition between two distinct quality control compartments. *Nature* **454**, 1088-1095.

**Kohrer, K. and Domdey, H.** (1991). Preparation of high molecular weight RNA. *Methods Enzymol* **194**, 398-405.

**Kong, F., Sivakumaran, K. and Kao, C.** (1999). The N-terminal half of the brome mosaic virus 1a protein has RNA capping-associated activities: specificity for GTP and s-adenosylmethionine. *Virology* **259**, 200-210.

**Kuehn, M. J., Herrmann, J. M. and Schekman, R.** (1998). COPII-cargo interactions direct protein sorting into ER-derived transport vesicles. *Nature* **391**, 187-190.

**Kushner, D. B., Lindenbach, B. D., Grdzelishvili, V. Z., Noueiry, A. O., Paul, S. M. and Ahlquist, P.** (2003). Systematic, genome-wide identification of host genes affecting replication of a positive-strand RNA virus. *Proc Natl Acad Sci USA* **100**, 15764-15769.

**Laliberté, J.-F. and Sanfaçon, H.** (2010). Cellular remodeling during plant virus infection. *Annu Rev Phytopathol* **48**, 69-91.

**Li, Z., Vizeacoumar, F. J., Bahr, S., Li, J., Warringer, J., Vizeacoumar, F. S., Min, R., VanderSluis, B., Bellay, J., DeVit, M. et al.** (2011). Systematic exploration of essential yeast gene function with temperature-sensitive mutants. *Nat Biotech* **29**, 361-367.

**Liu, L., Westler, W. M., Den Boon, J. A., Wang, X., Diaz, A., Steinberg, H. A. and Ahlquist, P.** (2009). An amphipathic α-helix controls multiple roles of brome mosaic virus protein 1a in RNA replication complex assembly and function. *PLoS Pathog* **5**, e1000351.

**Lord, C., Ferro-Novick, S. and Miller, E. A.** (2013). The highly conserved COPII coat complex sorts cargo from the endoplasmic reticulum and targets it to the golgi. *Cold SH Perspect Biol* **5**, a013367.

**Manford, Andrew G., Stefan, Christopher J., Yuan, Helen L., MacGurn, Jason A. and Emr, Scott D.** (2012). ER-to-plasma membrane tethering proteins regulate cell signaling and ER morphology. *Dev Cell* **23**, 1129-1140.

**Martelli, G. P. and Russo, M.** (1985). Virus-Host Relationships: Symptomatological and ultrastructural aspects. In *The plant viruses*, pp. 163-205: Springer.

**Marti, L., Fornaciari, S., Renna, L., Stefano, G. and Brandizzi, F.** (2010). COPII-mediated traffic in plants. *Trends Plant Sci* **15**, 522-528.

**Miller, E. A., Beilharz, T. H., Malkus, P. N., Lee, M. C. S., Hamamoto, S., Orci, L. and Schekman, R.** (2003). Multiple cargo binding sites on the COPII subunit Sec24p ensure capture of diverse membrane proteins into transport vesicles. *Cell* **114**, 497-509.

**Mo, C. and Bard, M.** (2005). A systematic study of yeast sterol biosynthetic protein–protein interactions using the split-ubiquitin system. *BBA-Mol Cell Biol L* **1737**, 152-160.

**Mossessova, E., Bickford, L. C. and Goldberg, J.** (2003). SNARE selectivity of the COPII coat. *Cell* **114**, 483-495.

**Novick, P., Field, C. and Schekman, R.** (1980). Identification of 23 complementation groups required for post-translational events in the yeast secretory pathway. *Cell* **21**, 205-215.

**O'Reilly, E. K., Paul, J. D. and Kao, C. C.** (1997). Analysis of the interaction of viral RNA replication proteins by using the yeast two-hybrid assay. *J Virol* **71**, 7526-32.

**Obrdlik, P., El-Bakkoury, M., Hamacher, T., Cappellaro, C., Vilarino, C., Fleischer, C., Ellerbrok, H., Kamuzinzi, R., Ledent, V., Blaudez, D. et al.** (2004). K+ channel interactions detected by a genetic system optimized for systematic studies of membrane protein interactions. *Proc Natl Acad Sci USA* **101**, 12242-12247.

**Pagant, S., Wu, A., Edwards, S., Diehl, F. and Miller, Elizabeth A.** (2015). Sec24 is a coincidence detector that simultaneously binds two signals to drive ER export. *Curr Biol* **25**, 403-412.

**Paul, D. and Bartenschlager, R.** (2013). Architecture and biogenesis of plus-strand RNA virus replication factories. *World J Virol* **2**, 32-48.

**Powers, J. and Barlowe, C.** (2002). Erv14p directs a transmembrane secretory protein into COPII-coated transport vesicles. *Mol Biol Cell* **13**, 880-891.

**Restrepo-Hartwig, M. A. and Ahlquist, P.** (1996). Brome mosaic virus helicase- and polymerase-like proteins colocalize on the endoplasmic reticulum at sites of viral RNA synthesis. *J Virol* **70**, 8908-16.

**Romero-Brey, I. and Bartenschlager, R.** (2014). Membranous replication factories induced by plus-strand RNA viruses. *Viruses* **6**, 2826-2857.

**Rosas-Santiago, P., Lagunas-Gómez, D., Barkla, B. J., Vera-Estrella, R., Lalonde, S., Jones, A., Frommer, W. B., Zimmermannova, O., Sychrová, H. and Pantoja, O.** (2015). Identification of rice cornichon as a possible cargo receptor for the Golgi-localized sodium transporter OsHKT1;3. *J Exp Bot* **66**, 2733-2748.

**Roth, S., Shira Neuman-Silberberg, F., Barcelo, G. and Schüpbach, T.** (1995). *cornichon* and the EGF receptor signaling process are necessary for both anterior-posterior and dorsal-ventral pattern formation in Drosophila. *Cell* **81**, 967-978.

**Sauvageau, E., Rochdi, M. D., Oueslati, M., Hamdan, F. F., Percherancier, Y., Simpson, J. C., Pepperkok, R. and Bouvier, M.** (2014). CNIH4 interacts with newly synthesized GPCR and controls their export from the endoplasmic reticulum. *Traffic* **15**, 383-400.

**Schwartz, M., Chen, J., Janda, M., Sullivan, M., den Boon, J. and Ahlquist, P.** (2002). A positive-strand RNA virus replication complex parallels form and function of retrovirus capsids. *Mol Cell* **9**, 505-514.

**Schwenk, J., Harmel, N., Zolles, G., Bildl, W., Kulik, A., Heimrich, B., Chisaka, O., Jonas, P., Schulte, U., Fakler, B. et al.** (2009). Functional proteomics identify cornichon proteins as auxiliary subunits of AMPA receptors. *Science* **323**, 1313-1319.

**Soderberg, O., Gullberg, M., Jarvius, M., Ridderstrale, K., Leuchowius, K.-J., Jarvius, J., Wester, K., Hydbring, P., Bahram, F., Larsson, L.-G. et al.** (2006). Direct observation of individual endogenous protein complexes in situ by proximity ligation. *Nat Meth* **3**, 995-1000.

**Taron, C. H., Wiedman, J. M., Grimme, S. J. and Orlean, P.** (2000). Glycosylphosphatidylinositol biosynthesis defects in Gpi11p- and Gpi13p-deficient yeast suggest a branched pathway and implicate Gpi13p in phosphoethanolamine transfer to the third mannose. *Mol Biol Cell* **11**, 1611-1630.

**Votsmeier, C. and Gallwitz, D.** (2001). An acidic sequence of a putative yeast Golgi membrane protein binds COPII and facilitates ER export. *Embo J* **20**, 6742-6750.

**Wang, J., Tan, D., Cai, Y., Reinisch, K. M., Walz, T. and Ferro-Novick, S.** (2014). A requirement for ER-derived COPII vesicles in phagophore initiation. *Autophagy* **10**, 708-709.

**Wang, X. and Ahlquist, P.** (2008). Brome mosaic virus (Bromoviridae). *Encyclopedia of Virology (B.W.J. Mahy and M.H.V. van Regenmortel, eds), Third Edition, Academic Press, Boston*., 381-386.

**Wang, X., Lee, W.-M., Watanabe, T., Schwartz, M., Janda, M. and Ahlquist, P.** (2005). Brome mosaic virus 1a nucleoside triphosphatase/helicase domain plays crucial roles in recruiting RNA replication templates. *J Virol* **79**, 13747-13758.

**Wei, T. and Wang, A.** (2008). Biogenesis of cytoplasmic membranous vesicles for plant potyvirus replication occurs at endoplasmic reticulum exit sites in a COPI- and COPII-dependent manner. *J Virol* **82**, 12252-12264.

**Wei, T., Zhang, C., Hong, J., Xiong, R., Kasschau, K. D., Zhou, X., Carrington, J. C. and Wang, A.** (2010). Formation of complexes at plasmodesmata for Potyvirus intercellular movement is mediated by the viral protein P3N-PIPO. *PLoS Pathog* **6**, e1000962.

**Yamanaka, T., Imai, T., Satoh, R., Kawashima, A., Takahashi, M., Tomita, K., Kubota, K., Meshi, T., Naito, S. and Ishikawa, M.** (2002). Complete inhibition of tobamovirus multiplication by simultaneous mutations in two homologous host genes. *J Virol* **76**, 2491-2497.

**Yamanaka, T., Ohta, T., Takahashi, M., Meshi, T., Schmidt, R., Dean, C., Naito, S. and Ishikawa, M.** (2000). TOM1, an Arabidopsis gene required for efficient multiplication of a tobamovirus, encodes a putative transmembrane protein. *Proc Natl Acad Sci USA* **97**, 10107-10112.

**Zhang, J., Diaz, A., Mao, L., Ahlquist, P. and Wang, X.** (2012). Host acyl coenzyme A binding protein regulates replication complex assembly and activity of a positive-strand RNA virus. *J Virol* **86**, 5110-5121.

**Zhang, J., Zhang, Z., Chukkapalli, V., Nchoutmboube, J. A., Li, J., Randall, G., Belov, G. A. and Wang, X.** (2016). Positive-strand RNA viruses stimulate host phosphatidylcholine synthesis at viral replication sites. *Proc Natl Acad Sci USA* **113**, E1064-E1073.

# Chapter 3 *Brome mosaic virus* remodels cytoplasmic ER subdomains and exploits the cellular early secretory pathway in *Nicotiana benthamiana*

## 3.1 Abstract

The cellular early secretory pathway is involved in protein trafficking between the ER and the Golgi for proper cellular processes, it is a conserved pathway among yeast, plants, and mammals. The endoplasmic reticulum (ER) membrane is the hub for coat protein complex II (COPII) vesicles to recruit specific cargo proteins. Once incorporated into the vesicles, cargo proteins are delivered to the Golgi apparatus, where they are modified and further targeted to their final destinations. Many positive-strand RNA viruses utilize host ER membranes and hijack the cellular early secretory pathway to build viral replication complexes (VRCs) during viral infection. Erv14 is a cargo receptor that facilitates cargo protein incorporation into the COPII vesicles in the cellular early secretory pathway. Our previous research has demonstrated that *brome mosaic virus* (BMV) requires Erv14 and several COPII components to traffic viral replication protein 1a to the perinuclear ER membrane in yeast. Here, I extend these findings to plants and demonstrate that BMV exploits specific cytoplasmic ER subdomains and subverts cellular early secretory pathway in *Nicotiana benthamiana*. While BMV 1a-mCherry (1a-mC) was highly mobile and trafficked along the ER membrane in *N. benthamiana*, BMV infection slowed down 1a-mC movement, most likely through the incorporation of BMV 1a-mC into VRCs. Moreover, BMV remodeled specific ER subdomains that are at three-way junctions and ER sheets, and suppressed the early secretory pathway. These findings demonstrate that cellular early

secretory pathway plays a conserved role during BMV infection in yeast and plants. I propose that specific localization of BMV to these sites takes advantage of their negative membrane curvature that favors VRC assembly.

## 3.2 Introduction

The endoplasmic reticulum (ER) network is composed of nuclear envelope, ER sheets and ER tubules that are interconnected with each other by three-way junctions (Shibata et al., 2006). Lunapark (Lnp) localizes to the three-way junctions and plays an essential role in the stabilization of three-way junctions in the ER network (Wang et al., 2016). Moreover, ER membrane is one of the major organelle membranes that are utilized by positive-strand RNA [(+)RNA] viruses for viral replication. Many (+)RNA viruses remodel host ER membranes and coopt cellular early secretory pathway for the assembly of viral replication complexes (VRC) during viral infection (Hsu et al., 2010; Jiang et al., 2015; Midgley et al., 2013; Rust et al., 2001). For instance, *turnip mosaic virus* (TuMV) viral protein $6K_2$ interacted with coat protein complex II (COPII) coat protein Sec24a to hijack COPII pathway for the biogenesis of VRCs during viral infection (Jiang et al., 2015). Poliovirus nonstructural proteins 2B and 2BC colocalized with COPII coat proteins Sec13 and Sec31 during viral infection, and might take advantage of early secretory pathway for the assembly and trafficking of VRCs (Rust et al., 2001). Therefore, cellular early secretory pathway plays important roles in the biogenesis of VRCs and viral infection.

*Brome mosaic virus* (BMV) is a model of (+)RNA viruses and it can replicate in yeast, facilitating understanding of virus-host interactions and viral replication mechanisms (Diaz

and Wang, 2014). The BMV replication protein 1a has an amphipathic alpha-helix, termed helix A, that inserts into the lipid bilayer of the perinuclear ER membrane to invaginate the outer perinuclear ER membrane to form viral spherules with a negative membrane curvature (Liu et al., 2009). In addition, BMV replication proteins 1a and $2a^{pol}$ colocalize with newly synthesized viral RNAs at the ER membrane in both BMV-infected barley protoplasts and BMV-infected yeast cells (Restrepo-Hartwig and Ahlquist, 1999; Restrepo-Hartwig and Ahlquist, 1996). These results suggest that BMV 1a is an important viral protein to initiate VRCs in diverse host cells.

By taking advantage of BMV-yeast system, we found that the cargo receptor Erv14 and several COPII components are required for trafficking of BMV 1a to the perinuclear ER to initiate VRC assembly during viral infection (Li et al., 2016). These findings suggest that the COPII pathway plays an important role in the biogenesis of BMV VRCs by promoting the trafficking of BMV 1a to the perinuclear ER membrane in yeast.

BMV induces the formation of VRCs at the perinuclear ER membrane in yeast and its natural host barley (Zhang et al., 2016). However, barley is not a good system for gene knockdown or overexpression analysis to examine the roles of host factors in BMV replication. Although BMV does not efficiently infect the model plant *Arabidopsis thaliana* (Fujisaki et al., 2003), it infects *Nicotiana benthamiana* (Gopinath et al., 2005). *N. benthamiana* is an excellent host for the majority of plant viruses and serves as a model plant for studying virus-plant interactions (Goodin et al., 2008). In contrast to the perinuclear ER localization of BMV 1a in yeast and barley, however, it was previously shown that BMV

induced three types of vesicles that varied in size from 60 nm to 360 nm in *N. benthamiana* (Bamunusinghe et al., 2011). In addition, the vesicles originated in cytoplasmic ER membranes, which is different from the sites of BMV VRCs in yeast and barley at the perinuclear ER membrane. In order to gain a better understanding of BMV replication sites in *N. benthamiana*, I set up a BMV-*N. benthamiana* system to examine the trafficking of BMV 1a and the sites where BMV forms VRCs as well as the role of cellular early secretory pathway during BMV infection.

Here I report that BMV remodels specific cytoplasmic ER subdomains and exploits the early secretory pathway during infection in *N. benthamiana*. BMV 1a-mC localized to specific ER subdomains at three-way junctions and ER sheets in addition to the perinuclear ER membrane. Accordingly, BMV infection rearranged ER subdomains that mainly colocalized with BMV 1a-mC at the three-way junctions and ER sheets. In addition, BMV suppressed the secretion of a soluble marker protein to the plant apoplast and affected the cellular early secretory pathway. Therefore, BMV targets to the specific ER subdomains and exploits cellular early secretory pathway to promote VRC assembly during viral infection.

## 3.3 Results

### 3.3.1 BMV 1a-mC localizes to three-way junctions and ER sheets besides the perinuclear ER membrane in *N. benthamiana*

BMV 1a localizes to the perinuclear ER membrane in both yeast and barley during replication (Zhang et al., 2016). However, barley is not a system that allow us to knock down

gene expression or over express targeted genes. I first established a system to check the localization pattern of BMV 1a-mC in leaf epidermal cells of *N. benthamiana*. BMV 1a-mC was cloned into an agrobacterium binary vector under the control of the enhanced CaMV 35S promoter. The resulting construct was transformed into agrobacterium. To visualize the subcellular localizations of BMV 1a-mC and ER membrane, I co-expressed BMV 1a-mC and GFP-HDEL (a soluble ER luminal marker) by agroinfiltration in leaf epidermal cells of *N. benthamiana* to examine the localizations of BMV 1a-mC in relation to ER membranes. BMV 1a-mC localized to both the perinuclear and cytoplasmic ER membranes. More specifically, BMV 1a-mC localized to three-way junctions and ER sheets of the cytoplasmic ER membrane in *N. benthamiana* cells (Figure 3.1). BMV 1a is a multifunctional viral protein (Ahola and Ahlquist, 1999; Kong et al., 1999; Wang et al., 2005), with the capability of targeting to and remodeling ER membrane to induce the assembly of VRCs. Thus, BMV 1a also serve as a marker to indicate the VRCs within a cell. Previous study has shown that BMV infection induces cytoplasmic ER membrane remodeling at the sites where BMV replication occurs in *N. benthamiana* (Bamunusinghe et al., 2011). This is consistent with our observation that BMV 1a-mC primarily localized to the cytoplasmic ER membrane in leaf epidermal cells of *N. benthamiana*. Moreover, we identified that BMV 1a-mC preferentially localized to three-way junctions and ER sheets of the cytoplasmic ER subdomains in epidermal cells, suggesting that those ER subdomains might be potentially used by BMV for viral replication (Figure 3.1).

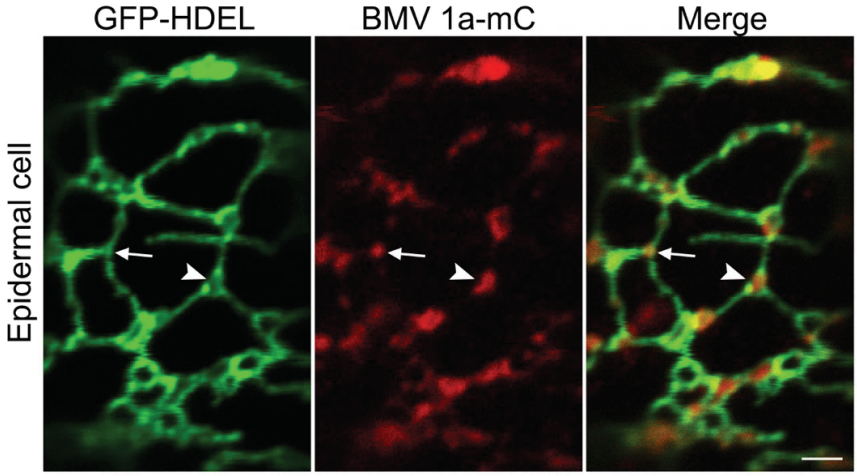


**Figure 3.1. The extended localization pattern of BMV 1a-mC at three-way junctions and ER sheets besides the perinuclear ER localization in leaf epidermal cells of *N. benthamiana*.**

Confocal microscopic images of a leaf epidermal cell co-expressing GFP-HDEL and BMV 1a-mC. GFP-HDEL and BMV 1a-mC were co-infiltrated into *N. benthamiana* epidermal cells. Leaf samples were collected 2 days after infiltration. The white arrow indicates three-way junction and white arrowhead indicates ER sheet. Scale bar: 2 μm.

### 3.3.2 The high mobility of BMV 1a-mC is inhibited by BMV infection in *N. benthamiana*

We next examined the spatiotemporal localization pattern of BMV 1a-mC. Time-lapse confocal microscope imaging showed that BMV 1a-mC rapidly moved along the ER membrane in leaf epidermal cells of *N. benthamiana* (Figure 3.2A). The white arrowheads pointed to a BMV 1a-mC dot structure that moved along the ER membrane at the time point 0, 4.77, and 9.54 seconds in a time-lapse experiment (Figure 3.2A). However, we could not distinguish whether the highly dynamic movement of BMV 1a-mC was because of its intrinsic ability or because of the dynamic movement of ER membrane. In contrast, the speedy movement of BMV 1a-mC slowed down in BMV-infected cells, as shown by the white arrowhead-pointed BMV 1a-mC localization at the time point 0, 4.77, and 9.54 (Figure

3.2B). The loss of movement of BMV 1a-mC could be a result of recruitment of BMV 1a-mC into VRCs during BMV replication.

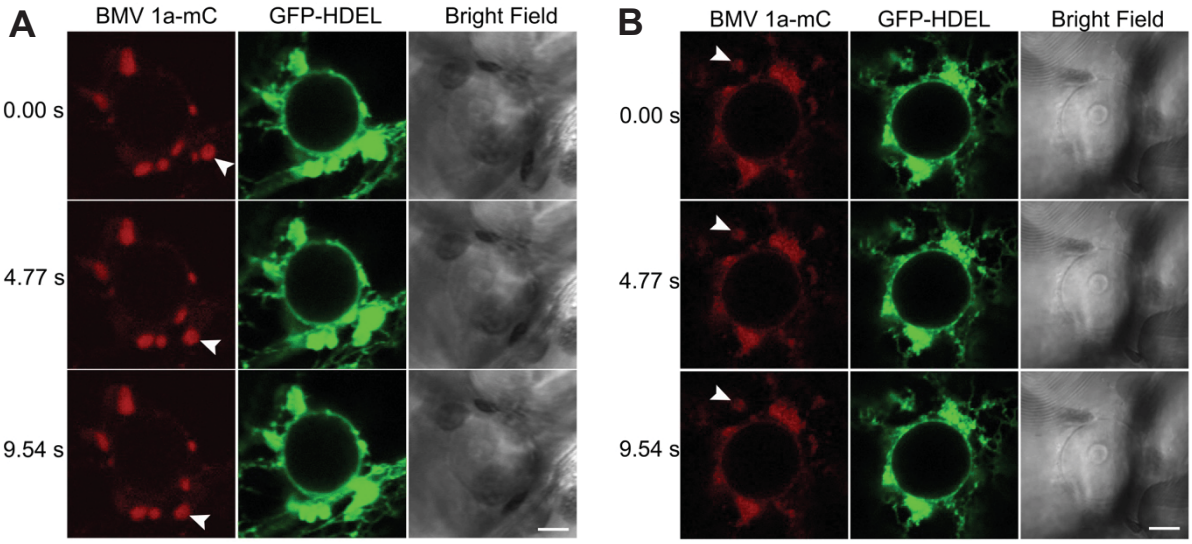


**Figure 3.2. BMV infection slows down the movement of BMV 1a-mC in leaf epidermal cells of *N. benthamiana*.**

**(A)** BMV 1a was highly dynamic in leaf epidermal cells of *N. benthamiana*. Time-lapse confocal microscopic images of a leaf epidermal cell co-expressing BMV 1a-mC and GFP-HDEL via agroinfiltration. White arrowheads indicate an example of BMV 1a-mC movement along the ER membrane in a leaf epidermal cell of *N. benthamiana*. **(B)** BMV infection slowed down the movement of BMV 1a-mC in leaf epidermal cells of *N. benthamiana*. Time-lapse confocal microscopic images of a BMV-infected leaf epidermal cell when co-expressing BMV 1a-mC and GFP-HDEL. White arrowheads indicate an example of BMV 1a-mC that stopped or slowed down the movement in a BMV-infected cell. The leaf epidermal cells were agroinfiltrated to express GFP-HDEL and each BMV genomic RNA. Leaf samples were collected 2 days after infiltration. Scale bars: 5 μm.

### 3.3.3 BMV-rearranged ER subdomains colocalize with BMV 1a-mC at the three-way junctions and ER sheets in *N. benthamiana*

Since BMV remodels host ER membranes in both plant and yeast, I next examined the ER morphology in cells during BMV infection. BMV RNA genomic RNAs, RNA1, RNA2

and RNA3, together with the ER marker GFP-HDEL were co-expressed by agroinfiltration in epidermal cells of *N. benthamiana*. It has been well established that BMV full replication can be detected 2 days after agroinfiltration in the infiltrated leaf tissue (Annamalai and Rao, 2005; Diaz et al., 2015; Gopinath et al., 2005). Two days after agroinfiltration, I found large dotted GFP-HEDL structures were present in BMV-infected leaf tissues, and furthermore, these dotted ER structures specifically localized to three-way junctions and ER sheets (Figure 3.3A). Interestingly, the localization pattern of BMV-rearranged ER subdomains was similar to the subcellular localization pattern of BMV 1a-mC during BMV infection, as both targeted to three-way junctions and ER sheets (Figures 3.3A and 3.1). This result suggests that BMV replication might be preferentially associated with three-way junctions and ER sheets.

We next checked whether BMV-rearranged ER subdomains colocalized with BMV 1a-mC. To do so, the *N. benthamiana* leaf tissues were agroinfiltrated with BMV genomic RNAs, GFP-HDEL, and BMV 1a-mC. Under these conditions, BMV 1a-mC primarily colocalized with BMV-rearranged ER subdomains at the three-way junctions and ER sheets (Figure 3.3B). Therefore, these results suggest that BMV might target to the ER subdomains at three-way junctions and ER sheets during viral replication in *N. benthamiana*.

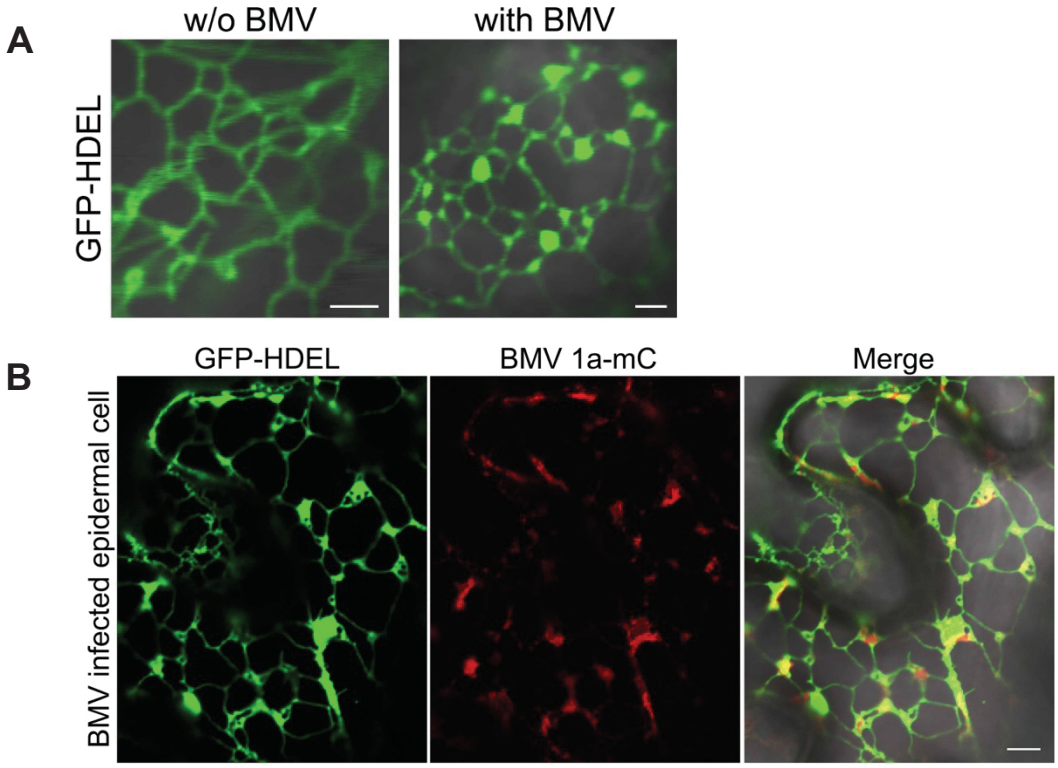


**Figure 3.3. BMV 1a-mC colocalizes with BMV-rearranged ER subdomains at three-way junctions and ER sheets in leaf epidermal cells of *N. benthamiana*.**

**(A)** BMV-induced ER membrane remodeling. Confocal microscopic images of leaf epidermal cells expressing GFP-HDEL in the absence or presence of BMV infection. Scale bars: 2 μm. **(B)** ER morphology of BMV-infected leaf epidermal cell co-expressing GFP-HDEL and BMV 1a-mC. Confocal microscopic image of BMV-infected leaf epidermal cells co-expressing GFP-HDEL and BMV 1a-mC. Leaf samples were collected 2 days after infiltration. Scale bar: 5 μm.

### 3.3.4 BMV suppresses the secretion of a soluble marker protein in *N. benthamiana*

To test whether BMV affects the anterograde pathway where cargo proteins are delivered to the Golgi from the ER membrane by COPII vesicles, we monitored a soluble marker protein, secYFP, which is transported from the ER to the apoplast. The fluorescence signal will be diffused away when it is exported out of the plant plasma membrane (Wei and Wang, 2008). A weak fluorescence signal of secYFP was observed in cells of healthy plants,

indicating an efficient export of secYFP. However, a significantly strong fluorescence signal was observed in BMV-infected cells (Figure 3.4). This result suggests that BMV infection inhibits host cellular early secretory pathways and subsequently suppresses secYFP protein trafficking from the ER to the Golgi apparatus or the secretion of secYFP out of the plasma membrane. Therefore, there is a potential interplay between the cellular early secretory pathway (COPII and COPI) and BMV during viral infection.

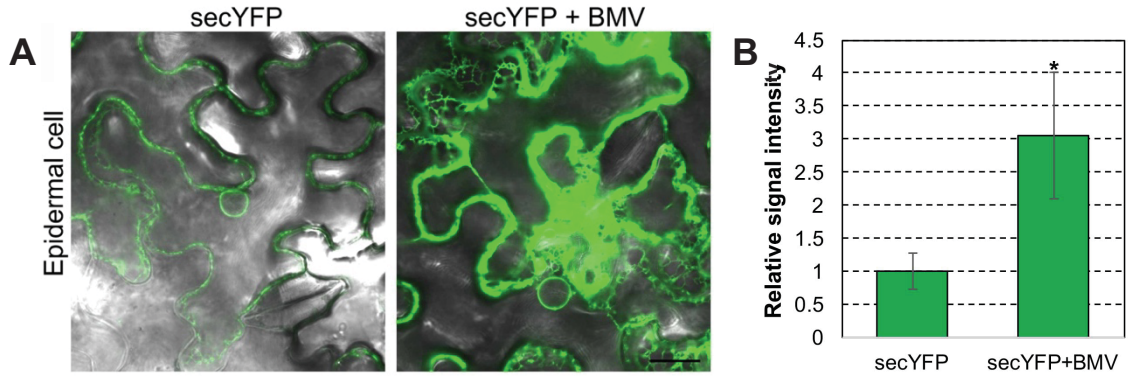


**Figure 3.4. BMV infection suppresses the secretion of secYFP out of the plasma membrane in leaf epidermal cells of *N. benthamiana*.**

**(A)** Confocal microscopic images of *N. benthamiana* leaf epidermal cells expressing secYFP in the absence or presence of BMV infection. The leaf epidermal cells were agroinfiltrated with secYFP and each BMV genomic RNA. Leaf samples were collected 3 days after infiltration. Scale bar: 20 μm. **(B)** Quantification of signal intensity. Relative signal intensity of secYFP with BMV infection as compared to that w/o BMV infection, the signal intensity was measured by Fiji (Image J) software. Error bars represent standard deviation. *$P$<0.05 (ANOVA single factor analysis of signal intensity of secYFP with BMV infection as compared to that w/o BMV infection).

### 3.3.5 BMV infection affects cellular early secretory pathway in *N. benthamiana*

Since BMV infection suppressed the secretion of secYFP out of the plasma membrane (Figure 3.4), we next examined how BMV infection affects COPII and COPI pathways by checking the localizations and protein expression levels of the small GTPase proteins:

secretion-associated RAS super family 1 (Sar1) and ADP-ribosylation factor 1 (Arf1). Both are involved in the formation and budding of vesicles that emerge from plant endomembrane systems (Cevher-Keskin, 2013). Sar1 is one of the five major components of COPII vesicles and required to initiate the assembly of COPII vesicles for protein trafficking from the ER to the Golgi apparatus (Nakano and Muramatsu, 1989). A dominant negative mutant Sar1(H74L) inhibits protein trafficking from the ER to the Golgi apparatus (Takeuchi et al., 2000). Arf1 is required to recruit COPI coat β-COP to the Golgi membrane to initiate the assembly of COPI vesicles (Donaldson et al., 1992). A dominant negative mutant Arf1(T31N), which prefers to bind to GDP as an inactive GDP-bound form, inhibits ER export and disrupts the binding of β-COP to the Golgi membrane, resulting in the collapse of Golgi into the ER membrane (Dascher and Balch, 1994; Stefano et al., 2006).

We tested whether BMV infection affects the localizations and abundance of Sar1 and Arf1, as well as the dominant negative mutants Sar1(H74L) and Arf1(T31N). The leaf epidermal cells were co-infiltrated with each of BMV genomic RNAs (agrobacterium at a concentration of $OD_{600}$ = 0.05), and Sar1-YFP, Arf1-YFP, or Sar1(H74L)-YFP (each agrobacterium at a concentration of $OD_{600}$ = 0.1), or Arf1(T31N)-YFP at a concentration of $OD_{600}$ = 0.05. Agroinfiltration of Arf1(T31N)-YFP at a concentration of $OD_{600}$ = 0.1 caused cell death (data not shown), consistent with a previous report that knockdown of COPI coat proteins causes acute cell death (Ahn et al., 2015). However, at a reduced concentration at $OD_{600}$ = 0.05, I did not observe obvious cell death. BMV infection reduced the protein accumulation levels of both Arf1-YFP and Arf1(T31N)-YFP, as the YFP signal intensity was

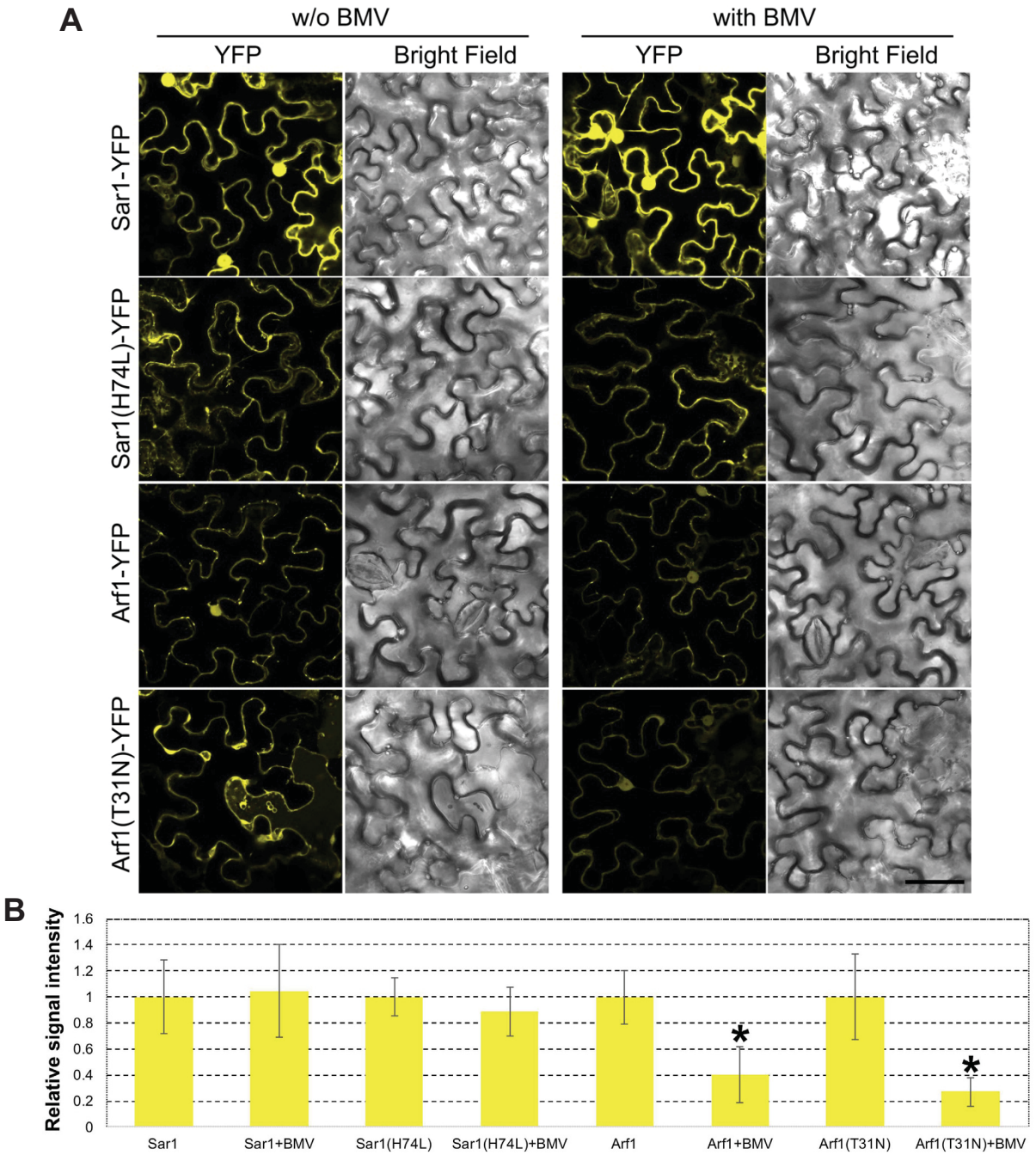


**Figure 3.5. BMV infection reduces the protein accumulation levels of Arf1-YFP and Arf1(T31N)-YFP in leaf epidermal cells of *N. benthamiana*.**

**(A)** Confocal microscopic images of *N. benthamiana* epidermal cells expressing Sar1-YFP, Sar1(H74L)-YFP, Arf1-YFP and Arf1(T31N)-YFP without (w/o) or with BMV infection. Leaf samples were collected 2 days after infiltration. Scale bar: 50 μm. **(B)** Quantification of signal intensity. Relative signal intensity of Sar1-YFP, Sar1(H74L)-YFP, Arf1-YFP and Arf1(T31N)-YFP with BMV infection as compared to those w/o BMV infection, the signal intensity was measured by Fiji (Image J) software. Error bars represent standard deviation. *$P$<0.05 (ANOVA single factor analysis of signal intensity of those with BMV infection as compared to those w/o BMV infection).

significantly lower during BMV infection, compared to the control (Figure 3.5B). However, BMV infection did not significantly affect the protein levels of Sar1-YFP and Sar1(H74L)-YFP (Figure 3.5B). Moreover, none of the localization patterns of Sar1-YFP, Sar1(H74L)-YFP, Arf1-YFP and Arf1(T31N)-YFP were significantly changed upon BMV infection (Figure 3.5A). Therefore, BMV infection reduced Arf1 protein accumulation, and hence, reduced ER export and affected COPI assembly at the Golgi membrane. This could potentially increase ER membrane pool to accommodate or favor BMV replication.

## 3.4 Discussion

### 3.4.1 BMV targets to three-way junctions and ER sheets for replication in *N. benthamiana*

BMV infection rearranged ER subdomains that are probably at three-way junctions and ER sheets in leaf epidermal cells of *N. benthamiana* (Figure 3.3). If BMV localizes to these specific ER subdomains, it can take advantage of the negative membrane curvature at three-way junctions for VRC assembly and the (poly)ribosomes on ER sheets for viral protein synthesis during viral infection. Therefore, three-way junctions and ER sheets might be structurally and functionally beneficial for BMV replication. ER tubules have a high positive membrane curvature, which is opposite to the negative membrane curvature of BMV VRCs. Thus, ER tubules may not favor BMV replication, especially when BMV initiates the invagination of the outer ER membrane into the ER lumen. Theoretically, the negative membrane curvature of three-way junctions might favor BMV during VRC initiation, by saving the energy that would be required for BMV to bend the high positive membrane

curvature of ER tubules into a negative membrane curvature. ER sheets have ribosomes studded on their flat membrane surface, and ribosomes are important for the synthesis of cellular proteins and viral proteins which are essential during viral replication. Considering the low membrane curvature on the flat membranes of ER sheets, it takes less energy for BMV to induce a negative membrane curvature on flat membranes than that on ER tubules. Previous study has demonstrated that BMV predominantly remodels the peripheral ER domain in *N. benthamiana* (Bamunusinghe et al., 2011; Chaturvedi and Rao, 2014). Here, we show a similar localization pattern of BMV 1a-mC at the cytoplasmic ER membrane in *N. benthamiana*, and further suggest that BMV might preferably remodel three-way junctions and ER sheets during infection in dicot plants (Figures 3.1, 3.3). The specific reason why BMV assembles VRCs at cytoplasmic ER but not at the perinuclear ER in *N. benthamiana* is not clear. It has been proposed that the ER composition may play a major role

The ER membrane-shaping proteins include reticulons (RTNs), Sey1 and Lunapark (Lnp1). The RTNs have been shown to be required for both BMV replication, in particular the VRC formation (Diaz et al., 2010). Our recent preliminary data showed that deletion of *SEY1* or *LNP1* in yeast also inhibited BMV replication (unpublished data), though the mechanism is unknown. BMV 1a interacts with and relocalizes RTNs from the peripheral ER to BMV VRCs at the perinuclear ER. RTNs may contribute to the maintenance of a positive membrane curvature in the neck of VRCs, and also might be incorporated into the interior of BMV VRCs to regulate the size of VRCs (Diaz et al., 2010). Although I have not determined the roles of Sey1 and Lnp1 in BMV replication in yeast, I hypothesize that three-way

junctions are crucial sites for BMV replication in *N. benthamiana* based on our preliminary data and the roles of Sey1 and Lnp1 in the formation and maintenance of three-way junctions (Chen et al., 2012; Wang et al., 2016).

### 3.4.2 BMV manipulates cellular early secretory pathway during viral infection

In yeast, Erv14 and COPII coat proteins Sec13, Sec24 and Sec31 are required for targeting BMV 1a to the perinuclear ER (Li et al., 2016), suggesting that BMV exploits COPII components for viral replication protein trafficking for its replication. Here, I found that BMV 1a-mC was highly mobile in *N. benthamiana* cells (Figure 3.2A) and BMV infection immobilized BMV 1a-mC (Figure 3.2B), suppressed secYFP secretion (Figure 3.4), and reduced the protein accumulation levels of Arf1 and Arf1(T31N) (Figure 3.5). By down-regulating Arf1 protein levels, BMV might inhibit COPI vesicle assembly, inhibit ER export, and cause the collapse of Golgi apparatus. These effects could in turn increase the ER membrane pools to benefit BMV infection.

In conclusion, BMV takes advantages of the structural and functional properties of specific ER subdomains at the three-way junctions and ER sheets during viral infection, and exploits cellular early secretory pathway to favor VRC assembly and viral RNA synthesis. These findings also reveal a role of cellular early secretory pathway in BMV infection that is functionally conserved between yeast and plants. This conservation suggests that further investigation of this process will provide broadly relevant new insights into the mechanisms through which viruses manipulate hosts. Moreover, it might be possible to inhibit virus infection by manipulating the homologs of membrane-shaping proteins. This application can

be tested by using BMV-*N. benthamiana* system along with the gene knockdown technique.

## 3.5 Materials and methods

### 3.5.1 Plant growth conditions

The *N. benthamiana* seeds were germinated on the soil in a pot covered by a transparent Zip plastic bag to maintain a high humidity condition during seed germination. About 2 weeks later, the plantlets were transferred to the soil and grown in a growth chamber at 24°C under a long-day photoperiod condition (16 h light and 8 h dark).

### 3.5.2 *Agrobacterium*-mediated BMV infection and protein expression in plant

The leaf epidermal cells of 4-5 weeks old plants were used for BMV infection and/or transient protein expression of BMV 1a-mC, GFP-HDEL, secYFP, Sar1-YFP, Sar1(H74L)-YFP, Arf1-YFP and Arf1(T31N)-YFP in *N. benthamiana* by agroinfiltration approach (Sparkes et al., 2006). The plant-expressing plasmids were transformed in agrobacteria by a modified freeze/thaw method (Höfgen and Willmitzer, 1988). Briefly, the agrobacteria competent cells were mixed with ~1 μg plasmid DNA and incubated on ice for 30 min, and then freeze with liquid nitrogen for 1 min. After incubation at 42°C for 5 min, the agrobacteria cells were grown at 30°C for 2-4 h before plating on the 1 x YT solid medium plate with kanamycin antibiotic.

As for the agrobacterium-mediated transient protein expression or BMV infection (Gopinath et al., 2005), the agrobacteria cells harboring plasmid of interest were grown

overnight at 30°C in 2 x YT liquid medium contained 50 μg·mL$^{-1}$ kanamycin, 10 μg·mL$^{-1}$ rifampicin, 10 mM MES (morpholine ethanesulfonic acid, pH=5.9), and 50 μM acetosynringone. The cells were sub-cultured in the same medium for 3.5 h with a start $OD_{600}$ value at 0.3 and harvested with a $OD_{600}$ value at ~1.0. After removing the medium, the cells were resuspended in the infiltration buffer (10 mM $MgCl_2$, 10 mM MES pH=5.9, and 150 uM acetosynringone), and incubated at room temperature for 3-24 h. Then the agrobacteria were infiltrated into the leaf tissues using a needleless 1-ml syringe by gentle pressure through the stomata on the lower epidermal surface (Sparkes et al., 2006). The leaf tissues were collected for confocal microscopy 2-3 days after infiltration.

### 3.5.3 Confocal microscopy

The leaf tissues of *N. benthamiana* were collected and immersed with water, and imaged immediately at room temperature using Argon/HeNe lasers with a 40 x water immersion objective (C-Apochromat 40x/1.2 W) of a Zeiss LSM Scanning 880 microscope at the Fralin microscopy facility at Virginia Tech. To assess the mobility of BMV 1a-mC in the leaf epidermal cells, time-lapse scanning analysis was performed with the Zeiss imaging system ZEN lite software. All the images were processed with Adobe Photoshop CS6 software.

## 3.6 References

**Ahn, H.-K., Kang, Y. W., Lim, H. M., Hwang, I. and Pai, H.-S.** (2015). Physiological functions of the COPI complex in higher plants. *Mol Cells* **38**, 866-875.

**Ahola, T. and Ahlquist, P.** (1999). Putative RNA capping activities encoded by brome mosaic virus: methylation and covalent binding of guanylate by replicase protein 1a. *J Virol* **73**, 10061-10069.

**Annamalai, P. and Rao, A. L. N.** (2005). Replication-independent expression of genome components and capsid protein of brome mosaic virus in planta: A functional role for viral replicase in RNA packaging. *Virology* **338**, 96-111.

**Bamunusinghe, D., Seo, J.-K. and Rao, A. L. N.** (2011). Subcellular localization and rearrangement of endoplasmic reticulum by brome mosaic virus capsid protein. *J Virol* **85**, 2953-2963.

**Cevher-Keskin, B.** (2013). ARF1 and SAR1 GTPases in endomembrane trafficking in plants. *Int J Mol Sci* **14**, 18181-18199.

**Chaturvedi, S. and Rao, A. L. N.** (2014). Live cell imaging of interactions between replicase and capsid protein of Brome mosaic virus using Bimolecular Fluorescence Complementation: Implications for replication and genome packaging. *Virology* **464–465**, 67-75.

**Chen, S., Novick, P. and Ferro-Novick, S.** (2012). ER network formation requires a balance of the dynamin-like GTPase Sey1p and the Lunapark family member Lnp1p. *Nat Cell Biol* **14**, 707-716.

**Dascher, C. and Balch, W. E.** (1994). Dominant inhibitory mutants of ARF1 block endoplasmic reticulum to Golgi transport and trigger disassembly of the Golgi apparatus. *J Biol Chem* **269**, 1437-48.

**Diaz, A. and Wang, X.** (2014). Bromovirus-induced remodeling of host membranes during viral RNA replication. *Curr Opin Virol* **9**, 104-110.

**Diaz, A., Wang, X. and Ahlquist, P.** (2010). Membrane-shaping host reticulon proteins play crucial roles in viral RNA replication compartment formation and function. *Proc Natl Acad Sci USA* **107**, 16291-16296.

**Diaz, A., Zhang, J., Ollwerther, A., Wang, X. and Ahlquist, P.** (2015). Host ESCRT proteins are required for bromovirus RNA replication compartment assembly and function. *PLoS Pathog* **11**, e1004742.

**Donaldson, J. G., Cassel, D., Kahn, R. A. and Klausner, R. D.** (1992). ADP-ribosylation factor, a small GTP-binding protein, is required for binding of the coatomer protein beta-COP to Golgi membranes. *Proc Natl Acad Sci USA* **89**, 6408-6412.

**Fujisaki, K., Hagihara, F., Kaido, M., Mise, K. and Okuno, T.** (2003). Complete nucleotide sequence of spring beauty latent virus, a bromovirus infectious to Arabidopsis thaliana. *Arch Virol* **148**, 165-175.

**Goodin, M. M., Zaitlin, D., Naidu, R. A. and Lommel, S. A.** (2008). Nicotiana benthamiana: Its history and future as a model for plant–pathogen interactions. *Mol Plant Microbe In*

**21**, 1015-1026.

**Gopinath, K., Dragnea, B. and Kao, C.** (2005). Interaction between brome mosaic virus proteins and RNAs: effects on RNA replication, protein expression, and RNA stability. *J Virol* **79**, 14222-14234.

**Höfgen, R. and Willmitzer, L.** (1988). Storage of competent cells for Agrobacterium transformation. *Nucleic Acids Res* **16**, 9877.

**Hsu, N.-Y., Ilnytska, O., Belov, G., Santiana, M., Chen, Y.-H., Takvorian, P. M., Pau, C., van der Schaar, H., Kaushik-Basu, N., Balla, T. et al.** (2010). Viral reorganization of the secretory pathway generates distinct organelles for RNA replication. *Cell* **141**, 799-811.

**Jiang, J., Patarroyo, C., Garcia Cabanillas, D., Zheng, H. and Laliberté, J.-F.** (2015). The vesicle-forming 6K2 protein of turnip mosaic virus interacts with the COPII coatomer Sec24a for viral systemic infection. *J Virol* **89**, 6695-6710.

**Kong, F., Sivakumaran, K. and Kao, C.** (1999). The N-terminal half of the brome mosaic virus 1a protein has RNA capping-associated activities: specificity for GTP and s-adenosylmethionine. *Virology* **259**, 200-210.

**Li, J., Fuchs, S., Zhang, J., Wellford, S., Schuldiner, M. and Wang, X.** (2016). An unrecognized function for COPII components in recruiting the viral replication protein BMV 1a to the perinuclear ER. *J Cell Sci* **129**, 3597-3608.

**Liu, L., Westler, W. M., Den Boon, J. A., Wang, X., Diaz, A., Steinberg, H. A. and Ahlquist, P.** (2009). An amphipathic α-helix controls multiple roles of brome mosaic virus protein 1a in RNA replication complex assembly and function. *PLoS Pathog* **5**, e1000351.

**Midgley, R., Moffat, K., Berryman, S., Hawes, P., Simpson, J., Fullen, D., Stephens, D. J., Burman, A. and Jackson, T.** (2013). A role for endoplasmic reticulum exit sites in foot-and-mouth disease virus infection. *J Gen Virol* **94**, 2636-2646.

**Nakano, A. and Muramatsu, M.** (1989). A novel GTP-binding protein, Sar1p, is involved in transport from the endoplasmic reticulum to the Golgi apparatus. *J Cell Biol* **109**, 2677-2691.

**Restrepo-Hartwig, M. and Ahlquist, P.** (1999). Brome mosaic virus RNA replication proteins 1a and 2a colocalize and 1a independently localizes on the yeast endoplasmic reticulum. *J Virol* **73**, 10303-10309.

**Restrepo-Hartwig, M. A. and Ahlquist, P.** (1996). Brome mosaic virus helicase- and polymerase-like proteins colocalize on the endoplasmic reticulum at sites of viral RNA synthesis. *J Virol* **70**, 8908-16.

**Rust, R. C., Landmann, L., Gosert, R., Tang, B. L., Hong, W., Hauri, H.-P., Egger, D.**

**and Bienz, K.** (2001). Cellular COPII proteins are involved in production of the vesicles that form the poliovirus replication complex. *J Virol* **75**, 9808-9818.

**Shibata, Y., Voeltz, G. K. and Rapoport, T. A.** (2006). Rough sheets and smooth tubules. *Cell* **126**, 435-439.

**Sparkes, I. A., Runions, J., Kearns, A. and Hawes, C.** (2006). Rapid, transient expression of fluorescent fusion proteins in tobacco plants and generation of stably transformed plants. *Nat Protoc* **1**, 2019-2025.

**Stefano, G., Renna, L., Chatre, L., Hanton, S. L., Moreau, P., Hawes, C. and Brandizzi, F.** (2006). In tobacco leaf epidermal cells, the integrity of protein export from the endoplasmic reticulum and of ER export sites depends on active COPI machinery. *Plant J* **46**, 95-110.

**Takeuchi, M., Ueda, T., Sato, K., Abe, H., Nagata, T. and Nakano, A.** (2000). A dominant negative mutant of Sar1 GTPase inhibits protein transport from the endoplasmic reticulum to the Golgi apparatus in tobacco and Arabidopsis cultured cells. *Plant J* **23**, 517-525.

**Wang, S., Tukachinsky, H., Romano, F. B. and Rapoport, T. A.** (2016). Cooperation of the ER-shaping proteins atlastin, lunapark, and reticulons to generate a tubular membrane network. *eLife* **5**, e18605.

**Wang, X., Lee, W.-M., Watanabe, T., Schwartz, M., Janda, M. and Ahlquist, P.** (2005). Brome mosaic virus 1a nucleoside triphosphatase/helicase domain plays crucial roles in recruiting RNA replication templates. *J Virol* **79**, 13747-13758.

**Wei, T. and Wang, A.** (2008). Biogenesis of cytoplasmic membranous vesicles for plant potyvirus replication occurs at endoplasmic reticulum exit sites in a COPI- and COPII-dependent manner. *J Virol* **82**, 12252-12264.

**Zhang, J., Zhang, Z., Chukkapalli, V., Nchoutmboube, J. A., Li, J., Randall, G., Belov, G. A. and Wang, X.** (2016). Positive-strand RNA viruses stimulate host phosphatidylcholine synthesis at viral replication sites. *Proc Natl Acad Sci USA* **113**, E1064-E1073.

# Chapter 4 Cornichon proteins are involved in maintaining ER morphology in yeast and *Nicotiana benthamiana*

## 4.1 Abstract

The endoplasmic reticulum (ER) network is generated and maintained by cellular factors such as membrane-shaping protein families. The Cornichon (CNI) protein family is conserved among eukaryotes, from Erv14 in yeast to CNI homologs (CNIHs) in plants and mammals. In yeast, Erv14 functions as a cargo receptor of coat protein complex II (COPII) vesicles to facilitate ER export of cargo proteins to their targeted destinations for proper cellular processes. In mammals, while HsCNIH1 and HsCNIH4 function as cargo receptors involved in cell proliferation and signal transduction, HsCNIH2 and HsCNIH3 function as partners of glutamate receptors involved in neuron signal transmission. However, the cellular function of CNIHs in plants is unclear. Here, I show that CNIHs of *Nicotiana benthamiana* (NbCNIHs) can functionally complement the loss of Erv14 in yeast, and play a significant role in maintaining ER morphology in *N. benthamiana*. Knockdown of *NbCNIH5* caused ER fragmentation by forming dotted ER structures that are separated from each other, and thus NbCNIH5 is unexpectedly involved in maintaining ER tubules. I further confirmed that Erv14 and another CNI Erv15 are both required for ER tubule maintenance, as deletions of *ERV14* and *ERV15* abolished ER tubule formation in the cortical ER region of yeast cells. Therefore, CNI proteins could be membrane-shaping proteins and play a conserved and significant role in maintaining ER morphology in plant and yeast.

## 4.2 Introduction

The endoplasmic reticulum (ER) is one of the largest organelles within the cell and exhibits a single continuous membrane that forms a network with dynamic and complex structures. ER is composed of nuclear envelope, ribosome-studded sheets and smooth tubules (Westrate et al., 2015). The nuclear envelope is one of the major domains of ER, which is composed of inner and outer nuclear membranes, nuclear pore complexes and the lamina in metazoa (Hetzer et al., 2005), or the lamina-like network in plant (Evans et al., 2011), or without the lamina in yeast (Taddei and Gasser, 2012). Expanding from nuclear envelope, another major domain, called peripheral ER, is formed. Peripheral ER is composed of a series of ER sheets and dynamic tubules. ER sheets are composed of two flat and closely apposed membranes with a well-maintained lumen space, and thus ER sheets have a low membrane curvature except at edges of the sheet. Furthermore, ER tubules radiate from nuclear envelope and ER sheets to form a mesh-like structure that dynamically interconnects all domains of ER. ER tubules have a high membrane curvature on the surface except the plane of tubule. The different structural features of ER sheets and ER tubules make them better suited for particular cellular functions (Westrate et al., 2015). The ribosome-studded ER sheets are the major subcellular locations for the biosynthesis of membrane and secretory proteins. In contrast, the ribosome-free ER tubules have less well known functions, but may be the major regions for lipid synthesis, vesicles budding and fusion, or contact sites with other organelle membranes (Shibata et al., 2006).

Many previous studies have been reported on the mechanistic formation of ER tubules

and ER sheets. Moreover, several integral membrane protein families are involved in the generation and maintenance of ER tubules. The reticulons (RTNs) are a membrane-shaping protein family involved in the generation of high membrane curvature. RTNs have a highly conserved carboxy-terminal reticulon homology domain. RTNs have been identified in many eukaryotes, including mammals, plants and yeast (Yang and Strittmatter, 2007). Specifically, there are four RTNs (RTN1, RTN2, RTN3, and RTN4/Nogo) in mammals, two RTNs (Rtn1 and Rtn2) in yeast, and 21 members in the reticulon-like protein subfamily (RTNLB) of *Arabidopsis thaliana* (Nziengui et al., 2007). Furthermore, another protein family, including DP1 in mammals and the yeast homolog of the polyposis locus protein 1 (Yop1), is also required to maintain the high membrane curvature for shaping ER tubules. Although RTNs and DP1/Yop1 protein families are not related in sequence, they both contain a conserved domain, which has two hydrophobic segments to form a hairpin structure for stabilizing the high membrane curvature of ER tubules. In addition, they both localize to the ER to promote tubule formation by forming immobile oligomers, subsequently maintaining the high membrane curvature of ER tubules and ER sheet edges (Hu et al., 2008; Shibata et al., 2008; Voeltz et al., 2006; Westrate et al., 2015). Therefore, RTNs and DP1/Yop1 proteins play crucial roles in generating and maintaining high membrane curvature of ER tubules, as well as stabilizing the high membrane curvature of ER sheet edges. Regarding with the maintenance of lumen and low curvature of flat membranes within ER sheets, ribosomes are involved in the stabilization of ER sheets, as removal of membrane-bound ribosomes from ER sheets causes the tubulation of ER membrane and loss of ER sheets (Puhka et al., 2007). Membrane-bound polysomes are required to separate rough ER proteins into sheets. The

lumen space between the two flat and closely apposed membranes is well maintained by luminal ER spacers, such as Climp63, which is one of the coiled-coil proteins (Shibata et al., 2010). Therefore, ribosomes, ER lumen spacer and membrane-shaping proteins all together coordinate the morphology of ER sheets, whereas the abundance of membrane-shaping proteins such as RTNs and DP1/Yop1, to some degree, determines the ratio of sheets to tubules (Shibata et al., 2010).

The ER tubules have to be interconnected with each other to develop a more complex ER network. A class of dynamin-related integral membrane GTPases, including atlastins (ATLs) in mammals and synthetic enhancement of Yop1 (Sey1) in yeast, have been found localize to the ER and mediate the fusion of ER membrane (Hu et al., 2009). In addition, Lnp1, a member of the conserved Lunapark (Lnp) family protein, is also involved in ER network formation in yeast. By binding to RTNs and Yop1, Lnp1 resides at three-way junctions. However, the localization of Lnp1 to three-way junctions, as well as the interaction between Lnp1 and Rtn1, are tightly regulated by Sey1 to balance the ER network formation in yeast (Chen et al., 2012). Recently, a comprehensive study was performed to understand the roles of ER-shaping proteins ATL, Lnp and RTNs in generating ER tubule network. This study has demonstrated that ATL and a balance between RTNs and ATL are required to maintain the ER network, and furthermore, Lnp is required for the stabilization of three-way junctions, instead of ER network formation in mammalian cells (Wang et al., 2016).

Cornichon (CNI) proteins are a conserved family of proteins among eukaryotes, from Erv14 in yeast to Cornichon homologs (CNIHs) in plants and mammals. Erv14 functions as a

cargo receptor of coat protein complex II (COPII) vesicles to facilitate the ER exit of membrane and secretory proteins to the Golgi apparatus, en route to their targeted destinations (Herzig et al., 2012; Pagant et al., 2015; Powers and Barlowe, 1998; Powers and Barlowe, 2002). However, we have very limited understanding of plant CNIHs. The most recent study on plant CNIHs has shown that a rice CNI protein functions as a cargo receptor for the ER exit of a sodium transporter to the Golgi apparatus (Rosas-Santiago et al., 2015). Here I report that an unexpected role of NbCNIH5 and Erv14/15 in maintaining ER morphology in plant and yeast, respectively. Knockdown of *NbCNIH5* in *N. benthamiana* led to the fragmented ER membrane to form dotted ER structures that are separated from each other. In parallel, deletions of *ERV14* and its paralog *ERV15* abolished ER tubules at the cortical ER region in yeast. Therefore, CNI proteins play an unexpected and conserved role of in maintaining ER morphology in plant and yeast.

## 4.3 Results

### 4.3.1 Sequence analysis of NbCNIHs

CNI proteins are a conserved family of proteins among eukaryotes. AtCNIH5 (AT3G12180) is one of the five CNIHs in *Arabidopsis* and has the highest nucleotide sequence similarity to Erv14 (46.28%). By using the nucleotide sequence of AtCNIH5 to BLAST the *N. benthamiana* draft genome-predicted proteins, we found nine CNIHs in *N. benthamiana* (Bombarely et al., 2012). Based on the percent identity of nucleotide sequences, these nine *CNIHs* of *N. benthamiana* (*NbCNIHs*) can be categorized into five groups. For the four groups that have two isoforms, each of *NbCNIHs* share between ~90% to 98% identity

(Figure 4.1A). More specifically, NbS00033235g0007.1 and NbS00059010g0003.1 share 95.27% identity, NbS00002151g0007.1 and NbS00044957g0003.1 are 98.33% identical, 95.6% identity is between NbS00002934g0013.1 and NbS00034361g0012.1, NbS00002749g0109.1 and NbS00015099g0002.1 has 90.91% identity. Therefore, we selected one representative gene from each group and named them specifically as: NbCNIH1 for NbS00059010g0003.1, NbCNIH2 for NbS00002151g0007.1, NbCNIH3 for NbS00034361g0012.1, NbCNIH4 for NbS00002749g0109.1 and NbCNIH5 for NbS00060547g0001.1 (Figure 4.1A). Amino acid sequence alignment showed that CNIHs among human (*Homo Sapiens*), *N. benthamiana* and yeast *Saccharomyces cerevisiae* were conserved throughout the full-length amino acid sequences (Figure 4.1B). Phylogenetic analysis indicated that NbCNIHs evolved into two separate clades: NbCNIH1, NbCNIH2 and NbCNIH3 as one clade, and NbCNIH4 and NbCNIH5 as the other one (Figure 4.1C). Therefore, NbCNIH2 and NbCNIH5 were selected to represent each clade for the follow-up complementation experiments in yeast and knockdown in *N. benthamiana* by virus-induced gene silencing (VIGS) approach.

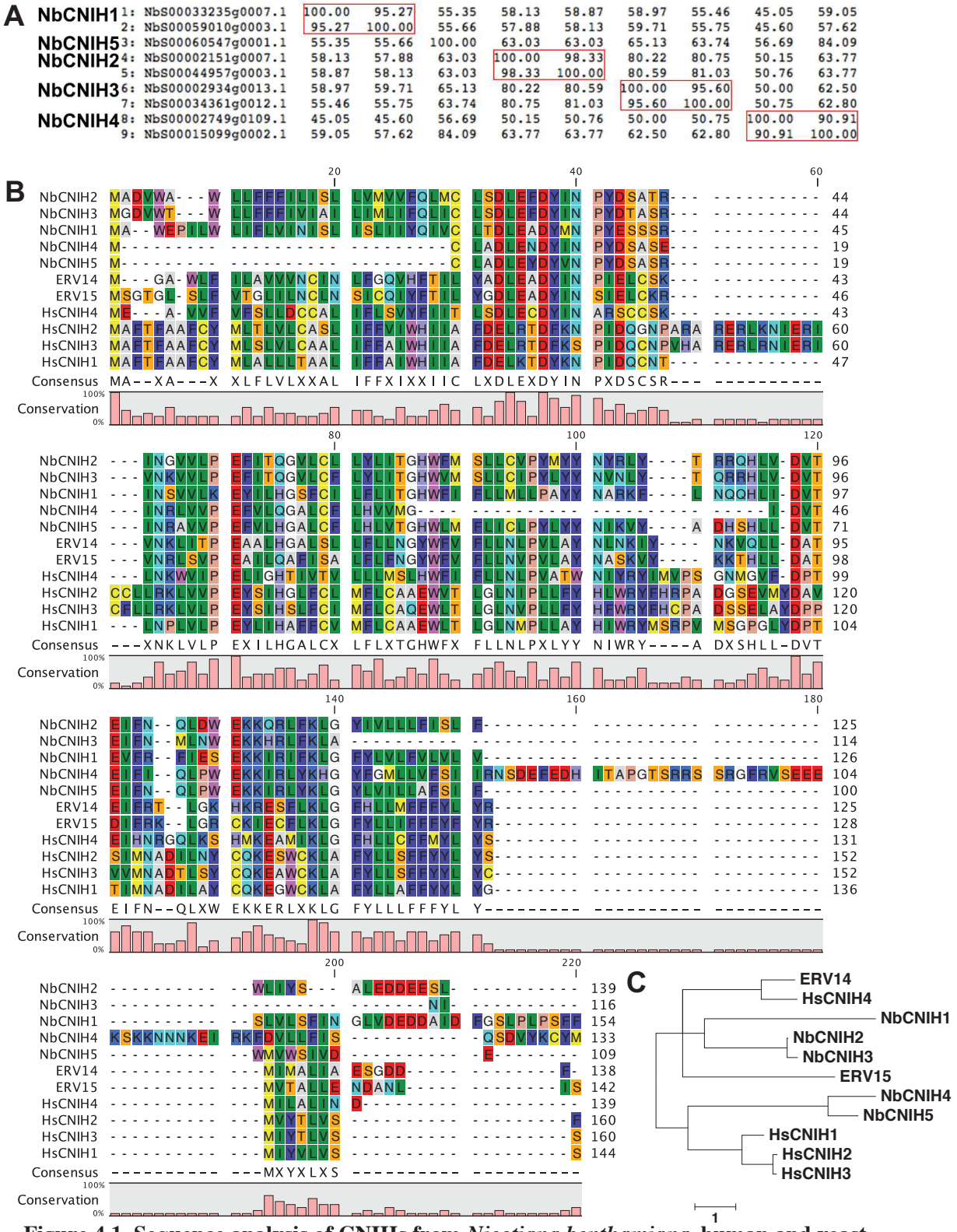


**Figure 4.1. Sequence analysis of CNIHs from *Nicotiana benthamiana*, human and yeast.**

**(A)** Percent identity of nucleotide sequences of *CNIHs* from *N. benthamiana*. Based on the draft genome version v0.4.4 of *N. benthamiana* (Sol Genomics Network), the nine *CNI* homologous gene names of *N. benthamiana* are NbS00033235g0007.1, NbS00059010g0003.1 (NbCNIH1 herein), NbS00002151g0007.1 (NbCNIH2), NbS00044957g0003.1, NbS00002934g0013.1,

NbS00034361g0012.1 (NbCNIH3), NbS00002749g0109.1 (NbCNIH4), NbS00015099g0002.1, and NbS00060547g0001.1 (NbCNIH5). The alignment of multiple nucleotide sequence was performed by using Clustal Omega. **(B)** Amino acid sequence alignment of NbCNIHs, HsCNIHs, Erv14 and Erv15 was performed by using the CLC Sequence Viewer 7 software program. **(C)** Phylogenetic analysis of the amino acid sequences of NbCNIHs, HsCNIHs, Erv14 and Erv15 was performed by Maximum Likelihood method based on the JTT matrix-based model (Jones et al., 1992) using MEGA7 software program (Kumar et al., 2016). The tree with the highest log likelihood (-2936.7298) is shown and is drawn to scale.

### 4.3.2 NbCNIHs complement the defective distribution of BMV 1a-mC in yeast *erv14*Δ mutant cells

Because deleting *ERV14* disrupts the perinuclear ER localization of BMV 1a in yeast (Li et al., 2016), we first examined whether NbCNIH2 and NbCNIH5 could complement the defective localization pattern of BMV 1a-mC in *erv14*Δ cells. In *erv14*Δ cells, ~83% cells had disrupted BMV 1a-mC localization patterns such as dots and clusters, but only ~17% cells, as compared to ~56% in wt cells, had normal BMV 1a-mC localization pattern at the perinuclear ER membrane (Li et al., 2016). Each of NbCNIH2 and NbCNIH5 was expressed from a low-copy-number plasmid under the control of *ERV14* endogenous promoter to achieve a similar expression level to endogenous Erv14. BMV 1a-mC was then expressed along with each NbCNIH in *erv14*Δ cells (Figure 4.2A). We found that yeast cells expressing NbCNIH2 had ~56%, and NbCNIH5 had ~53% of cells showing a ring pattern of BMV 1a-mC. These numbers were similar to that expressing wt Erv14 (~59%), with more than 2-fold increase in all three cases as compared to those expressing an empty vector (Figure 4.2B). We concluded that NbCNIH2 and NbCNIH5 are functionally equivalent to Erv14 in yeast.

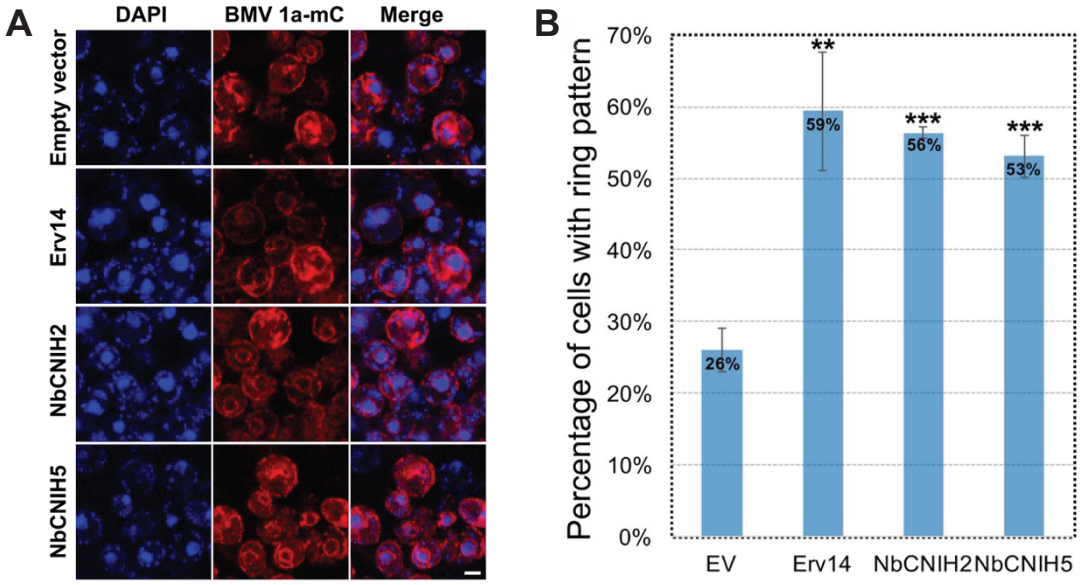


**Figure 4.2. NbCNIH2 and NbCNIH5 complement the defective distribution of BMV 1a-mC in *erv14*Δ mutant cells.**

**(A)** Confocal microscopic images of *erv14*Δ cells when BMV 1a-mC was co-expressed with an empty vector, or with Erv14, NbCNIH2 or NbCNIH5. Representative images of BMV 1a-mC localizations are shown. Nuclei were stained with DAPI (blue). Scale bar: 2 μm. **(B)** Percentage of cells with the BMV 1a-mC ring distribution pattern in *erv14*Δ cells when co-expressed with an empty vector (n=1352), or with Erv14 (n=1285), NbCNIH2 (n=1331) or NbCNIH5 (n=1258). Error bars represent standard deviation. $^{**}P<0.01$ and $^{***}P<0.001$ (ANOVA single factor analysis of percentage of BMV 1a-mC ring pattern in *erv14*Δ cells when supplemented with Erv14, NbCNIH2 or NbCNIH5 as comparison to that with an empty vector). Statistical analysis of BMV 1a localization pattern was performed as previously described (Li et al., 2016).

### 4.3.3 Knockdown of *NbCNIH5* remodels ER membrane

In order to gain a better understanding of the cellular functions of plant CNIHs, I explored the roles of NbCNIH2 and NbCNIH5 in plant development. I first designed primers to knockdown *NbCNIH2* and *NbCNIH5* by using tobacco rattle virus (TRV)-based VIGS approach, then performed RT-PCR to check gene expression levels of *NbCNIH2* and *NbCNIH5* in the knockdown plants by using gene-specific primers. The RT-PCR result

showed that knockdown of *NbCNIH2* reduced gene expression level of *NbCNIH2* not *NbCNIH5* as compared to the vector control of *GFP* knockdown plant (Figure 4.3). As for *NbCNIH5* knockdown plant, the gene expression level of *NbCNIH5* was reduced but not *NbCNIH2* as compared to the vector control of *GFP* knockdown plant (Figure 4.3). Therefore, a specific and effective knockdown of the target gene expression by VIGS approach has been achieved.

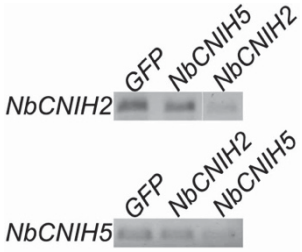


**Figure 4.3. RT-PCR analysis of *NbCNIH2* and *NbCNIH5* in the knockdown plants.**
RT-PCR analysis of *NbCNIH2* and *NbCNIH5* expression levels in the total RNA extracted from *GFP*, *NbCNIH2* and *NbCNIH5* knockdown plants. cDNA of *GFP*, *NbCNIH2* and *NbCNIH5* were reverse transcribed from 160 ng total RNA respectively, and then used as templates for PCR amplification of *NbCNIH2* and *NbCNIH5* with 25 cycles and 24 cycles, respectively.

I next examined the ER morphology of *NbCNIH2* and *NbCNIH5* knockdown plants. Surprisingly, a dramatic ER membrane rearrangement was observed in *NbCNIH5* but not *NbCNIH2* knockdown plants (Figure 4.4). Normally, the peripheral ER membrane contains ER tubules and ER sheets, which were observed in *NbCNIH2* knockdown plant (Figure 4.4). However, the remodeled-ER membrane structures such as dotted or clustered ER structures were observed in *NbCNIH5* knockdown cells (Figure 4.4). In some cells, the dotted structures were still connected to each other by ER tubules but in some other cells, dotted structures were not connected by ER tubules, suggesting that knocking down *NbCNIH5* blocked ER tubules in particular.

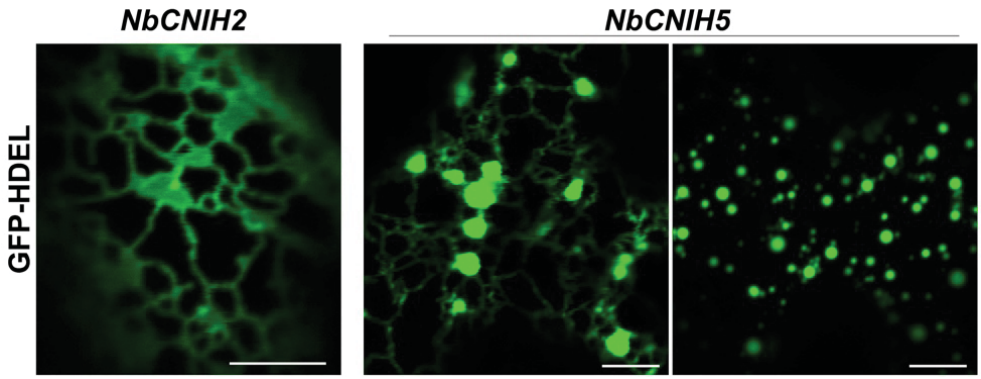


**Figure 4.4. ER morphology in leaf epidermal cells with the gene expression of *NbCNIH2* or *NbCNIH5* knocked down.**

Confocal microscopic images of *NbCNIH2* or *NbCNIH5* knockdown cells expressing GFP-HDEL. Leaf samples were collected 2 days after infiltration. Note the dots were connected by ER tubules in the cell as shown in the middle. Scale bars: 5 μm.

### 4.3.4 Knockdown of *NbCNIH5* fragments ER membrane

To further characterize the remodeled-ER membrane structures in *NbCNIH5* knockdown plant, we performed fluorescence recovery after photobleaching (FRAP) analysis to determine whether those dotted ER structures were still connected with each other. FRAP analysis of normal ER structure in *NbCNIH2* knockdown plant demonstrated that the ER membrane is highly dynamic, as the GFP-HDEL signal intensity rapidly recovered from photobleaching within 2-3 seconds (Figure 4.5A, D). As shown in Figure 4.5A, the GFP signal intensity was bleached down to 45% ± 7% (n=3) but rapidly recovered to 73% ± 6% (n=3) in 2.4 seconds as compared to the prephotobleaching signal intensity (Figure 4.5D, a single representative example of FRAP analysis). FRAP analysis of dotted ER structures in many *NbCNIH5* knockdown cells demonstrated that those dotted ER membranes were completely separated from each other because no ER tubules connecting these dotted structures were observed (Figure 4.5B). This conclusion was reached because the GFP-

HDEL signal intensity, when bleached down, did not show any recovery even after 60 s (Figure 4.5D, a single representative of FRAP analysis). However, in some cells, ER tubules were still present and connected to the dotted ER structures. In such cells, GFP-HDEL signal was rapidly recovered within 2-3 seconds after photobleaching (Figure 4.5C). When bleached down to 50% ± 6% (n=3) of prephotobleaching signal intensity, GFP-HDEL signal recovered to 70% ± 9% (n=3) in 2.4 seconds (Figure 4.5D), a recovery rate that is similar to that of normal ER membranes. Therefore, the results suggest that NbCNIH5 plays an critical role in maintaining the normal ER morphology, especially ER tubules.

### 4.3.5 CNI proteins are required for cortical ER tubule maintenance in yeast

The unexpected role of NbCNIH5 in maintaining ER morphology in plant stimulated us to test whether this surprising role of CNI protein in ER morphology maintenance is conserved in other organisms, such as yeast. Erv14 and Erv15 are the two CNIHs in yeast, so we examined the ER morphology in yeast *erv14*/*erv15*Δ double deletion mutants. We transformed an ER marker GFP-Scs2 into wt and *erv14*/*erv15*Δ cells. As expected, the ER tubules at the cortical ER region were disrupted in the *erv14*/*erv15*Δ mutant as compared to wt (Figure 4.6). However, the perinuclear ER membrane was not affected in *erv14*/*erv15*Δ cells, because the ring localization pattern of GFP-Scs2 was observed in both wt and *erv14*/*erv15*Δ mutant cells (Figure 4.6). Therefore, this result suggests that CNI proteins play a conserved and important role in maintaining ER tubules in plant and yeast.

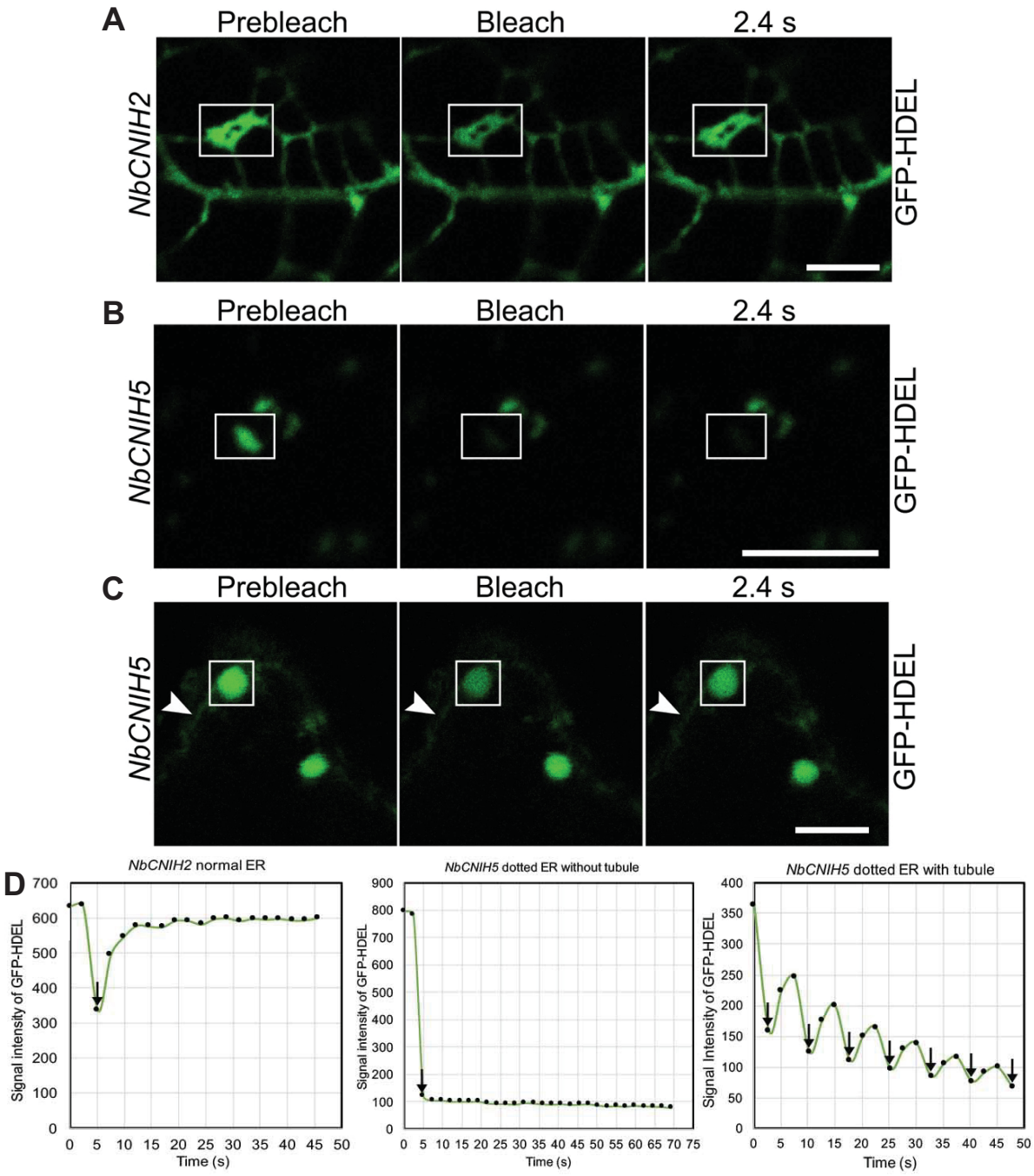


**Figure 4.5. FRAP analysis of ER membrane in leaf epidermal cells of *NbCNIH2* and *NbCNIH5* knockdown plants.**

**(A)** Representative FRAP analysis of ER morphology in *NbCNIH2* knockdown cells that had a highly dynamic ER membrane. Confocal microscopic images of *NbCNIH2* knockdown cells expressing GFP-HDEL, GFP-HDEL signal rapidly recovered from photobleaching within 2.4 s. **(B, C)** Representative FRAP analysis of dotted ER structures in *NbCNIH5* knockdown cells. Confocal microscopic images of *NbCNIH5* knockdown cells expressing GFP-HDEL, dotted ER structures did not recover after photobleaching if there were no ER tubules connecting those dotted ER structures

(B), or dotted ER structures rapidly recovered after photobleaching if ER tubules connected those dotted ER, white arrowhead indicates ER tubules (C). Leaf samples were collected 2 days after infiltration. The white boxes indicate the regions for photobleaching Scale bars: 5 μm. **(D)** Quantification of signal intensity of a single dotted structure of GFP-HDEL in (A), (B) and (C) during a 45 to 70-second period. Black arrows indicate the time point when performing photobleaching with a laser intensity of 80%.

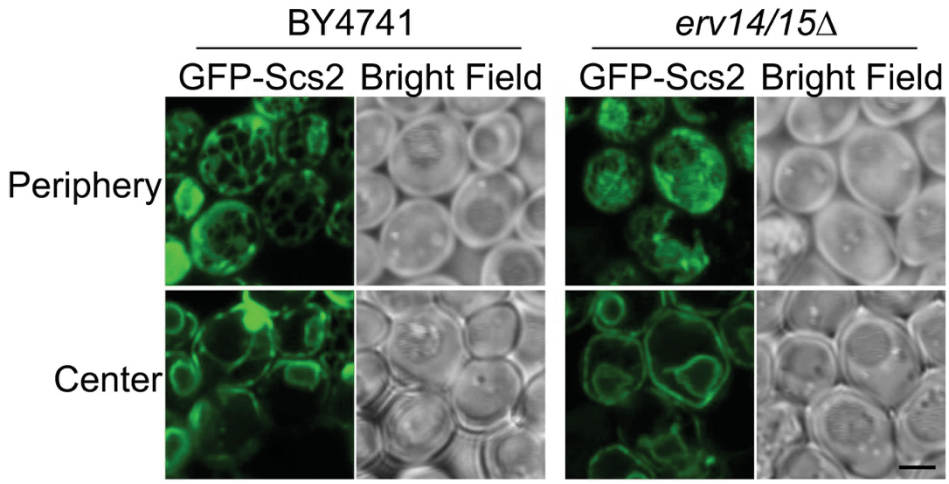


**Figure 4.6. ER morphology in yeast wt and *erv14/erv15*Δ cells.**

Confocal microscopic images of the distribution of GFP-Scs2 (an ER marker) in wt (BY4741) and *erv14/erv15Δ* cells. Live cells were collected for imaging with focuses at the peripheral and central regions of yeast cells. Scale bar: 2 μm.

## 4.4 Discussion

The ER is a complex organelle that composed of nuclear envelope and peripheral ER domains. ER membranes play important cellular roles in protein and lipid synthesis, protein quality control, and calcium storage and stress response (Schwarz and Blower, 2016). The ER morphology is well-maintained by membrane-shaping protein families, including RTNs and DP1/Yop1 proteins, a dynamin-related GTPase family protein and Lnp proteins, and furthermore, it also requires a balance between ATL and RTNs to maintain the ER morphology, otherwise it will cause ER fragmentation (Wang et al., 2016). Therefore, there

is a tight cooperation among the abundance of membrane-shaping proteins to determine and maintain the ER structures, and furthermore, safeguard normal cellular functions.

Previous studies have shown that many conditional changes cause the ER fragmentation in mammalian cells. For instance, it can cause a reversible ER fragmentation by increasing the cytosolic calcium concentration in cells (Subramanian and Meyer, 1997). This is probably because that calcium alters membrane curvature to favor the formation of vesicles and other structures, by binding the divalent calcium cations to and hence neutralizing the negative charge of phospholipid head groups (Mullock and Luzio, 2013). Alternatively, it can also induce a reversible ER fragmentation in nerve cells by the stimulation of a glutamate receptor and ion channel protein called N-methyl-D-aspartate receptor (NMDA receptor), or the activation of non-NMDA receptor with the glutamate receptor agonist kainic acid, or a high concentration of potassium (Kucharz et al., 2009; Kucharz et al., 2011; Sokka et al., 2007). Although the normal ER morphology is required for cellular functions, the fragmented ER might still be functionally connected with each other by the vesicular transportation. At least, this has been demonstrated in cells when expressing a mutant version of serine protease inhibitor, Z-$\alpha_1$-antitrypsin, which causes ER fragmentation (Dickens et al., 2016). Therefore, many factors are involved in ER morphology maintenance, including the abundance of membrane-shaping proteins, calcium or potassium concentration, and glutamate receptor.

Here, I report a novel role of CNI proteins in maintaining ER morphology in *N. benthamiana* and yeast. Knockdown of *NbCNIH5* remodeled ER membranes to form dotted ER structures and led to the collapse of ER tubules, which subsequently caused the ER

fragmentation in plant (Figure 4.4 and 4.5). Deletions of *ERV14* and its paralog *ERV15* in yeast disrupted ER tubules at the cortical ER region (Figure 4.6). In tobacco plant, overexpression of RTNLB13, a member of RTNLB family in *Arabidopsis thaliana*, caused ER lumen fragmentation in leaf epidermal cells, by inducing constrictions into the membrane and reducing diffusion of soluble proteins within ER lumen (Tolley et al., 2008). This phenotype in *Arabidopsis* is consistent with that in mammals, as the abundance and balance of membrane-shaping proteins play an important role in ER morphology maintenance.

Phylogenetic analysis of NbCNIH5 and human CNIHs showed that NbCNIH5 is closely related to HsCNIH2 and HsCNIH3 (Figure 4.1C). HsCNIH2 and HsCNIH3 play important roles in trafficking and activity of a group of glutamate receptors in mammalian central nervous system, termed AMPA (α-amino-3-hydroxy-5-methyl-4-isoxazole propionic acid) receptors (Herring et al., 2013; Jackson and Nicoll, 2009; Schwenk et al., 2009). These receptors have four subunits, which assemble into heterop or homotetramers, and mediate the fast-excitatory signal transmission. As cargo receptors, HsCNIH2 and HsCNIH3 facilitate the incorporation of AMPA receptors into COPII vesicles. At the same time, HsCNIH2 and HsCNIH3 will travel to the plasma membranes as auxiliary factors of AMPA receptor complexes (Haering et al., 2014). Therefore, it is possible that NbCNIH5 functions as a regulator or chaperone of glutamate receptors in addition to its roles as a cargo receptor involved in the trafficking of regulators of glutamate receptor in plant.

Nevertheless, it is less possible that NbCNIH5 functions as a glutamate receptor in plant, because one of the well-known functions of glutamate receptor-like proteins (GLRs) in plants

is to facilitate calcium influx across the plasma membrane (Kwaaitaal et al., 2011; Li et al., 2013; Michard et al., 2011; Qi et al., 2006). Furthermore, it requires the activation of glutamate receptor or calcium influx to induce ER fragmentation in nerve cells. Therefore, if NbCNIH5 functions as a glutamate receptor, we might not expect an increased cellular calcium concentration to cause ER fragmentation in *NbCNIH5* knockdown plant. However, we found that knockdown of *NbCNIH5* caused ER fragmentation in leaf epidermal cells of *N. benthamiana* (Figure 4.4 and 4.5). Based on these results, it is more likely that NbCNIH5 functions as a regulator or chaperone of glutamate receptor and negatively regulates glutamate receptor. It is also likely that NbCNIH5 functions as a cargo receptor involved in the trafficking of regulators of glutamate receptor. Either way, it fits our working model that knockdown of *NbCNIH5* might activate the downstream function of glutamate receptors, increase the cytoplasmic calcium concentration, and eventually cause ER stress to induce ER fragmentation. It is also possible that NbCNIH5 functions as a membrane-shaping protein directly involved in ER morphology maintenance, or as a cargo receptor involved in membrane-shaping protein distribution and thus, to indirectly influence ER morphology. In this scenario, knockdown of *NbCNIH5* might disturb the balance or distribution of membrane-shaping proteins to cause ER fragmentation.

Therefore, I hypothesize that NbCNIH5 might function as a cargo receptor involved in the trafficking of a regulator or chaperone of glutamate receptor, or that NbCNIH5 itself as a regulator or chaperone of glutamate receptor. NbCNIH5 or its cargos negatively regulate glutamate receptor and thus, affect the balance of calcium concentration in cells and cause

ER stress to fragment ER membrane. However, all of the possibilities should be await tested in our future study (discussed in Chapter 6). In conclusion, CNI proteins play a crucial role in maintaining ER morphology in *N. benthamiana* and yeast, indicating that CNIHs might be also involved in ER morphology maintenance in *Drosophila* and mammals.

## 4.5 Materials and methods

### 4.5.1 Plant growth conditions and yeast cell culture

The growth conditions of *N. benthamiana* plants were the same as in Chapter 3. Yeast strain YPH500 with *ERV14* deletion mutant was used in the complementation experiment on BMV 1a-mC localization, HA-tagged Erv14, NbCNIH2 and NbCNIH5 were expressed under the control of *ERV14* endogenous promoter from a low-copy-number plasmid. The yeast strain BY4741 and its *ERV14* and *ERV15* double deletion mutant were transformed with an ER marker GFP-Scs2 to examine the ER tubules at the cortical ER region of the resulting yeast cells. The yeast cells were grown in defined synthetic medium containing 2% galactose as a carbon source at 30°C. Uracil, or leucine and uracil were omitted to maintain plasmid(s) selection. Cells were grown in galactose medium for two passages (36 to 48 h) and harvested at the exponential stage with the optical density at 600 nm ($OD_{600}$) between 0.4 and 1.0.

### 4.5.2 Cloning of *NbCNIH* fragments and TRV-based VIGS in *N. benthamiana*

The knockdown of target gene expression of *NbCNIH2* and *NbCNIH5* in *N. benthamiana* was performed by using the TRV-based VIGS method (Senthil-Kumar and Mysore, 2014). A 400 bp fragment of *NbCNIH2* coding region with EcoRI and XhoI was amplified by using

primers gcgggatccgaattcATGGCAGATGTTTGGGCAT and gcgggatccctcgagCTTCC AAGGCACTGTAGA, and a 292 bp fragment of *NbCNIH5* coding region with EcoRI and XhoI was amplified by using primers gcgggatccgaattcGTGCTTGGCAGACCTT GAAT and gcgggatccctcgagCGAAAAGGCAAGAAGTATCA. The DNA fragments of NbCNIH2 and NbCNIH5 were verified by sequencing before cloning into the pTRV2 vector by T4 ligase (New England Biolabs) via the EcoRI and XhoI sites.

The resulting pTRV2-NbCNIH2 and pTRV2-NbCNIH5 vectors were transformed into the agrobacterium strain GV3101 by a modified freeze/thaw method (Höfgen and Willmitzer, 1988). The pTRV1 with pTRV2-NbCNIH2 or NbCNIH5 were agroinfiltrated into the leaf epidermal cells of *N. benthamiana* at a concentration of $OD_{600}$ value 0.25 for each TRV genomic RNA to knockdown the gene expression levels of *NbCNIH2* and *NbCNIH5*. The pTRV1 along with pTRV2-PDS were used as a technical control while with pTRV2-GFP as a negative vector control. Transient expression of GFP-HDEL was performed 2-3 weeks after infiltration when the *PDS* knockdown plant displayed bleaching phenotype on leaves.

### 4.5.3 Plant RNA extraction and RT-PCR analysis

The leaf tissues of VIGS-mediated *NbCNIH2*, *NbCNIH5* and *GFP* knockdown plants were harvested and grounded into fine powders with liquid nitrogen. Plant RNA was extracted from the fine powder of leaf tissues by using a hot phenol method (Kohrer and Domdey, 1991). The total RNA was used for RT-PCR analysis to check the gene expression levels of *NbCNIH2* and *NbCNIH5* in the knockdown plants. Briefly, genomic DNA was removed from RNA samples by RQ1 RNase-Free DNase (Promega, Cat. no. M610A)

digestion at 37°C for 30 min, and then incubated at 65°C for 10 min with RQ1 DNase Stop Solution (Promega, Cat. no. M199A) to terminate the reaction by inactivating the DNase. About 1600 ng DNase-treated plant RNA were used for cDNA synthesis by using iScript Select cDNA Synthesis kit (Bio-Rad, Cat. no. 170-8897), and 1/10 of the resulting cDNA were used as templates for PCR to amplify *NbCNIH2* with 25 cycles using gene-specific primers AAGTGGATCGGTTTCCTCG and GGAACTCTTGAAGCCAAATTT, and to amplify *NbCNIH5* with 24 cycles using gene-specific primers gcgggatccgaattcGTGCTTGGC AGACCTTGAAT and ATTCGTCCACAA TGCTCCA. All PCR reactions were performed along with a cDNA template that reverse transcribed from the RNA of *GFP* knockdown plant, a negative control for comparing to the gene expression levels of *NbCNIH2* and *NbCNIH5* in the knockdown plants.

### 4.5.4 Confocal microscopy and fluorescence recovery after photobleaching (FRAP) analysis

For the complementation experiment on BMV 1a-mC localization with NbCNIHs in yeast, 2 $OD_{600}$ unit cells were harvested and fixed with 4% (v/v) formaldehyde. The cell wall was removed by lyticase at 30°C for 1 h and permeabilized with 0.1% Triton X-100 for 15 min at room temperature. The nuclei were stained with DAPI for 10 min and samples were observed using Argon/HeNe lasers with a 100 x oil immersion objective (Alpha Plan-Apochromat 100x/1.46 Oil DIC) of a Zeiss LSM Scanning 880 microscope or a Zeiss epifluorescence microscope (Observer.Z1) at the Fralin microscopy facility at Virginia Tech. For the examination of ER tubules in yeast, the live cells were harvested and imaged

immediately using the same setting of Zeiss LSM Scanning 880 microscope as for the imaging of fixed yeast cells.

The leaf tissues of *N. benthamiana* were collected and immersed with water, and imaged at room temperature using Argon/HeNe lasers with a 40 x water immersion objective (C-Apochromat 40x/1.2 W) of a Zeiss LSM Scanning 880 microscope at the Fralin microscopy facility at Virginia Tech. To assess the continuity of ER lumen, FRAP analysis was performed with the Zeiss imaging system ZEN lite software. All the images were processed with Adobe Photoshop CS6 software.

## 4.6 References

**Bombarely, A., Rosli, H. G., Vrebalov, J., Moffett, P., Mueller, L. A. and Martin, G. B.** (2012). A draft genome sequence of Nicotiana benthamiana to enhance molecular plant-microbe biology research. *Mol Plant Microbe In* **25**, 1523-1530.

**Chen, S., Novick, P. and Ferro-Novick, S.** (2012). ER network formation requires a balance of the dynamin-like GTPase Sey1p and the Lunapark family member Lnp1p. *Nat Cell Biol* **14**, 707-716.

**Dickens, J. A., Ordóñez, A., Chambers, J. E., Beckett, A. J., Patel, V., Malzer, E., Dominicus, C. S., Bradley, J., Peden, A. A., Prior, I. A. et al.** (2016). The endoplasmic reticulum remains functionally connected by vesicular transport after its fragmentation in cells expressing Z-α1-antitrypsin. *FASEB J* **30**, 4083-4097.

**Evans, D. E., Shvedunova, M. and Graumann, K.** (2011). The nuclear envelope in the plant cell cycle: structure, function and regulation. *Ann Bot-London* **107**, 1111-1118.

**Haering, S., Tapken, D., Pahl, S. and Hollmann, M.** (2014). Auxiliary subunits: shepherding AMPA receptors to the plasma membrane. *Membranes* **4**, 469-490.

**Herring, Bruce E., Shi, Y., Suh, Young H., Zheng, C.-Y., Blankenship, Sabine M., Roche, Katherine W. and Nicoll, Roger A.** (2013). Cornichon proteins determine the subunit composition of synaptic AMPA receptors. *Neuron* **77**, 1083-1096.

**Herzig, Y., Sharpe, H. J., Elbaz, Y., Munro, S. and Schuldiner, M.** (2012). A systematic approach to pair secretory cargo receptors with their cargo suggests a mechanism for cargo selection by Erv14. *PLoS Biol* **10**, e1001329.

**Hetzer, M. W., Walther, T. C. and Mattaj, I. W.** (2005). Pushing the envelope: structure, function, and dynamics of the nuclear periphery. *Annu Rev Cell Dev Biol* **21**, 347-380.

**Höfgen, R. and Willmitzer, L.** (1988). Storage of competent cells for Agrobacterium transformation. *Nucleic Acids Res* **16**, 9877.

**Hu, J., Shibata, Y., Voss, C., Shemesh, T., Li, Z., Coughlin, M., Kozlov, M. M., Rapoport, T. A. and Prinz, W. A.** (2008). Membrane proteins of the Endoplasmic Reticulum induce high-curvature tubules. *Science* **319**, 1247-1250.

**Hu, J., Shibata, Y., Zhu, P.-P., Voss, C., Rismanchi, N., Prinz, W. A., Rapoport, T. A. and Blackstone, C.** (2009). A class of dynamin-like GTPases involved in the generation of the tubular ER network. *Cell* **138**, 549-561.

**Jackson, A. C. and Nicoll, R. A.** (2009). Neuroscience: AMPA receptors get 'pickled'.

*Nature* **458**, 585-586.

**Jones, D. T., Taylor, W. R. and Thornton, J. M.** (1992). The rapid generation of mutation data matrices from protein sequences. *Comput Appl Biosci* **8**, 275-282.

**Kohrer, K. and Domdey, H.** (1991). Preparation of high molecular weight RNA. *Methods Enzymol* **194**, 398-405.

**Kucharz, K., Krogh, M., Ng, A. N. and Toresson, H.** (2009). NMDA receptor stimulation induces reversible fission of the neuronal endoplasmic reticulum. *PLoS ONE* **4**, e5250.

**Kucharz, K., Wieloch, T. and Toresson, H.** (2011). Potassium-induced structural changes of the endoplasmic reticulum in pyramidal neurons in murine organotypic hippocampal slices. *J Neurosci Res* **89**, 1150-1159.

**Kumar, S., Stecher, G. and Tamura, K.** (2016). MEGA7: Molecular evolutionary genetics analysis version 7.0 for bigger datasets. *Mol Biol Evol* **33**, 1870-1874.

**Kwaaitaal, M., Huisman, R., Maintz, J., Reinstädler, A. and Panstruga, R.** (2011). Ionotropic glutamate receptor (iGluR)-like channels mediate MAMP-induced calcium influx in Arabidopsis thaliana. *Biochem J* **440**, 355-373.

**Li, F., Wang, J., Ma, C., Zhao, Y., Wang, Y., Hasi, A. and Qi, Z.** (2013). Glutamate receptor-like channel3.3 is involved in mediating glutathione-triggered cytosolic calcium transients, transcriptional changes, and innate immunity responses in Arabidopsis. *Plant Physiol* **162**, 1497-1509.

**Li, J., Fuchs, S., Zhang, J., Wellford, S., Schuldiner, M. and Wang, X.** (2016). An unrecognized function for COPII components in recruiting the viral replication protein BMV 1a to the perinuclear ER. *J Cell Sci* **129**, 3597-3608.

**Michard, E., Lima, P. T., Borges, F., Silva, A. C., Portes, M. T., Carvalho, J. E., Gilliham, M., Liu, L.-H., Obermeyer, G. and Feijó, J. A.** (2011). Glutamate receptor–like genes form Ca2+ channels in pollen tubes and are regulated by pistil D-serine. *Science* **332**, 434-437.

**Mullock, B. M. and Luzio, J. P.** (2013). Theory of organelle biogenesis: a historical perspective. pp 1-18.

**Nziengui, H., Bouhidel, K., Pillon, D., Der, C., Marty, F. and Schoefs, B.** (2007). Reticulon-like proteins in Arabidopsis thaliana: structural organization and ER localization. *FEBS Lett* **581**, 3356-3362.

**Pagant, S., Wu, A., Edwards, S., Diehl, F. and Miller, Elizabeth A.** (2015). Sec24 is a coincidence detector that simultaneously binds two signals to drive ER export. *Curr Biol* **25**, 403-412.

**Powers, J. and Barlowe, C.** (1998). Transport of Axl2p depends on Erv14p, an ER–vesicle

protein related to the drosophila cornichon gene product. *J Cell Biol* **142**, 1209-1222.

**Powers, J. and Barlowe, C.** (2002). Erv14p directs a transmembrane secretory protein into COPII-coated transport vesicles. *Mol Biol Cell* **13**, 880-891.

**Puhka, M., Vihinen, H., Joensuu, M. and Jokitalo, E.** (2007). Endoplasmic reticulum remains continuous and undergoes sheet-to-tubule transformation during cell division in mammalian cells. *J Cell Biol* **179**, 895-909.

**Qi, Z., Stephens, N. R. and Spalding, E. P.** (2006). Calcium entry mediated by GLR3.3, an Arabidopsis glutamate receptor with a broad agonist profile. *Plant Physiol* **142**, 963-971.

**Rosas-Santiago, P., Lagunas-Gómez, D., Barkla, B. J., Vera-Estrella, R., Lalonde, S., Jones, A., Frommer, W. B., Zimmermannova, O., Sychrová, H. and Pantoja, O.** (2015). Identification of rice cornichon as a possible cargo receptor for the Golgi-localized sodium transporter OsHKT1;3. *J Exp Bot* **66**, 2733-2748.

**Schwarz, D. S. and Blower, M. D.** (2016). The endoplasmic reticulum: structure, function and response to cellular signaling. *Cell Mol Life Sci* **73**, 79-94.

**Schwenk, J., Harmel, N., Zolles, G., Bildl, W., Kulik, A., Heimrich, B., Chisaka, O., Jonas, P., Schulte, U., Fakler, B. et al.** (2009). Functional proteomics identify cornichon proteins as auxiliary subunits of AMPA receptors. *Science* **323**, 1313-1319.

**Senthil-Kumar, M. and Mysore, K. S.** (2014). Tobacco rattle virus–based virus-induced gene silencing in Nicotiana benthamiana. *Nat Protoc* **9**, 1549-1562.

**Shibata, Y., Shemesh, T., Prinz, W. A., Palazzo, A. F., Kozlov, M. M. and Rapoport, T. A.** (2010). Mechanisms determining the morphology of the peripheral ER. *Cell* **143**, 774-788.

**Shibata, Y., Voeltz, G. K. and Rapoport, T. A.** (2006). Rough sheets and smooth tubules. *Cell* **126**, 435-439.

**Shibata, Y., Voss, C., Rist, J. M., Hu, J., Rapoport, T. A., Prinz, W. A. and Voeltz, G. K.** (2008). The reticulon and Dp1/Yop1p proteins form immobile oligomers in the tubular endoplasmic reticulum. *J Biol Chem* **283**, 18892-18904.

**Sokka, A.-L., Putkonen, N., Mudo, G., Pryazhnikov, E., Reijonen, S., Khiroug, L., Belluardo, N., Lindholm, D. and Korhonen, L.** (2007). Endoplasmic reticulum stress inhibition protects against excitotoxic neuronal injury in the rat brain. *J Neurosci* **27**, 901-908.

**Subramanian, K. and Meyer, T.** (1997). Calcium-induced restructuring of nuclear envelope and Endoplasmic Reticulum calcium stores. *Cell* **89**, 963-971.

**Taddei, A. and Gasser, S. M.** (2012). Structure and function in the budding yeast nucleus. *Genetics* **192**, 107-129.

**Tolley, N., Sparkes, I. A., Hunter, P. R., Craddock, C. P., Nuttall, J., Roberts, L. M., Hawes, C., Pedrazzini, E. and Frigerio, L.** (2008). Overexpression of a plant reticulon remodels the lumen of the cortical endoplasmic reticulum but does not perturb protein transport. *Traffic* **9**, 94-102.

**Voeltz, G. K., Prinz, W. A., Shibata, Y., Rist, J. M. and Rapoport, T. A.** (2006). A class of membrane proteins shaping the tubular endoplasmic reticulum. *Cell* **124**, 573-586.

**Wang, S., Tukachinsky, H., Romano, F. B. and Rapoport, T. A.** (2016). Cooperation of the ER-shaping proteins atlastin, lunapark, and reticulons to generate a tubular membrane network. *eLife* **5**, e18605.

**Westrate, L., Lee, J., Prinz, W. and Voeltz, G.** (2015). Form follows function: the importance of endoplasmic reticulum shape. *Annu Rev Biochem* **84**, 791-811.

**Yang, Y. S. and Strittmatter, S. M.** (2007). The reticulons: a family of proteins with diverse functions. *Genome Biol* **8**, 234-234.

# Chapter 5 Critical roles of Cornichon proteins in *Arabidopsis* pollen development and bacterial pathogen infection

## 5.1 Abstract

Pollen development is strictly controlled by a complex network in a sequential and cooperative manner, whereas abnormal pollen development, including either abnormal pollen wall or pollen cell development, would be detrimental to seed plants during fertilization. Cornichon (CNI) proteins are structurally related transmembrane proteins among eukaryotes, from Erv14 in yeast to CNI homologs (CNIHs) in plants and mammals. Erv14 functions as a cargo receptor of COPII vesicles that is involved in the ER exit of cargo proteins. However, we have very limited understanding of cellular functions of plant CNIHs. Here, I show that CNIHs of *Arabidopsis thaliana* (AtCNIHs) are unexpectedly involved in pollen development and are important for bacterial pathogen infection. Heterozygous *atcnih1* and *atcnih4* mutants displayed abnormal pollen development with reduced starch accumulation in pollen, and aberrant pollen morphology with blebs protruding away from pollen upon the $I_2$-KI staining. Homozygous *atcnih2*, *atcnih3* and *atcnih5* mutant plants grew just like wild-type (wt) plants but exhibited a reduced susceptibility to bacterial pathogen *Pseudomonas syringae* pv. *tomato* DC3000 (*Pst* DC3000). Our data suggest that AtCNIHs function as cargo receptors and are involved in the trafficking of cargo proteins that are important for pollen development or bacterial pathogen infection.

## 5.2 Introduction

The pollen grain is the male haploid microgametophyte in seed plants, which comprises a bi- or tri-nucleate cell covered with a pollen wall. Both bicellular and tricellualr pollen grains possess a large vegetative cell. Bicellular pollen grain contains a single generative cell while tricellular pollen grain contains a pair of sperm cells. The pollen wall protects male gamethophytes from microbial attack and environmental stresses, as well as facilitates pollination by attaching to insect pollinators and adhesion to the stigmatic surfaces. The pollen wall is made up of two layers with exine for the outer layer and intine for the inner layer. The exine is composed of a chemically resistant polymer sporopollenin and divided into an outer sculptured layer, sexine that contains tectum and bacula, and an inner unsculptured layer, nexine that covers the intine. The exine carries all the morphological traits that are necessary for pollen identification, while the cavities of exine sculptures are filled with a lipid-rich pollen coat. The intine is mainly made of pectin and cellulose that are very similar to the primary composition of common plant cell walls, and plays important roles in maintaining structural integrity of pollen cell. Underneath the intine is the plasma membrane and cytoplasm of pollen cell (Blackmore et al., 2007; Edlund et al., 2004; Frenguelli, 2003; Jiang et al., 2013; Quilichini et al., 2015).

The processes of pollen wall development are controlled by a complex regulatory network. There are four distinct cell layers developed from the non-reproductive cells of anthers and composed of tapetum, middle layer, endothecium, and epidermis. The synthesis of exine wall is under the sporophytic control and requires at least three major developmental

processes, including primexine formation, callose wall formation and sporopollenin synthesis. The exine is developed from early microspore cytoplasm and tapetum. Furthermore, tapetum plays an important role in the synthesis and deposition of sporopollenin on the outer surface of pollen wall, because the sporopollenin is synthesized via catalytic reactions in tapetum and then deposited on the primexine and callose walls (Ariizumi and Toriyama, 2011; Quilichini et al., 2014). In contrast to the exine wall, the synthesis of intine wall is under the control of microspore cytoplasm and gametophytic gene expression from haploid microspore, and furthermore, is similar to plant cell wall formation that mainly associated with polysaccharide metabolism (Shi et al., 2015).

Pollen is produced inside anthers, following three developmental stages: microsporogenesis, post-meiotic development of microspores, and microspore mitosis (Gómez et al., 2015). Pollen mother cells undergo meiosis to produce tetrads of haploid unicellular microspores, and then microspores are released into the anther locule, a closed fluid-filled cavity, to start post-meiotic development. The free microspores expand themselves by forming a single large vacuole to displace the microspore nucleus to an eccentric position against the microspore wall, then the microspores undergo an asymmetric cell division to produce a larger vegetative cell and a smaller generative cell; moreover, the generative cell undergoes a symmetric cell division to produce two sperm cells (Gómez et al., 2015; Wilson and Zhang, 2009). Pollen produce male gametes and transfer them to ovules for double fertilization (Berger et al., 2008). Specifically, most pollen possess apertures, which are generally thin or opening parts of exine through which the pollen tube emerged from the

vegetative cell (Edlund et al., 2004; Frenguelli, 2003). Pollen tube is essential to transport and deliver the two sperm cells to embryo sac of ovule for double fertilization to produce embryo and endosperm respectively (Berger et al., 2008). There are three furrow-like equatorial apertures in *Arabidopsis* pollen, and the number of apertures is closely related to the survival of pollen. Previous study showed that the plasma membrane of pollen grain with more apertures is more likely to break than the ones from wt with three apertures in *Arabidopsis*, suggesting that there is a tradeoff between the number of apertures and the survival of pollen in plant (Prieu et al., 2016). Therefore, pollen development is vital to produce viable male gametes for fertilization in seed plants, and many cellular factors are essential to the biosynthesis and regulation of pollen development.

Plant pathogens evolve the ability to exploit cellular nutrient transportation machinery to compete with host cells for essential nutrients, including sugars, organic acids and metals in the apoplastic fluids, and colonize the intercellular spaces of plant cells (Jones and Wildermuth, 2011; Ma et al., 2017; Rico and Preston, 2008). As such, plant pathogens can promote their growth under favorable environmental conditions and nutrients in plants to cause serious diseases (Fatima and Senthil-Kumar, 2015). Importantly, successful pathogens have the capability of regulating the transport of plant nutrients across the plasma membrane to gain access to nutrients from the apoplast and at the same time suppressing plant immune responses to pathogen infection. The nutrient transporters residing on the plant plasma membrane are involved in nutrient efflux to the apoplast while targeted by plant pathogens to regulate the nutrient and metabolite contents in the apoplastic fluids for providing essential

nutrients to plant pathogens.

*Pseudomonas syringae* is a hemibiotrophic foliar pathogen and infects the aerial portions of plants. In a successful disease cycle, *P. syringae* strains live in two lifestyles that are spatially and temporally interconnected, with an initial epiphytic phase on plant surface and a subsequent endophytic phase in the apoplast after invading through plant openings such as wounds and stomata (Xin and He, 2013). *P. syringae* pv *tomato* (*Pst*) is a pathogenic agent that causes bacterial speck disease in tomato (*Solanum lycopersicon*), while the virulent strain *Pst* DC3000 is broadly used to infect *Arabidopsis* plants in current laboratory setting (Whalen et al., 1991). The *Pst* DC3000 produces polar flagella (15 nm in diameter) and a few surface appendages Hrp pili (8 nm in diameter) encoded by hypersensitive response and pathogenicity genes. Specifically, flagella are used for bacterial movement while Hrp pili are involved in protein secretion and regulation of bacterial type III secretion system during plant-bacterial interactions (He and Jin, 2003; Jin et al., 2001; Katagiri et al., 2002; Roine et al., 1997; Wei et al., 2000). More importantly, *Pst* DC3000 has the capability of manipulating plant nutrient transporters on the plasma membrane, such as sugar transporters, to acquire essential nutrients for its growth and proliferation (Chen et al., 2010; Wang et al., 2012; Yamada et al., 2016). Previous studies have demonstrated that *Pst* DC3000 uses virulence factors to alter host immune responses to bacterial infection, but we have very limited understanding of how *Pst* DC3000 affects host cellular machinery to regulate nutrient and metabolite contents in the apoplastic fluids during bacterial infection (Xin and He, 2013).

In yeast, about 45 proteins depend on Erv14 for their localizations to the plasma

membrane, such as transporters of glucose (Hxt2, Hxt3, Hxt5 and Hxt6), iron (Ftr1 and Fth1), copper (Qdr2), ammonium (Mep2 and Ato3) and plasma membrane ATP-binding cassette (Yor1, Snq2 and Pdr5) (Herzig et al., 2012; Pagant et al., 2015). Like other cargo receptors, Erv14 interacts with its client cargos and bridges them to COPII vesicles for the ER exit of cargo proteins and trafficking to their final destinations. Similarly, *Arabidopsis* AtCNIH5, one member of AtCNIHs, has been found to interact with ~500 cellular proteins in a yeast two-hybrid screen. These proteins include many transporters of amino acids, sugars, and metals (Jones et al., 2014). I hypothesize that AtCNIHs function as cargo receptors involved in the trafficking and distribution of nutrient transporters that are involved in *Pst* DC3000 infection. Furthermore, it is possible that *Pst* DC3000 might manipulate AtCNIHs to control the trafficking of nutrient transporters to favor bacterial growth. Interestingly, *Pst* DC3000 infection upregulates expression of sugar transporter SWEETs (sugars will eventually be exported transporters) in *Arabidopsis*. In addition, RNAi of rice *SWEET11* exhibited an enhanced resistance to bacterial pathogen (Chen et al., 2010). Interestingly, plants have developed a defense strategy by regulating sugar transporter activity to prevent nutrient loss and compete with pathogens for extracellular sugars. For instance, the phosphorylation-dependent regulation of sugar transporter 13 (STP13) for plant antibacterial defenses (Yamada et al., 2016). Specifically, STP13 physically associates with flagellin receptor flagellin-sensitive 2 and its co-receptor brassinosteroid insensitive 1-associated receptor kinase 1 (BAK1). Upon recognition of pathogen-associated molecular patterns during pathogen infection, BAK1 phosphorylates STP13 and enhances the monosaccharide uptake activity of STP13 to limit the amounts of sugars in the apoplast and deprive an energy source

for bacterial growth and proliferation (Chinchilla et al., 2007; Yamada et al., 2016). Therefore, it is promising to develop a novel strategy by manipulating nutrient transporters that are necessary for plant pathogen growth to make plants resistant or less susceptible to plant pathogens.

Here, I show that AtCNIHs play crucial roles in pollen development and bacterial pathogen infection. AtCNIH1 and AtCNIH4 are unexpectedly involved in pollen development, as some pollen in *atcnih1* and *atcnih4* heterozygous mutants were abnormal when stained with $I_2$-KI or when geminated. AtCNIH2, AtCNIH3 and AtCNIH5, on the other hand, are involved in bacterial pathogen infection because homozygous *atcnih2*, *atcnih3* and *atcnih5* mutant plants were less susceptible to *Pst* DC3000 than that of wt plants. Therefore, AtCNIHs might function as cargo receptors involved in the trafficking of nutrient transporters and/or plant pathogen defense-related proteins to the plasma membrane, and some CNIH-dependent cargos are required for pollen development or *Pst* DC3000 infection. Currently, researchers are trying to develop plants resistant to pathogens by manipulating host nutrient transporters. However, it may require the knockout or knockdown of several nutrient transporters simultaneously to achieve efficient and sustainable resistance. Since the trafficking of a group of nutrient transporters depends on AtCNIHs, we provide a proof of concept that it is possible to develop an alternate strategy to control plant pathogens by blocking the targeting of nutrient transporters with manipulating one or several AtCNIHs.

## 5.3 Results

### 5.3.1 Sequence analysis of AtCNIHs

CNI proteins are a conserved family of transmembrane proteins among eukaryotes and have been well studied in *Drosophila*, mammals and yeast (Bökel et al., 2006; Castro et al., 2007; Herring et al., 2013; Herzig et al., 2012; Powers and Barlowe, 1998; Powers and Barlowe, 2002; Roth et al., 1995; Sauvageau et al., 2014; Schwenk et al., 2009). There are five *CNIHs* in *A. thaliana* but their functions have not been studied. Among the five CNIHs, AtCNIH1, AtCNIH4 and AtCNIH5 can partially complement the defective localization of BMV 1a in yeast mutant lacking *ERV14* (*erv14Δ*) (Li et al., 2016). Nucleotide sequence analysis of *CNIHs* from yeast and *A. thaliana* showed that *AtCNIHs* shared less than 50% identity with *ERV14*. While *AtCNIH2* and *AtCNIH3* shared 90.77% identity (Figure 5.1A), neither could complement the defective localization of BMV 1a in *erv14Δ* cells (Li et al., 2016). Amino acid sequence alignment showed that CNIHs of *A. thaliana*, human (*Homo sapiens*) and yeast *Saccharomyces cerevisiae* were conserved throughout the length of the encoded proteins (Figure 5.1B). Phylogenetic analysis demonstrated that the AtCNIHs clustered into a single clade relative to human and yeast homologs. AtCNIH2 and AtCNIH3 evolved more recently than AtCNIH1, AtCNIH4 and AtCNIH5 (Figure 5.1C). This could be one of the reasons why AtCNIH1, AtCNIH4 and AtCNIH5, but not AtCNIH2 and AtCNIH3, could functionally complement the loss of Erv14 in yeast. Based on the sequence analysis of AtCNIHs and Erv14, AtCNIHs might function as cargo receptors to mediate the ER exit of cellular proteins en route to their targeted destinations.

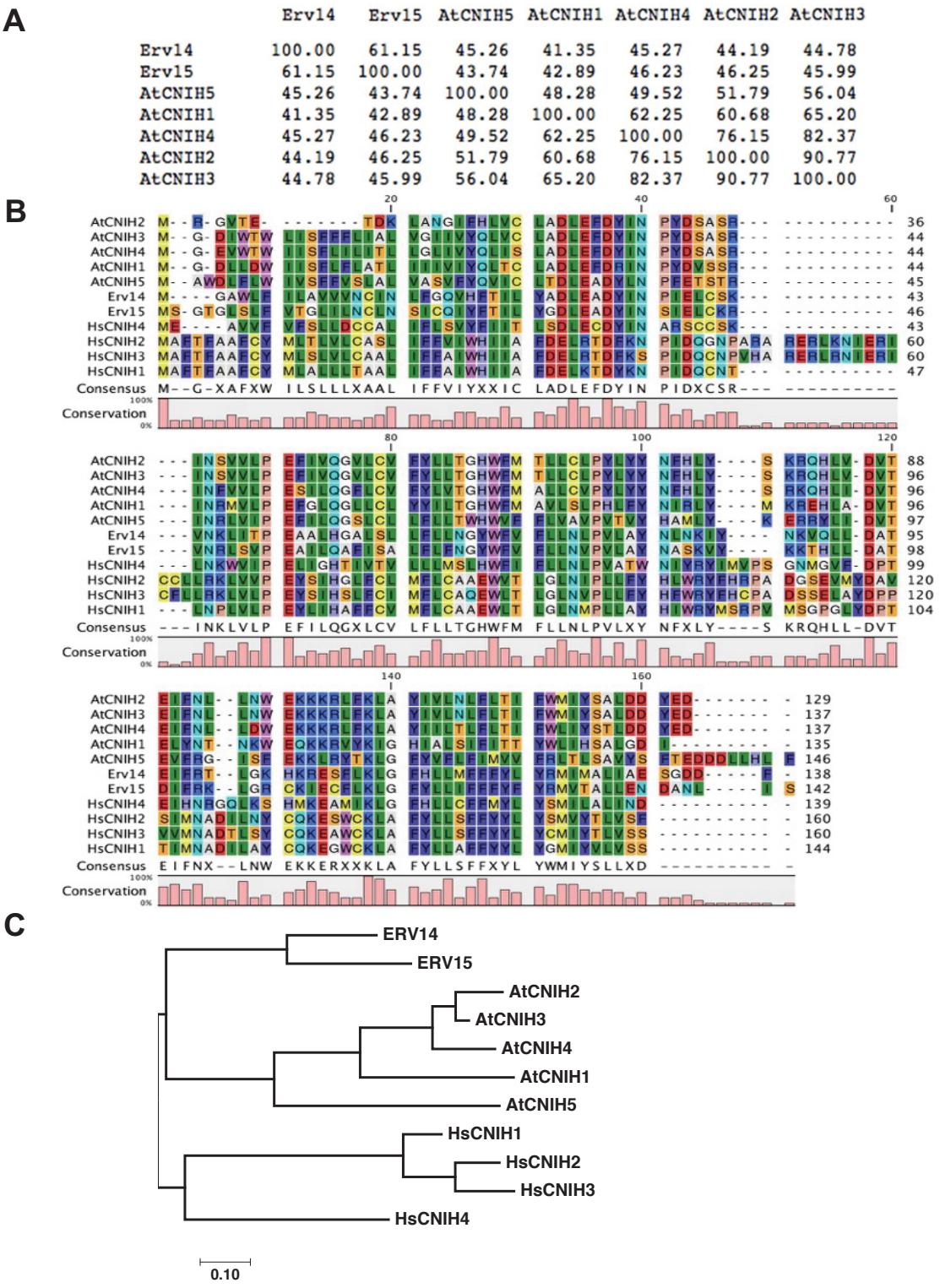


**Figure 5.1. Sequence analysis of CNIHs from *Arabidopsis thaliana*, human and yeast.**

**(A)** Percent identity of nucleotide sequence of *CNIHs* from *A. thaliana* and yeast. The accession numbers of AtCNIHs are AT4G12090 for *AtCNIH1*, AT1G12340 for *AtCNIH2*, AT1G12390 for *AtCNIH3*, AT1G62880 for *AtCNIH4* and AT3G12180 for *AtCNIH5*. The alignment of multiple nucleotide sequences was performed by using Clustal Omega. **(B)** Amino acid sequence alignment of

AtCNIHs, HsCNIHs, Erv14 and its paralog Erv15 was performed by using the CLC Sequence Viewer 7 software program. **(C)** Phylogenetic analysis of the amino acid sequences of AtCNIHs, HsCNIHs, Erv14 and its paralog Erv15 was performed by Maximum Likelihood method based on the JTT matrix-based model (Jones et al., 1992) using MEGA7 software program (Kumar et al., 2016). The tree with the highest log likelihood (-2191.3214) is shown and is drawn to scale.

### 5.3.2 Identification of homozygous *Arabidopsis cnih* knockout mutants

We obtained the seeds of *atcnih* T-DNA insertion mutants from The Arabidopsis Biological Resource Center (ABRC). They all are in the Columbia genetic background. The T-DNA insertion in *atcnih2*, *atcnih3* and *atcnih5* mutants confer kanamycin resistance, while *atcnih1* and *atcnih4* mutants have BASTA resistance. The T-DNA insertion sites of each mutant were shown in Figure 5.2.

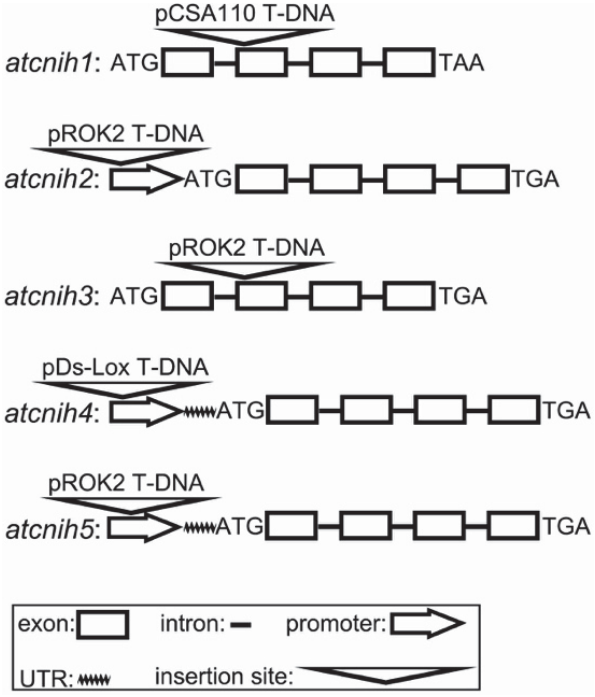


**Figure 5.2. Diagram of T-DNA insertion sites of *atcnih1*, *atcnih2*, *atcnih3*, *atcnih4* and *atcnih5* mutants.**

The annotated genome of each *atcnih* mutant, with T-DNA vectors and insertion sites are shown. The diagram was draw according to the annotations of each mutant from TAIR SeqViewer Whole Genome View, but not draw to the scale of actual size in each region.

BASTA and PCR analysis were employed for the selection of homozygous *atcnih1* and *atcnih4* mutants. On the other hand, PCR analysis was employed for the selection of homozygous *atcnih2*, *atcnih3* and *atcnih5* mutants because the expression of kanamycin resistant gene may be silenced in these mutants. Homozygous *atcnih2*, *atcnih3* and *atcnih5* mutants were identified and confirmed by PCR-assisted segregation analysis. No segregation of T-DNA insertion sites had occurred after two subsequent generations (Figure 5.3). No visible or significant phenotypic alterations were associated with homozygous *atcnih2*, *atcnih3* and *atcnih5* mutants, suggesting that *AtCNIH2*, *AtCNIH3* and *AtCNIH5* may play redundant roles in plant growth and development.

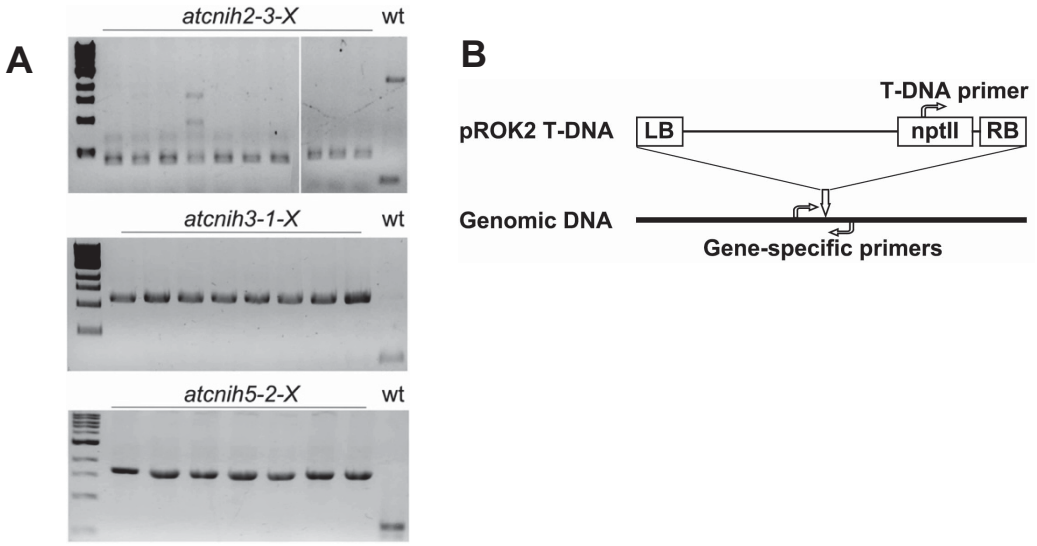


**Figure 5.3. PCR-based T-DNA segregation analysis of *atcnih2*, *atcnih3* and *atcnih5* mutants in the second generation of screening.**

**(A)** PCR analysis of *atcnih2*, *atcnih3* and *atcnih5* mutants. **(B)** Illustration of primers designed for PCR analysis. Gene-specific primers residing upstream and downstream of the T-DNA insertion sites, along with a primer from the nptII (kanamycin resistant gene) of pROK2 vector (Baulcombe et al., 1986) were designed for amplifying a DNA fragment, containing partial T-DNA vector and genomic DNA from the mutant. Genomic DNA was extracted from leaf tissues of mutants and wt and were used as templates for PCR analysis. All different plants from a given mutant showed no segregation of T-DNA insertion sites. The molecular marker is a 1 kb DNA ladder (New England Biolabs).

In contrast, no homozygous *atcnih1* or *atcnih4* mutant had been identified after three generations. PCR analysis was employed for the herbicide resistant *atcnih1* and *atcnih4* plants in the fourth generation. The result showed that *atcnih1* plants had segregation of T-DNA insertion sites in the 13 herbicide resistant plants, with 2 plants had nothing been amplified while 11 plants had a DNA fragment with a same size as wt (Figure 5.4A). It should be noted that although we tried primers from either left or right border of T-DNA vector, no DNA fragment, which is different from that of wt, was ever amplified from *atcnih1* mutant that (Figure 5.4A, B). These results suggest that *atcnih1* mutant might either has incorrect T-DNA insertion sites as indicated by that 11 of the herbicide resistant *atcnih1* plants had a wt band been amplified (Figure 5.4A). It is also possible that the mutant has multiple copies of T-DNA inserted in one target locus as shown by that 2 of the herbicide resistant *atcnih1* plants had no band been amplified (Figure 5.4A). If *atcnih1* mutant had multiple copies of T-DNA insertion, it is possible that these 2 *atcnih1* plants with no band been amplified might be homozygous, whereas the rest 11 *atcnih1* plants might be heterozygous. In contrast to *atcnih1* mutant, only one *atcnih4* plant survived after BASTA selection. This *atcnih4* plant had an expected T-DNA insertion site (Figure 5.4A), suggesting that this *atcnih4* plant might be a homozygous *atcnih4* mutant since no wt band had been amplified from this mutant (Figure 5.4A). Both *atcnih1* and *atcnih4* mutants need to be further analyzed to identify and confirm homozygous mutants. On the other hand, the results also suggest that *AtCNIH1* and *AtCNIH4* might be important for plant reproductive tissue development, including either ovule or pollen development, since we did not observe any visible or significant growth defective phenotype at the vegetative growth stage of *atcnih1*

and *atcnih4* mutants. Therefore, we hypothesized that *atcnih1* and *atcnih4* mutants might be homozygous lethal, or male lethal with abnormal pollen development, or female lethal with abnormal ovule development when harboring the T-DNA inserted gene versions of *AtCNIH1* and *AtCNIH4*.

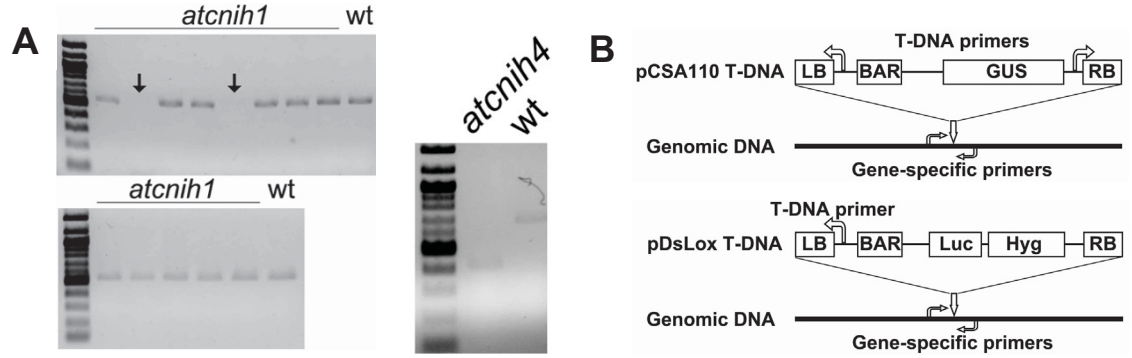


**Figure 5.4. PCR-based T-DNA segregation analysis of *atcnih1* and *atcnih4* mutants in the fourth generation of screening.**

**(A)** PCR analysis of *atcnih1* and *atcnih4* mutants. **(B)** Illustration of primers designed for PCR analysis. Gene-specific primers reside upstream and downstream of T-DNA insertion sites, along with primers from either left or right border of pCSA110 vector (McElver et al., 2001) were designed for amplifying a DNA fragment composed of partial T-DNA and genomic DNA from *atcnih1* mutant, or gene-specific primers along with a primer from the left border of pDs-Lox vector (Woody et al., 2007) were designed for amplifying a DNA fragment composed of partial T-DNA and genomic DNA from *atcnih4* mutant. Genomic DNA was extracted from leaf tissues of mutants and wt and were used as templates for PCR analysis. Black arrows indicate the potential *atcnih1* mutant with multiple copies of T-DNA insertion at the target site. The molecular marker is a 100 bp DNA ladder (New England Biolabs).

### 5.3.3 AtCNIH1 and AtCNIH4 are involved in pollen development

To identify the possible reasons for continued segregation of T-DNA insertion in *atcnih1* and *atcnih4* mutants, we checked the reproductive tissues of both mutants in the fourth generation of screening. We first checked whether there were any aborted seeds developed in

the siliques due to embryo lethality. However, no aborted seeds were observed in the siliques of mutant plants that were resistant to BASTA (Figure 5.5). This result suggested that: 1) ovule development is normal; 2) pollen with the T DNA-inserted copy of *AtCNIH1* or *4* is defective; 3) homozygous lethal might not be the reason for not getting homozygous mutants; 4) heterozygous mutants are generated between wt pollen and mutant ovule.

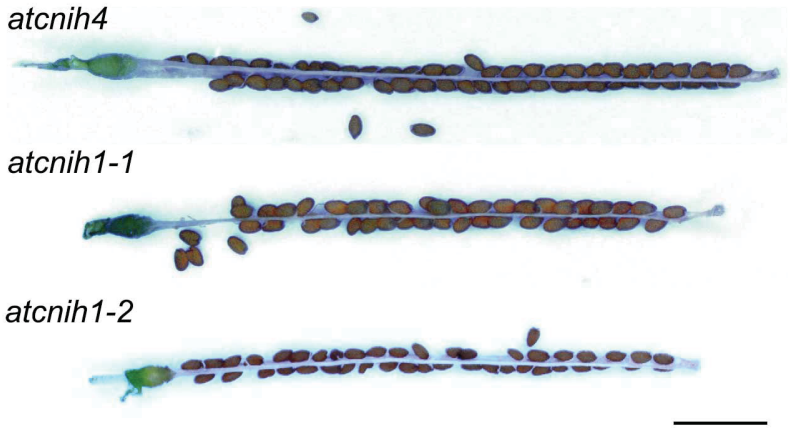


**Figure 5.5. Normal seeds developed in herbicide resistant *atcnih1* and *atcnih4* mutants.**
Stereomicroscopic images of siliques from *atcnih1* and *atcnih4* mutants that survived after BASTA selection. At least three siliques from each plant had been analyzed. The representative images of silique from each mutant are shown. Scale bar: 2 cm.

Next, we checked pollen of *atcnih1* and *atcnih4* mutants by iodine staining and pollen germination analysis, two approaches commonly used to test pollen functionality (Michard et al., 2011). To check the starch accumulation in pollen, we performed iodine staining ($I_2$-KI solution) of pollen grains from wt, *atcnih1* and *atcnih4* mutants. Iodine is often used as a starch indicator and stains subjects containing starch to blue or dark blue depending on the levels of starch. Incubating with $I_2$-KI solution, pollen of *atcnih1* and *atcnih4* mutants showed abnormal morphological traits with several blebs developed on pollen surface while less starch accumulation in pollen with light blue staining color, as compared to the round-

shaped and dark blue color of wt pollen (Figure 5.6A). Interestingly, the pollen grains from *atcnih4* mutant were not completely separated, as some pollen grains coupled together (Figure 5.6A, indicated by black arrow). There were at least two or three blebs developed on pollen surface of *atcnih1* and *atcnih4* mutants (Figure 5.6A). *In vitro* pollen germination analysis showed that pollen from both *atcnih1* and *atcnih4* mutants germinated faster than that from wt (Figure 5.6B). These results suggest that pollen development has been significantly affected and would lead to defective pollen when harboring the T-DNA-inserted *AtCNIH1* or *AtCNIH4* allele. In the pollen germination liquid medium or on germination plate, no blebs were ever observed, suggesting that the protrusions in $I_2$-KI-stained pollen grains were dependent on either $I_2$ or potassium. Therefore, it is more likely that the T-DNA-inserted *AtCNIH1* and *AtCNIH4* allele might not be able to be inherited through pollen to the offspring, but instead through ovule. Overall, these results suggest that both AtCNIH1 and AtCNIH4 are required for pollen development and their functions are not redundant, requiring each of them to maintain normal pollen functions.

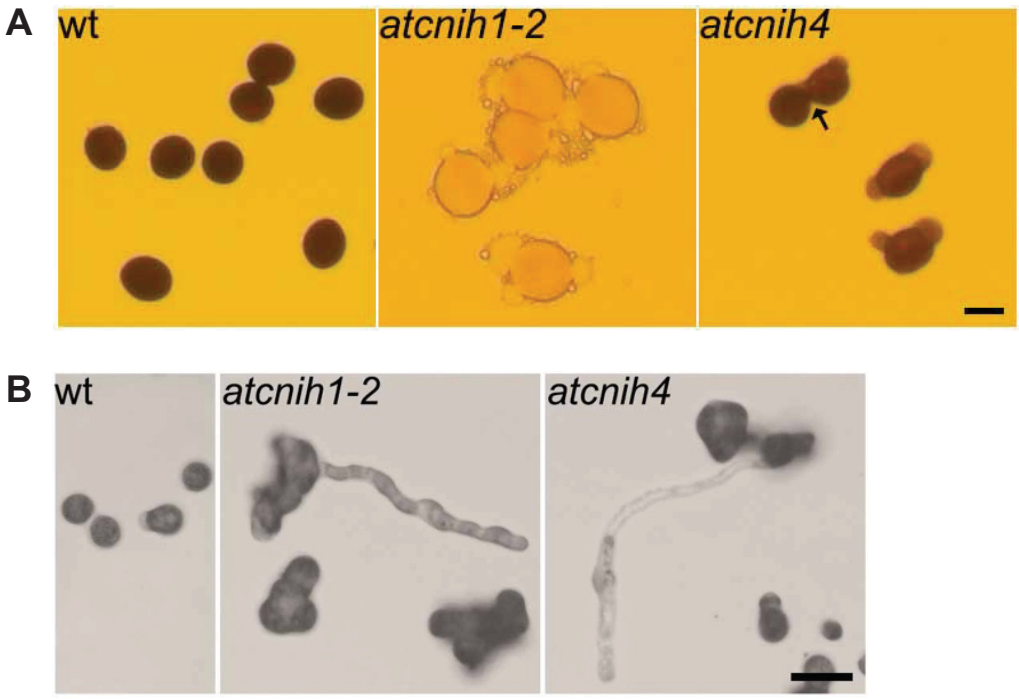


**Figure 5.6. Abnormal pollen development of herbicide resistant *atcnih1* and *atcnih4* mutants in the fourth generation of screening.**

**(A)** Staining pollen from wt, *atcnih1* and *atcnih4* mutants with $I_2$-KI solution. The bright field microscopic images of $I_2$-KI stained pollen from wt, *atcnih1* and *atcnih4* mutants are shown. Black arrow indicates the unseparated pollen grains from *atcnih4* mutant. Scale bar: 20 μm. **(B)** *In vitro* pollen germination analysis of wt, *atcnih1* and *atcnih4* mutants on solid medium (Michard et al., 2011). The representative bright field microscopic images of germinated pollen from wt, *atcnih1* and *atcnih4* mutants are shown. The pollen grain tube germinated faster in *atcnih1* and *atcnih4* mutants than that in wt. Scale bar: 50 μm.

### 5.3.4 Homozygous *atcnih* mutants are less susceptible to *Pst* DC3000

Sugar transporters such as Hxt3 and Hxt5 are dependent on Erv14 for trafficking to the plasma membrane in yeast (Herzig et al., 2012; Pagant et al., 2015). SWEETs are the homologs of sugar transporters in plant and bacterial infection can upregulate expression levels of *AtSWEETs* (Chen et al., 2010). I hypothesize that AtCNIHs function as cargo receptors in targeting SWEETs to the plasma membrane, and thus support bacterial infection.

The *Arabidopsis-P. syringae* interaction is a well-established system to study molecular plant-bacterial interactions (Katagiri et al., 2002; Nobuta and Meyers, 2005) and in particular, the virulent strain *Pst* DC3000 is widely used for experiments with *Arabidopsis* (Whalen et al., 1991; Xin and He, 2013). In order to understand the roles of plant CNIHs in plant pathogen infection, we checked whether plant CNIHs are involved in plant bacterial pathogen infection. We used *Pst* DC3000 to inoculate the homozygous *atcnih2*, *atcnih3* and *atcnih5* mutants to determine whether AtCNIH2, AtCNIH3 and AtCNIH5 are involved in *Pst* DC3000 infection.

We first examined whether *Pst* DC3000 infection could affect *AtCNIHs* expression by surveying a web-based gene expression analysis tool Genevestigator V3 microarray database. *Pst* DC3000 infection significantly increased levels of accumulated *AtCNIH2* and *AtCNIH3* transcripts by 10-fold ($P<0.05$) at 24 h post bacterial inoculation, as compared to the control. However, *AtCNIH1* was not detected while no significant change of *AtCNIH4* and *AtCNIH5* transcripts was found (Hruz et al., 2008; Hruz et al., 2011; Zimmermann et al., 2004). This information suggested that *Pst* DC3000 induces AtCNIH2 or AtCNIH3 to facilitate the trafficking of nutrient transporters to the plasma membrane and promote nutrient efflux to the apoplast for bacterial growth and proliferation.

Since *Pst* DC3000 infection dramatically increased the gene expression levels of *AtCNIH2* and *AtCNIH3*, we predicted that knockout *atcnih* mutants might inhibit *Pst* DC3000 infection through the regulation of nutrient transporters (Chen et al., 2014; Chen, 2014; Chen et al., 2010; Rico and Preston, 2008). To test the hypothesis, I inoculated wt,

homozygous *atcnih2*, *atcnih3* and *atcnih5* mutants with *Pst* DC3000 and checked bacterial growth at 4 days post bacterial inoculation. On leaves of *Pst* DC3000-infected *atcnih2*, *atcnih3* and *atcnih5* mutants, less bacterial speck symptom was developed at 4 days post bacterial inoculation than that in wt (Figure 5.7A). Quantification of bacterial colony-forming unit (CFU) on leaf tissues demonstrated that *atcnih2*, *atcnih3* and *atcnih5* mutants significantly inhibited *Pst* DC3000 growth and a 6-, 10-, and 11-fold reduction of CFU than that of wt were observed at 4 days post bacterial inoculation, respectively (Figure 5.7B). The results were consistent with our hypothesis that AtCNIHs function as cargo receptors involved in the trafficking of nutrient transporters, among others, and affected nutrient efflux in *atcnih* mutants affected bacterial infection (Figure 5.7). Therefore, it is possible to inhibit bacterial pathogens that rely on host nutrient transporters for growth by blocking nutrient transporters with manipulating one or few AtCNIHs.

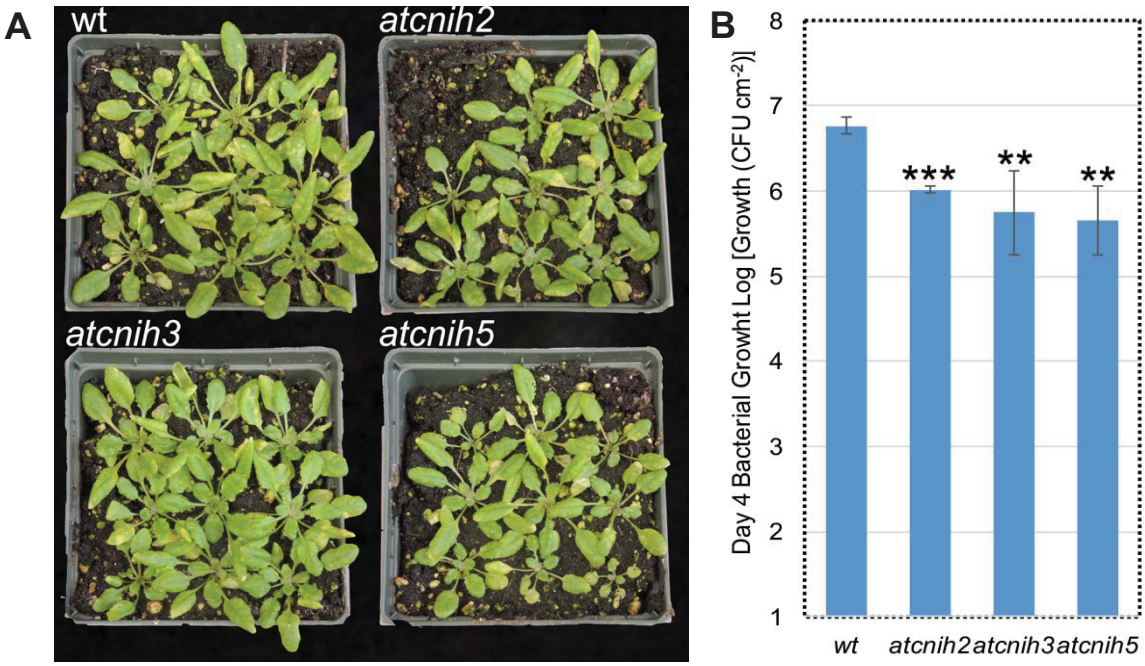


**Figure 5.7. Reduced susceptibility to *Pst* DC3000 in homozygous *atcnih2*, *atcnih3*, and *atcnih5* mutant plants.**

**(A)** Disease symptom on leaf tissues of *Pst* DC3000-inoculated wt, homozygous *atcnih2*, *atcnih3* and *atcnih5* mutants at 4 days post bacterial inoculation. Leaves were spray-inoculated with a concentration of $OD_{600}$=0.1 for *Pst* DC3000. **(B)** Bacterial growth analysis of *Pst* DC3000 inoculated wt, homozygous *atcnih2*, *atcnih3* and *atcnih5* mutants at 4 days post bacterial inoculation. The bacterial concentration was calculated as CFU. Error bars represent standard deviation (n=6). $^{**}P<0.01$ and $^{***}P<0.001$ (ANOVA single factor analysis of bacterial growth on mutants as compared to that on wt). Three individual bacterial *Pst* DC3000 growth experiments were performed, and a representative result is shown.

## 5.4 Discussion

CNI proteins are a conserved family of proteins among eukaryotes, including yeast, plants and mammals. Erv14, one of CNIHs in yeast, functions as a cargo receptor of COPII vesicles by interacting with its cargo proteins and COPII coat protein Sec24 to facilitate the incorporation of cargo proteins into the COPII vesicles. Cargo proteins subsequently exit the ER along with the vesicles to the Golgi complex and eventually to their final destinations: plasma membranes, chloroplasts, or extracellular space, among others. About 45 yeast proteins, including many transporters of amino acids, sugars and metals, depend on Erv14 for their trafficking to the Golgi or plasma membrane (Herzig et al., 2012; Pagant et al., 2015). Similar in plant, AtCNIH5 has been found to interact with ~500 cellular proteins (Membrane-based Interactome Network Database, http://cas-biodb.cas.unt.edu/project/mind/index.php). These interactors include pathogen resistance-related leucine-rich repeat protein kinase family proteins, glutamate receptor-like family proteins, and many transporters of amino acids, sugars, metals and elements (Jones et al., 2014). In our previous study (Li et al., 2016), we found that AtCNIH1, AtCNIH4 and AtCNIH5 are functionally equivalent to Erv14 in yeast. In this study, I further identified that AtCNIH1 and AtCNIH4 are important for pollen

development, while AtCNIH2, AtCNIH3 and AtCNIH5 are involved in bacterial pathogen *Pst* DC3000 infection (Figures 5.6 and 5.7). Therefore, I proposed that AtCNIHs might function as cargo receptors for the trafficking of various cargo proteins that are involved in many cellular processes, including nutrient efflux across the plant plasma membrane, pollen development and plant immune responses to pathogen infection.

### 5.4.1 The possible roles of AtCNIH1 and AtCNIH4 in pollen development

Pollen development is strictly controlled by a complex regulatory network to ensure proper development of pollen cell and wall for producing viable male gametes. Several protein families are known to be involved in pollen development, including arabinogalactan proteins, SWEETs and pectin lyase-like superfamily protein (Cao, 2012; Chen, 2014; Pereira et al., 2014; Wu et al., 2016).

Arabinogalactan proteins (AGPs) are complex proteoglycans, a family of non-enzymatic cell surface hydroxyproline-rich glycoproteins. AGPs have been found throughout the entire plant kingdom and mainly expressed at cell surface and play important roles in plant development, such as root and pollen development (Nguema-Ona et al., 2012). AGPs are dynamically expressed in the reproductive tissues of *A. thaliana*. Interestingly, AGPs are detected in the tapetal cells during pollen development, including microsporogenesis and post-meiotic development of microspores (Coimbra et al., 2007; Pereira et al., 2014). Furthermore, the tapetum is a specialized tissue for exporting all essential nutrients and other materials into the locular fluid to support pollen development (Ma, 2005), indicating an important role of AGPs in pollen development. For instance, knockdown or knockout of both

*AtAGP6* and *AtAGP11* caused abnormal pollen development with aborted pollen, while the aborted pollen showed morphological abnormalities, including condensed cytoplasm, membrane blebbing and small lytic vacuoles (Coimbra et al., 2009). In addition to the important role of AGPs in pollen development, AGPs play critical roles in pollen germination and pollen tube growth (Coimbra et al., 2010; Levitin et al., 2008). Previous study showed that *atagp6/11* mutant had precocious germination of pollen, suggesting that AtAGP6 and AtAGP11 play a role in preventing an early and wasteful pollen germination to ensure a timely pollen germination (Coimbra et al., 2010).

Similarly, we observed abnormal morphologies and *in vitro* faster germination of pollen from *atcnih1* and *atcnih4* mutants (Figure 5.6), even though they might be heterozygous mutants (Figure 5.4). AtCNIH1 and AtCNIH4 are closely related to AtCNIH5 (Figure 5.1C). It needs to note that one putative interactor of AtCNIH5 is anther-specific protein AGP1-like protein (ALP, AT3G26110) (Jones et al., 2014), which is essential to pollen fertility and had been found highly expressed in both tapetum and microspores (Wu et al., 2016). Therefore, it is possible that AtCNIH1 and AtCNIH4 function as cargo receptors involved in the trafficking of AGPs to specific subcellular loci to ensure normal pollen development, whereas knockout of *AtCNIH1* and *AtCNIH4* disturb the trafficking and distribution of AGPs in reproductive tissues and subsequently affect pollen development.

Sugar efflux transporters, i.e., SWEETs are essential to pollen development (Slewinski, 2011). For instance, SWEET8/RPG1 is required for pollen wall development and essential to pollen viability. *AtSWEET8/RPG1* was highly expressed in microspores and tapetum during

male meiosis, while *atsweet8*/*rpg1* mutant displayed aberrant primexine formation of microspores at tetrad stage and had an impaired exine pattern formation due to defective sporollenin deposition on pollen surface with severely reduced male fertility (Guan et al., 2008). This is in agreement with the role of AtSWEET8 in glucose efflux from tapetum to provide essential carbohydrate sources for pollen development (Chen, 2014). Not surprisingly, pollen of *atcnih1* and *atcnih4* mutants had less starch accumulation than wt (Figure 5.6A), suggesting that pollen of *atcnih1* and *atcnih4* mutants might have abnormal transportation of sugars from tapetum to pollen cell. Given that at least nine members of AtSWEETs family protein have been found to interact with AtCNIH5 (Jones et al., 2014), it is possible that AtCNIH1 and AtCNIH4 interact with some members of AtSWEETs, serve as cargo receptors for SWEETs and affect the trafficking and distribution of sugars in the anther during pollen development.

Another interesting interactor of AtCNIH5 is pectin lyase-like superfamily protein (AT2G43880) (Jones et al., 2014). These proteins mainly function in the degradation of pectin and play important roles in pollen development, especially in microspore separation (Cao, 2012). Previous studies have shown that tetrad pollen formation in quartet mutant is associated with the persistence of pectin in pollen mother cell and causes the microspores to fail to separate completely and remain group together with exine deposition to form pollen tetrads (Rhee et al., 2003; Rhee and Somerville, 1998). Here, we found that some pollen grains from *atcnih4* mutant coupled together (Figure 5.6A), suggesting that some microspores of *atcnih4* mutant might separate partially but not completely. It is possible that

some members of pectin lyase-like superfamily might not be efficiently transported to pollen mother cell wall when lacking suitable cargo receptors for their ER exit, and subsequently affect the degradation of pectin on microspores and result in incompletely separation of pollen grains.

It is likely that AtCNIH1 and AtCNIH4 play multiple roles in the regulation and coordination of pollen development and pollen germination. While the indirect role of AtCNIH1 and AtCNIH4 in cargo protein trafficking is favored, the possibility that AtCNIH1 and/or AtCNIH4 might be directly involved in pollen development cannot be totally ruled out. It is necessary to determine which specific pollen development stages and/or what specific pollen morphological traits have been affected in both mutants.

It also needs to note that each of AtCNIH1 and AtCNIH4 is required for pollen development, indicating that each is required differently for maintaining pollen development and/or functions. They may facilitate trafficking of different cargo proteins that are essential for pollen development,

### 5.4.2 The possible roles of AtCNIH2, AtCNIH3 or AtCNIH5 in supporting *Pst* DC3000 infection

Nutrients are required for the growth and development of plants and pathogens (Dordas, 2008). Many plant pathogens exploit and manipulate host nutrient transporters to acquire essential nutrients for their growth and multiplication (Fatima and Senthil-Kumar, 2015). For instance, bacteria and oomycetes upregulate the gene expression levels of plasma membrane-

localized sugar efflux transporters, known as SWEETs (Chen et al., 2010). Additionally, bacterial pathogens promote sugar transport to extracellular space in plants as carbohydrate sources for bacterial growth (Antony et al., 2010; Chandran, 2015; Chen, 2014; Chen et al., 2010). Interestingly, data are available showing that *Pst* DC3000 infection significantly increases transcript levels of *AtCNIH2* and *AtCNIH3*, the putative cargo receptors for SWEETs. The increased expression of AtCNIH2 and AtCNIH3 might be to accelerate the trafficking of the enhanced levels of SWEETs. Similar to the important roles of SWEETs in pollen development, SWEETs can also regulate sugar contents in the apoplastic fluids and thus, regulate bacterial growth.

Surprisingly, there are five plant glutamate receptor-like proteins (GLRs) in AtCNIH5 interactors: AtGLR3.4 (AT1G05200), AtGLR1.1 (AT3G04110), AtGLR1.3 (AT5G48410), AtGLR3.2 (AT4G35290) and AtGLR2.9 (AT2G29100) (Jones et al., 2014). HsCNIH2 and HsCNHI3 have been found function as auxiliary subunits of ionotropic glutamate receptors (iGluRs) (Herring et al., 2013; Schwenk et al., 2009), while plant GLRs play an important role in plant pathogen defense response (Forde and Roberts, 2014). Therefore, it is possible that AtCNIH2, AtCNIH3 and AtCNIH5 might function as auxiliary subunits of GLRs and negatively regulate GLRs activity to be involved in plant pathogen infection. Plant GLRs have broader ligand specificity than their mammalian iGluRs counterparts and might function as non-specific amino acid sensors rather than glutamate sensors, in view of their ubiquitous expression pattern in different plant tissues and the evidence that some individual GLRs have been identified to be gated by up to seven amino acids (Forde and Roberts, 2014). More

importantly, GLRs, especially members in the clade 3 of GLRs family, play important roles in plant pathogen defense responses (Forde and Roberts, 2014). For instance, AtGLR3.3 is involved in plant immune response to bacterial and oomycete pathogens. Knockout of *AtGLR3.3* failed to activate pathogen-induced defense genes and increased susceptibility to *Pst* DC3000 and *Hyaloperonospora arabidopsidis* (*Hpa)* (Li et al., 2013; Manzoor et al., 2013). Homozygous *atcnih2*, *atcnih3* and *atcnih5* mutants showed a reduced susceptibility to *Pst* DC3000 (Figure 5.7). This is consistent with our hypothesis that AtCNIH2, AtCNIH3 and AtCNIH5 might function as negative regulators of GLRs, whereas knockout of *AtCNIH2*, *AtCNIH3* and *AtCNIH5* could enhance the activity of GLRs to elevate plant immune response to bacterial pathogen infection and inhibit bacterial growth. We would expect a constitutively enhanced expression of pathogen-induced defense genes in homozygous *atcnih2*, *atcnih3* and *atcnih5* mutants as compared to that in wt, if GLRs were not negatively regulated by plants when lacking *AtCNIH2*, *AtCNIH3* or *AtCNIH5*.

Some other proteins that involved in plant pattern-triggered immune response have also been identified to interact with AtCNIH5, including BAK1-interacting receptor-like kinase 1 (BIR1) (AT5G48380) and FLG22-induced receptor-like kinase 1 (FRK1) (AT2G19190). Plant pathogen-induced defense responses are negatively controlled to avoid detrimental effects on plant development caused by the constitutive activation of pathogen-induced defense genes or autoimmunity responses. BIR1, a plasma membrane protein, negatively regulates multiple plant pathogen resistant signaling pathways because knockout of *BIR1* caused cell death and constitutive defense responses (Gao et al., 2009). Because AtCNIH2,

AtCNIH3 and AtCNIH5 are similar to each other (Figure 5.1C), AtCNIH2 and AtCNIH3 might possibly also interact with and involved in trafficking of BIR1. Knockout of each of *AtCNIH2, 3, or 5* might partially inhibit, but not totally block, BIR1 trafficking to the plasma membrane and result in significantly enhanced defense response to pathogen (Figure 5.7).

Based on our current studies in *Arabidopsis*, the cellular functions of AtCNIHs are both diverse and redundant as AtCNIHs may function as cargo receptors to mediate the trafficking of multiple cellular proteins to their targeted destinations for proper cellular processes, including pollen development and plant bacterial pathogen responses. Even though different group of cargo proteins might rely on different AtCNIHs, it is likely that plants evolve to have a functional redundancy strategy to ensure the normal cellular functions of AtCNIHs in plant development and active plant pathogen-induced defense responses.

The cellular functions of AtCNIHs are redundant. First, AtCNIH1, AtCNIH4 and AtCNIH5 are functionally equivalent to Erv14 in yeast (Figure 2.10, Chapter 2). Second, no growth defects were observed in homozygous knockout mutant of *atcnih2*, *atcnih3*, and *atcnih5*, suggesting that each of their functions can be complemented by other CNIH(s). Third, some cargo proteins might depend on several AtCNIHs for trafficking. Plant bacterial pathogen might coopt AtCNIHs-mediated protein secretory pathway to favor their growth and proliferation because *Pst* DC3000 infection increased the gene expression of *AtCNIH2* or *AtCNIH3*. AtCNIHs might function as a central hub to sort and control the trafficking and distribution of numerous cellular proteins that are involved in various cellular processes. At least AtCNIH2, AtCNIH3 and AtCNIH5 are involved in bacterial pathogen infection, as

homozygous *atcnih2*, *atcnih3* and *atcnih5* mutants showed reduced susceptibility to *Pst* DC3000 (Figure 5.7). Our data also support the concept of functional diversity of AtCNIHs because knocking out of each AtCNIH1 or AtCNIH4 led to defective pollen grains. The functional diversity and redundancy properties of AtCNIHs, to some degree, can safeguard the normal cellular functions of AtCNIHs in plant development and plant pathogen-induced defense responses.

In conclusion, we demonstrate that knockout mutants of AtCNIHs affect pollen development and susceptibility to virulent bacteria. Specifically, AtCNIH1 and AtCNIH4 are important for pollen development, whereas at least AtCNIH2, AtCNIH3 and AtCNIH5 are involved in *Pst* DC3000 infection. Therefore, our data not only reveal an unexpected role of CNI family protein in plant reproductive development, but also provide a proof of concept evidence of an alternate strategy to control bacterial pathogen by manipulating the expression or the presence of CNIHs.

## 5.5 Materials and methods

### 5.5.1 Seed germination and plant growth conditions

The seeds of T-DNA insertion mutants were ordered from ABRC. The stock numbers of each germplasm are: CS811998 for AT4G12090 (*atcnih1*) (McElver et al., 2001), SALK_096437C for AT1G12340 (*atcnih2*), SALK_083076C for AT1G12390 (*atcnih3*) and SALK_130850 for AT3G12180 (*atcnih5*) (Alonso et al., 2003), and CS859174 for AT1G62880 (*atcnih4*) that originated from Wisconsin DsLox Project (Woody et al., 2007).

The homozygous mutants with expected T-DNA insertion sites were identified by PCR-based segregation analysis.

Seeds were germinated on a wet filter paper in a Petri dish wrapped by Parafilm to keep humidity inside, put Petri dishes at 4°C for 2 days to break dormancy, then moved to a growth chamber and cultured under long-day conditions (22°C and 16 h light) for 7-10 days until seeds germinated. Plantlets were transferred to soil and grown under the same culture conditions as seed germination in the growth chamber. It was very important to keep individual plants of the same mutant line isolated from neighboring plants to avoid cross contamination. The individual plants were separated from each other by floral sleeves that were made of wax paper and help to harvest seeds from each individual plant. The seeds were dried and then stored in 1.5-ml microcentrifuge tubes at room temperature.

### 5.5.2 Plant DNA extraction and PCR identification of *atcnih* mutants

Genomic DNA was extracted from plant leaf tissues as previously described with minor modifications (Edwards et al., 1991). Briefly, the leaf tissues were collected using the 1.5-ml microcentrifuge tube cap to pinch out a disc of leaf tissue into the microcentrifuge tube, and freeze at -80°C before grinding. DNA extraction buffer (200 mM Tris-HCl, pH=7.5, 250 mM NaCl, 25 mM EDTA and 0.5% SDS, 150 ul) was added to each microcentrifuge tube, leaf tissues were ground into fine powder, 300 ul of DNA extraction buffer were added to each tube and vortexed for 5 s. After spinning down at 13,000 rpm for 1 min, 350 µl supernatant was transferred to a new tube and mixed with 350 µl isopropanol. DNA was precipitated by incubating with isopropanol at room temperature for 5 min. DNA pellet was washed with

70% ethanol, dried and dissolved in 60 µl $H_2O$. About 2 µl of genomic DNA of each plant sample was used for PCR analysis using gene-specific primers and T-DNA primers (Table 5.1) for identifying *atcnih* mutants (Figures 5.2, 5.3B, 5.4B). All the homozygous mutants were screened along with a negative control using DNA from wt plant.

**Table 5.2. Primers used for PCR analysis of *atcnih* mutants**

| Genes and T-DNA vectors | Gene-specific and T-DNA Primers |
|---|---|
| *AtCNIH1* | TGAATAAATAAGTAGCTTTTTAT |
| | AAATGAATGAGTA AATTGTCTAA |
| *AtCNIH2* | GCTAATCAAAATCCGAGCC |
| | TTACTCAGTAGAAGCAGCAC |
| *AtCNIH3* | TAACTTCTCTTTTCTGAATTTG |
| | AGATGGAAGTTGTAGTATAGA |
| *AtCNIH4* | TTAATAGATTAAATGG AGTAGTA |
| | TACGTTCTTTTGGTTTTTGAC |
| *AtCNIH5* | TGGCTTGTATAGGCCTAAAT |
| | AATTTTTTAGCTAATTCGAACAA |
| pCSA110 | TATGAGATGGGTTTTTATGATT (right border) |
| | TGTGTTATTAAGTTGTCTAAGCGTCA (left border) |
| pROK2 | AACTCGTCAAGAAGGCGAT |
| pDs-Lox | GTCCGCAATGTGTTATTAAGTTG |

### 5.5.3 Stereomicroscopy of *atcnih* seeds

The fresh siliques were collected from *atcnih1* and *atcnih4* mutants, the valves were opened and separated with tweezers, and then imaged immediately with a camera of ZEISS SteREO Discovery.V12 stereomicroscope in Dr. Amy Brunner lab at the Department of Forestry Resources and Environmental Conservation at Virginia Tech, at least three siliques were analyzed from each mutant plant.

### 5.5.4 *In vitro* pollen germination and iodine staining analysis

The fresh pollen grains were germinated at room temperature overnight on solid medium (10 mM $CaCl_2$, 1 mM KCl, 1.6 mM boric acid, 1 mM MES-pH 6.5 NaOH and 2% plant agar)

(Michard et al., 2011). The fresh pollen grains were stained with $I_2$-KI solution, which was prepared as following: 2 g KI was dissolved in 10 ml $H_2O$, 1 g of $I_2$ was then added, followed by adding $H_2O$ to a final volume of 300 ml. The solution was covered with foil and stored at room temperature. The iodine stained pollen grains and germinated pollen grains were imaged under the bright field channel of Zeiss inverted epifluorescence microscope (Observer.Z1) at the Fralin microscopy facility at Virginia Tech.

### 5.5.5 Plant bacterial pathogen inoculation on *atcnih* mutants

The inoculation of plant bacterial pathogen *Pst* DC3000 on homozygous *atcnih2*, *atcnih3* and *atcnih5* mutants was performed as previously described with minor modifications (Yao et al., 2013). Briefly, *Pst* DC3000 was streaked from -80°C glycerol stock onto a King's B medium (King et al., 1954) with 15 $\mu g \cdot ml^{-1}$ tetracycline (KB + Tet medium) and cultured overnight at 28°C, re-streaked and cultured overnight again on KB + Tet medium at 28°C. The bacteria were collected and re-suspended in 10 mM MgSO4 with 0.025% Silwet L-77 at $OD_{600}$ = 0.1, The plants were pretreated with water and sealed in a Zip plastic bag 1 day before bacterial inoculation to maintain humidity and keep stomata open to facilitate bacterial infection. Individual plant was sprayed completely with *Pst* DC3000 inside the Zip plastic bag and removed the bag after 1 day post infection. Six leaves were collected 4 days post bacterial inoculation from each mutant line. Leaf discs were cut with a 1.5-ml microcentrifuge tube cap to have a same area of leaf tissues from each plant, were then put into a 1.5-ml microcentrifuge tube with 200 µl 10 mM MgSO4 and 3 glass beads. Leaf tissues were then broken down by using a bead beater for 40 s and repeated 2 more times to

completely break down the leaf tissues. Serial dilutions of bacteria were prepared and 10 µl diluted sample were spread onto KB + Tet plates, Petri dishes were incubated at room temperature for 4-5 days and colony numbers of bacteria were counted to calculate CPU developed on each plant.

## 5.6 References

**Alonso, J. M., Stepanova, A. N., Leisse, T. J., Kim, C. J., Chen, H., Shinn, P., Stevenson, D. K., Zimmerman, J., Barajas, P., Cheuk, R. et al.** (2003). Genome-wide insertional mutagenesis of Arabidopsis thaliana. *Science* **301**, 653-657.

**Antony, G., Zhou, J., Huang, S., Li, T., Liu, B., White, F. and Yang, B.** (2010). Rice xa13 recessive resistance to bacterial blight is defeated by induction of the disease susceptibility gene Os-11N3. *Plant Cell* **22**, 3864-3876.

**Ariizumi, T. and Toriyama, K.** (2011). Genetic regulation of sporopollenin synthesis and pollen exine development. *Annu Rev Plant Biol* **62**, 437-460.

**Baulcombe, D. C., Saunders, G. R., Bevan, M. W., Mayo, M. A. and Harrison, B. D.** (1986). Expression of biologically active viral satellite RNA from the nuclear genome of transformed plants. *Nature* **321**, 446-449.

**Berger, F., Hamamura, Y., Ingouff, M. and Higashiyama, T.** (2008). Double fertilization-caught in the act. *Trends Plant Sci* **13**, 437-443.

**Blackmore, S., Wortley, A. H., Skvarla, J. J. and Rowley, J. R.** (2007). Pollen wall development in flowering plants. *New Phytol* **174**, 483-498.

**Bökel, C., Dass, S., Wilsch-Bräuninger, M. and Roth, S.** (2006). Drosophila Cornichon acts as cargo receptor for ER export of the TGFα-like growth factor Gurken. *Development* **133**, 459-470.

**Cao, J.** (2012). The pectin lyases in Arabidopsis thaliana: evolution, selection and expression profiles. *PLoS ONE* **7**, e46944.

**Castro, C. P., Piscopo, D., Nakagawa, T. and Derynck, R.** (2007). Cornichon regulates transport and secretion of TGFα-related proteins in metazoan cells. *J Cell Sci* **120**, 2454-2466.

**Chandran, D.** (2015). Co-option of developmentally regulated plant SWEET transporters for pathogen nutrition and abiotic stress tolerance. *IUBMB Life* **67**, 461-471.

**Chen, C.-c., Chien, W.-F., Lin, N.-C. and Yeh, K.-C.** (2014). Alternative functions of Arabidopsis YELLOW STRIPE-LIKE3: From metal translocation to pathogen defense. *PLoS ONE* **9**, e98008.

**Chen, L.-Q.** (2014). SWEET sugar transporters for phloem transport and pathogen nutrition. *New Phytol* **201**, 1150-1155.

**Chen, L.-Q., Hou, B.-H., Lalonde, S., Takanaga, H., Hartung, M. L., Qu, X.-Q., Guo, W.-J., Kim, J.-G., Underwood, W., Chaudhuri, B. et al.** (2010). Sugar transporters for intercellular exchange and nutrition of pathogens. *Nature* **468**, 527-532.

**Chinchilla, D., Zipfel, C., Robatzek, S., Kemmerling, B., Nurnberger, T., Jones, J. D. G., Felix, G. and Boller, T.** (2007). A flagellin-induced complex of the receptor FLS2 and BAK1 initiates plant defence. *Nature* **448**, 497-500.

**Coimbra, S., Almeida, J., Junqueira, V., Costa, M. L. and Pereira, L. G.** (2007). Arabinogalactan proteins as molecular markers in Arabidopsis thaliana sexual reproduction. *J Exp Bot* **58**, 4027-4035.

**Coimbra, S., Costa, M., Jones, B., Mendes, M. A. and Pereira, L. G.** (2009). Pollen grain development is compromised in Arabidopsis agp6 agp11 null mutants. *J Exp Bot* **60**, 3133-3142.

**Coimbra, S., Costa, M., Mendes, M. A., Pereira, A. M., Pinto, J. and Pereira, L. G.** (2010). Early germination of Arabidopsis pollen in a double null mutant for the arabinogalactan protein genes AGP6 and AGP11. *Sex Plant Reprod* **23**, 199-205.

**Dordas, C.** (2008). Role of nutrients in controlling plant diseases in sustainable agriculture. A review. *Agron Sustain Dev* **28**, 33-46.

**Edlund, A. F., Swanson, R. and Preuss, D.** (2004). Pollen and stigma structure and function: The role of diversity in pollination. *Plant Cell* **16**, S84-S97.

**Edwards, K., Johnstone, C. and Thompson, C.** (1991). A simple and rapid method for the preparation of plant genomic DNA for PCR analysis. *Nucleic Acids Res* **19**, 1349.

**Fatima, U. and Senthil-Kumar, M.** (2015). Plant and pathogen nutrient acquisition strategies. *Front Plant Sci* **6**, 750.

**Forde, B. G. and Roberts, M. R.** (2014). Glutamate receptor-like channels in plants: a role as amino acid sensors in plant defence? *F1000Prime Reports* **6**, 37.

**Frenguelli, G.** (2003). Pollen structure and morphology. *Postêpy Dermatologii i Alergologii* **20**, 200.

**Gao, M., Wang, X., Wang, D., Xu, F., Ding, X., Zhang, Z., Bi, D., Cheng, Y. T., Chen, S., Li, X. et al.** (2009). Regulation of cell death and innate immunity by two receptor-like kinases in Arabidopsis. *Cell Host Microbe* **6**, 34-44.

**Gómez, J. F., Talle, B. and Wilson, Z. A.** (2015). Anther and pollen development: A conserved developmental pathway. *J Integr Plant Biol* **57**, 876-891.

**Guan, Y.-F., Huang, X.-Y., Zhu, J., Gao, J.-F., Zhang, H.-X. and Yang, Z.-N.** (2008). RUPTURED POLLEN GRAIN1, a member of the MtN3/saliva gene family, is crucial for exine pattern formation and cell integrity of microspores in Arabidopsis. *Plant Physiol* **147**, 852-863.

**He, S. Y. and Jin, Q.** (2003). The Hrp pilus: learning from flagella. *Curr Opin Microbiol* **6**, 15-19.

**Herring, Bruce E., Shi, Y., Suh, Young H., Zheng, C.-Y., Blankenship, Sabine M., Roche, Katherine W. and Nicoll, Roger A.** (2013). Cornichon proteins determine the subunit composition of synaptic AMPA receptors. *Neuron* **77**, 1083-1096.

**Herzig, Y., Sharpe, H. J., Elbaz, Y., Munro, S. and Schuldiner, M.** (2012). A systematic approach to pair secretory cargo receptors with their cargo suggests a mechanism for cargo selection by Erv14. *PLoS Biol* **10**, e1001329.

**Hruz, T., Laule, O., Szabo, G., Wessendorp, F., Bleuler, S., Oertle, L., Widmayer, P., Gruissem, W. and Zimmermann, P.** (2008). Genevestigator V3: A reference expression database for the meta-analysis of transcriptomes. *Adv Bioinformat* **2008**, 5.

**Hruz, T., Wyss, M., Docquier, M., Pfaffl, M. W., Masanetz, S., Borghi, L., Verbrugghe, P., Kalaydjieva, L., Bleuler, S., Laule, O. et al.** (2011). RefGenes: Identification of reliable and condition specific reference genes for RT-qPCR data normalization. *BMC Genomics* **12**, 156.

**Jiang, J., Zhang, Z. and Cao, J.** (2013). Pollen wall development: the associated enzymes and metabolic pathways. *Plant Biol* **15**, 249-263.

**Jin, Q., Hu, W., Brown, I., McGhee, G., Hart, P., Jones, A. L. and He, S. Y.** (2001). Visualization of secreted Hrp and Avr proteins along the Hrp pilus during type III secretion in Erwinia amylovora and Pseudomonas syringae. *Mol Microbiol* **40**, 1129-1139.

**Jones, A. M. and Wildermuth, M. C.** (2011). The phytopathogen Pseudomonas syringae pv. tomato DC3000 has three high-affinity iron-scavenging systems functional under iron limitation conditions but dispensable for pathogenesis. *J Bacteriol* **193**, 2767-2775.

**Jones, A. M., Xuan, Y., Xu, M., Wang, R.-S., Ho, C.-H., Lalonde, S., You, C. H., Sardi, M. I., Parsa, S. A., Smith-Valle, E. et al.** (2014). Border control-a membrane-linked interactome of Arabidopsis. *Science* **344**, 711-716.

**Jones, D. T., Taylor, W. R. and Thornton, J. M.** (1992). The rapid generation of mutation data matrices from protein sequences. *Comput Appl Biosci* **8**, 275-282.

**Katagiri, F., Thilmony, R. and He, S. Y.** (2002). The Arabidopsis thaliana-Pseudomonas syringae interaction. *The Arabidopsis Book / American Society of Plant Biologists* **1**, e0039.

**King, E. O., Ward, M. K. and Raney, D. E.** (1954). Two simple media for the demonstration of pyocyanin and fluorescin. *J Lab Clin Med* **44**, 301-307.

**Kumar, S., Stecher, G. and Tamura, K.** (2016). MEGA7: Molecular evolutionary genetics analysis version 7.0 for bigger datasets. *Mol Biol Evol* **33**, 1870-1874.

**Levitin, B., Richter, D., Markovich, I. and Zik, M.** (2008). Arabinogalactan proteins 6 and 11 are required for stamen and pollen function in Arabidopsis. *Plant J* **56**, 351-363.

**Li, F., Wang, J., Ma, C., Zhao, Y., Wang, Y., Hasi, A. and Qi, Z.** (2013). Glutamate receptor-like channel3.3 is involved in mediating glutathione-triggered cytosolic calcium transients, transcriptional changes, and innate immunity responses in Arabidopsis. *Plant Physiol* **162**, 1497-1509.

**Li, J., Fuchs, S., Zhang, J., Wellford, S., Schuldiner, M. and Wang, X.** (2016). An unrecognized function for COPII components in recruiting the viral replication protein BMV 1a to the perinuclear ER. *J Cell Sci* **129**, 3597-3608.

**Ma, H.** (2005). Molecular genetic analyses of microsporogenesis and microgametogenesis in flowering plants. *Annu Rev Plant Biol* **56**, 393-434.

**Ma, Z., Zhu, L., Song, T., Wang, Y., Zhang, Q., Xia, Y., Qiu, M., Lin, Y., Li, H., Kong, L. et al.** (2017). A paralogous decoy protects Phytophthora sojae apoplastic effector PsXEG1 from a host inhibitor. *Science* **355**, 710-714.

**Manzoor, H., Kelloniemi, J., Chiltz, A., Wendehenne, D., Pugin, A., Poinssot, B. and Garcia-Brugger, A.** (2013). Involvement of the glutamate receptor AtGLR3.3 in plant defense signaling and resistance to Hyaloperonospora arabidopsidis. *Plant J* **76**, 466-480.

**McElver, J., Tzafrir, I., Aux, G., Rogers, R., Ashby, C., Smith, K., Thomas, C., Schetter, A., Zhou, Q., Cushman, M. A. et al.** (2001). Insertional mutagenesis of genes required for seed development in Arabidopsis thaliana. *Genetics* **159**, 1751-1763.

**Michard, E., Lima, P. T., Borges, F., Silva, A. C., Portes, M. T., Carvalho, J. E., Gilliham, M., Liu, L.-H., Obermeyer, G. and Feijó, J. A.** (2011). Glutamate receptor–like genes form Ca2+ channels in pollen tubes and are regulated by pistil D-serine. *Science* **332**, 434-437.

**Nguema-Ona, E., Coimbra, S., Vicré-Gibouin, M., Mollet, J.-C. and Driouich, A.** (2012). Arabinogalactan proteins in root and pollen-tube cells: distribution and functional aspects. *Ann Bot-London* **110**, 383-404.

**Nobuta, K. and Meyers, B. C.** (2005). Pseudomonas versus Arabidopsis: Models for genomic research into plant disease resistance. *BioScience* **55**, 679-686.

**Pagant, S., Wu, A., Edwards, S., Diehl, F. and Miller, Elizabeth A.** (2015). Sec24 is a coincidence detector that simultaneously binds two signals to drive ER export. *Curr Biol* **25**, 403-412.

**Pereira, A. M., Masiero, S., Nobre, M. S., Costa, M. L., Solís, M.-T., Testillano, P. S., Sprunck, S. and Coimbra, S.** (2014). Differential expression patterns of arabinogalactan proteins in Arabidopsis thaliana reproductive tissues. *J Exp Bot* **65**, 5459-5471.

**Powers, J. and Barlowe, C.** (1998). Transport of Axl2p depends on Erv14p, an ER–vesicle protein related to the drosophila cornichon gene product. *J Cell Biol* **142**, 1209-1222.

**Powers, J. and Barlowe, C.** (2002). Erv14p directs a transmembrane secretory protein into COPII-coated transport vesicles. *Mol Biol Cell* **13**, 880-891.

**Prieu, C., Matamoro-Vidal, A., Raquin, C., Dobritsa, A., Mercier, R., Gouyon, P.-H. and Albert, B.** (2016). Aperture number influences pollen survival in Arabidopsis mutants. *Am J Bot* **103**, 452-459.

**Quilichini, T. D., Douglas, C. J. and Samuels, A. L.** (2014). New views of tapetum ultrastructure and pollen exine development in Arabidopsis thaliana. *Ann Bot-London* **114**, 1189-1201.

**Quilichini, T. D., Grienenberger, E. and Douglas, C. J.** (2015). The biosynthesis, composition and assembly of the outer pollen wall: A tough case to crack. *Phytochemistry* **113**, 170-182.

**Rhee, S. Y., Osborne, E., Poindexter, P. D. and Somerville, C. R.** (2003). Microspore separation in the quartet 3 mutants of Arabidopsis is impaired by a defect in a developmentally regulated polygalacturonase required for pollen mother cell wall degradation. *Plant Physiol* **133**, 1170-1180.

**Rhee, S. Y. and Somerville, C. R.** (1998). Tetrad pollen formation in quartet mutants of Arabidopsis thaliana is associated with persistence of pectic polysaccharides of the pollen mother cell wall. *Plant J* **15**, 79-88.

**Rico, A. and Preston, G. M.** (2008). Pseudomonas syringae pv. tomato DC3000 uses constitutive and apoplast-induced nutrient assimilation pathways to catabolize nutrients that are abundant in the tomato ppoplast. *Mol Plant Microbe In* **21**, 269-282.

**Roine, E., Wei, W., Yuan, J., Nurmiaho-Lassila, E.-L., Kalkkinen, N., Romantschuk, M. and He, S. Y.** (1997). Hrp pilus: An hrp-dependent bacterial surface appendage produced by Pseudomonas syringae pv. tomato DC3000. *Proc Natl Acad Sci USA* **94**, 3459-3464.

**Roth, S., Shira Neuman-Silberberg, F., Barcelo, G. and Schüpbach, T.** (1995). *cornichon* and the EGF receptor signaling process are necessary for both anterior-posterior and dorsal-ventral pattern formation in Drosophila. *Cell* **81**, 967-978.

**Sauvageau, E., Rochdi, M. D., Oueslati, M., Hamdan, F. F., Percherancier, Y., Simpson, J. C., Pepperkok, R. and Bouvier, M.** (2014). CNIH4 interacts with newly synthesized GPCR and controls their export from the endoplasmic reticulum. *Traffic* **15**, 383-400.

**Schwenk, J., Harmel, N., Zolles, G., Bildl, W., Kulik, A., Heimrich, B., Chisaka, O., Jonas, P., Schulte, U., Fakler, B. et al.** (2009). Functional proteomics identify cornichon proteins as auxiliary subunits of AMPA receptors. *Science* **323**, 1313-1319.

**Shi, J., Cui, M., Yang, L., Kim, Y.-J. and Zhang, D.** (2015). Genetic and biochemical mechanisms of pollen wall development. *Trends Plant Sci* **20**, 741-753.

**Slewinski, T. L.** (2011). Diverse functional roles of monosaccharide transporters and their homologs in vascular plants: a physiological perspective. *Mol Plant* **4**, 641-662.

**Wang, K., Senthil-kumar, M., Ryu, C.-M., Kang, L. and Mysore, K. S.** (2012). Phytosterols play a key role in plant innate immunity against bacterial pathogens by regulating nutrient efflux into the apoplast. *Plant Physiol* **158**, 1789-1802.

**Wei, W., Plovanich-Jones, A., Deng, W.-L., Jin, Q.-L., Collmer, A., Huang, H.-C. and He, S. Y.** (2000). The gene coding for the Hrp pilus structural protein is required for type III secretion of Hrp and Avr proteins in Pseudomonas syringae pv. tomato. *Proc Natl Acad Sci USA* **97**, 2247-2252.

**Whalen, M. C., Innes, R. W., Bent, A. F. and Staskawicz, B. J.** (1991). Identification of Pseudomonas syringae pathogens of Arabidopsis and a bacterial locus determining avirulence on both Arabidopsis and soybean. *Plant Cell* **3**, 49-59.

**Wilson, Z. A. and Zhang, D.-B.** (2009). From Arabidopsis to rice: pathways in pollen development. *J Exp Bot* **60**, 1479-1492.

**Woody, S. T., Austin-Phillips, S., Amasino, R. M. and Krysan, P. J.** (2007). The WiscDsLox T-DNA collection: An Arabidopsis community resource generated by using an improved high-throughput T-DNA sequencing pipeline. *J Plant Res* **120**, 157-165.

**Wu, T., Feng, F., Ye, C. and Li, Y.** (2016). Characterization of a pollen-specific agp1-like protein in Arabidopsis thalian. *J App Biol Biotech* **1**, 010-014.

**Xin, X.-F. and He, S. Y.** (2013). Pseudomonas syringae pv. tomato DC3000: A model pathogen for probing disease susceptibility and hormone signaling in plants. *Annu Rev Phytopathol* **51**, 473-498.

**Yamada, K., Saijo, Y., Nakagami, H. and Takano, Y.** (2016). Regulation of sugar transporter activity for antibacterial defense in Arabidopsis. *Science* **354**, 1427-1430.

**Yao, J., Withers, J. and He, S. Y.** (2013). Pseudomonas syringae infection assays in Arabidopsis. In *Jasmonate Signaling: Methods and Protocols*, (eds A. Goossens and L. Pauwels), pp. 63-81. Totowa, NJ: Humana Press.

**Zimmermann, P., Hirsch-Hoffmann, M., Hennig, L. and Gruissem, W.** (2004). GENEVESTIGATOR. Arabidopsis microarray database and analysis toolbox. *Plant Physiol* **136**, 2621-2632.

# Chapter 6 Conclusions and future directions

## 6.1 Conclusions and working models

Positive-strand RNA [(+)RNA] viruses rearrange host intracellular membranes to assemble viral replication complexes (VRCs) during viral replication. Different viruses utilize specific intracellular membranes to initiate VRC assembly. With a better understanding of host factors involved in targeting viral replication proteins to their destination organelles, it becomes possible to manipulate such host targets to inhibit or block viral infection before VRC assembly. In this work, I used the BMV-yeast system to identify host factors that are involved in targeting BMV 1a to the perinuclear ER membrane and thus, BMV replication. In Chapter 2, I demonstrated that cargo receptor Erv14 and several components of COPII vesicles, Sec13, Sec24 and Sec31, are involved in BMV 1a's association with the perinuclear ER membrane (Li et al., 2016). These findings not only reveal novel host factors involved in BMV VRC biogenesis and BMV replication, but also suggest a possible novel function of the COPII pathway in targeting proteins to the perinuclear ER membrane, in addition to its canonical function of the protein ER export.

The Cornichon protein family is a functionally and structurally conserved family of proteins among eukaryotes from Erv14 in yeast to CNIHs in plants. Because there is very limited information on plant CNIHs, I set to examine the cellular functions of CNIHs in plant development and pathogen infection. BMV does not infect dicot plants, such as model plant *Arabidopsis thaliana* (Fujisaki et al., 2009), but does infect another model dicot plant *Nicotiana benthamiana* (Annamalai and Rao, 2005; Diaz et al., 2015; Gopinath et al., 2005).

Using BMV-*N. benthamiana* system in combination with virus-induced gene silencing (VIGS) technique (Senthil-Kumar and Mysore, 2014), I examined the roles of NbCNIHs in plant development, and studied how BMV affects cellular machinery in plants. In Chapter 4, I showed that NbCNIH5 and Erv14/15 play an unanticipated role in maintaining ER morphology, especially ER tubules, in *N. benthamiana* and yeast. In addition, I examined how BMV exploits cellular early secretory pathway in Chapter 3. Taking advantage of available *Arabidopsis cnih* knockout mutants, I also examined the cellular functions of AtCNIHs in plant development and their roles in the infection of a pathogenic bacterium. In Chapter 5, I reported that while each of AtCNIH1 and AtCNIH4 is necessary for pollen development and functions, AtCNIH2, AtCNIH3 and AtCNIH5 are involved in bacterial pathogen *Pst* DC3000 infection. Thus, I concluded that CNIHs play important roles in plant pathogen infection, ER morphology maintenance and pollen development. All these functions are not previously reported and not expected.

Based on the data presented in Chapters 2-5 and below (section 6.2.2), I propose a working model for BMV 1a trafficking to the perinuclear ER membrane to initate VRC formation (Figure 6.1). BMV 1a might be translated in association with specific ER subdomains, such as ER exit sites (ERES), and subsequently transported to the perinuclear ER membrane to initiate spherule formation. COPII coat proteins (Sec13, Sec24 and Sec31) and Erv14, as well as coat protein complex I (COPI) coat proteins (Sec21 and Sec33) (shown below in Figure 6.5), are involved in the process. I propose to follow up on two future directions to : 1) test the hypothesis that an unexpected role of the COPII pathway is to target

certain cellular proteins to the perinuclear ER membrane, in addition to its canonical role to transport cellular cargo proteins out of the ER, and 2) determine the initial protein expression site of BMV 1a and identify cellular machineries involved in BMV 1a trafficking to the perinuclear ER membrane in yeast.

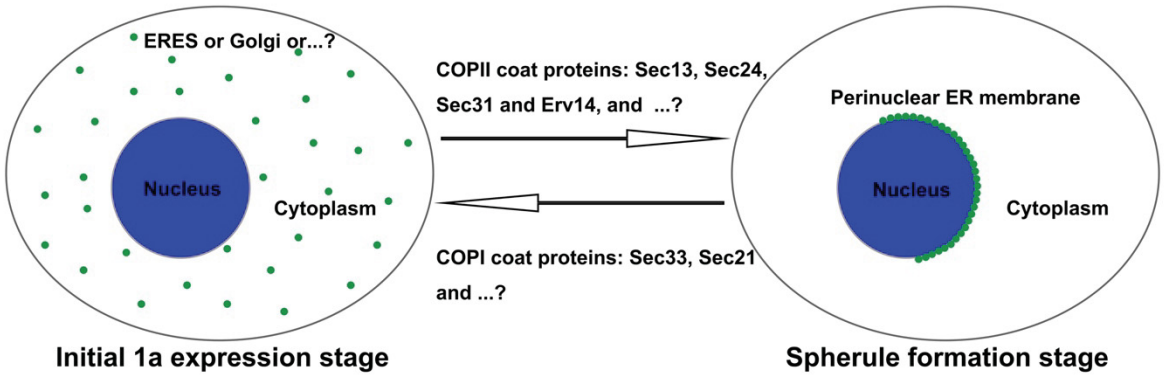


**Figure 6.1. A working model for the trafficking of BMV 1a protein at the early stage of viral infection in yeast.**

BMV 1a is initially translated by ribosomes in the cytoplasm or rough ER and can be detected at about 1.5-2 h after induction in synthetic medium with galactose as a carbon source, and then gradually relocated to the perinuclear ER membrane at about 2-4 h after galactose induction (Figure 6.4). BMV 1a localizes to the perinuclear ER membrane after overnight expression. Erv14 and COPII coat proteins such as Sec24, Sec13 and Sec31 are required for BMV 1a targeting to the perinuclear ER, whereas COPI coat proteins such as Sec33 and Sec21 might antagonize BMV 1a targeting to the perinuclear ER membrane (Figure 6.5). Green dots represent BMV 1a protein.

I also propose a working model on the roles of CNI proteins in plant pathogen infection, ER morphology maintenance and pollen development. Plant CNIHs, such as NbCNIH2 and 5 as well as AtCNIH1, 4 and 5, functionally replaced Erv14 in yeast, suggesting that plant CNIHs might function as cargo receptors in the trafficking of various cargo proteins to their targeted destinations in plants. These cargo proteins subsequently participate in cellular processes such as ER morphology maintenance, pollen development, and plant immune response to pathogen infection. As such, CNI proteins are indirectly involved in the

aforementioned processes.

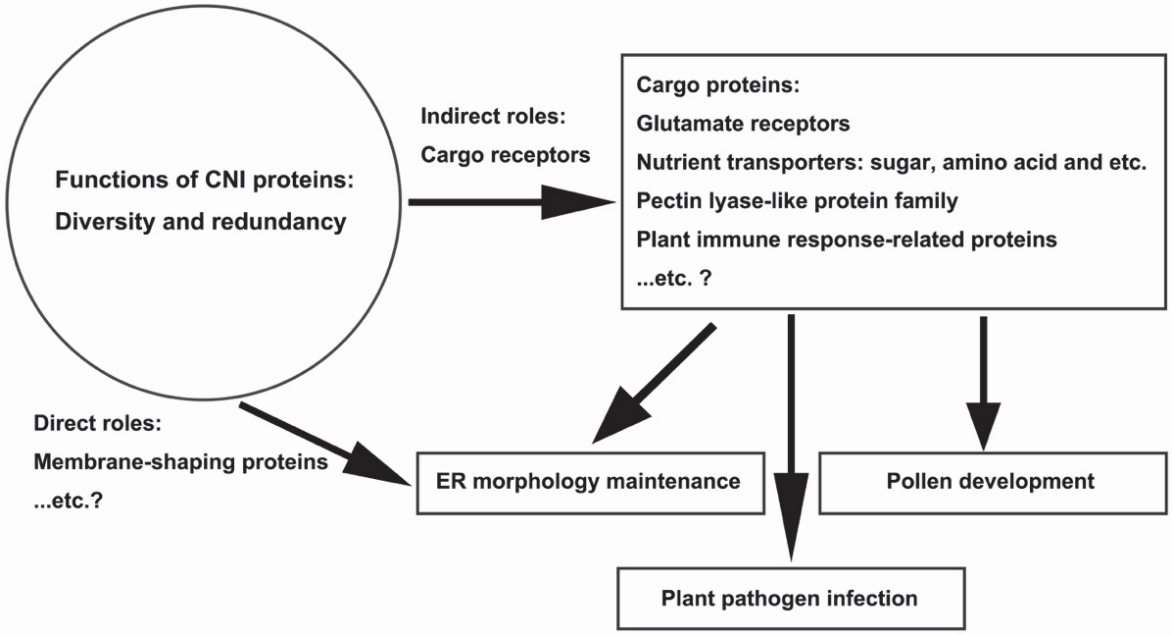


**Figure 6.2. A working model for possible roles of CNI proteins in plant pathogen infection, ER morphology maintenance and pollen development.**

Plant CNIHs have both diverse and redundant cellular functions. They might function in a direct or indirect manner to participate in plant pathogen infection, ER morphology maintenance and pollen development. Plant CNIHs might facilitate the ER exit of various groups of cargo proteins to the Golgi apparatus, en route to their targeted destinations for proper cellular processes. These may include pollen development, ER morphology, and the regulation of plant pathogen infection. More specifically, the putative cargo proteins of plant CNIHs might include proteins related to plant immune response, glutamate receptors, pectin lyase-like protein family and nutrient transporters such as amino acid, sugar and metal. It is also possible that CNI proteins might function as novel membrane-shaping proteins that directly stabilize ER tubules in yeast and plant.

For future directions on plant CNIH functions as cargo receptors, I propose to: 1) identify cargo proteins of plant CNIHs; 2) connect plant CNIHs, cargo proteins to ER morphology maintenance, pollen development, and/or plant pathogen infection based on the cellular functions of candidate cargo proteins and perform in-depth follow up assays. In addition, we will test whether CNI proteins are novel membrane-shaping proteins that directly maintain

ER tubules in plant and yeast.

## 6.2 Future directions

### 6.2.1 The possible roles of COPII vesicles in the trafficking of cellular perinuclear ER proteins

*Rationale and preliminary data:*

COPII is required for anterograde secretory pathway to recruit cargo proteins from the ER into COPII vesicles and depart for the Golgi apparatus (D'Arcangelo et al., 2013; Gomez-Navarro and Miller, 2016; Venditti et al., 2014). Surprisingly, I found that COPII coat proteins and cargo receptor are required for targeting BMV 1a to the perinuclear ER membrane in yeast (Li et al., 2016). It is possible that BMV 1a redirects COPII pathway from its canonical function for targeting itself to the perinuclear ER. Alternatively, COPII pathway plays an unrecognized role in targeting cellular proteins to the perinuclear ER, and BMV 1a exploits this function for its own trafficking. To determine whether certain cellular ER proteins require the COPII pathway for their perinuclear ER targeting in yeast, we first selected cellular proteins that reside at the perinuclear ER and examined their localizations in yeast mutant with the disrupted COPII pathway. Subcellular localizations of yeast proteins have been largely determined based on the signal of GFP, which was fused to the C-terminus of the majority yeast proteins (~4,200). Among them, 302 proteins localize to the ER membrane (Huh et al., 2003). I selected 125 proteins that are evenly distribute at the perinuclear ER membrane based on *Saccharomyces* Genome Database

(www.yeastgenome.org). Among COPII coats, Sec24 is the cargo adaptor that interacts with and recruits diverse cargo proteins into COPII vesicles (Miller et al., 2003). Importantly, BMV 1a distribution was affected in almost every cell in a *sec24* temperature sensitive (*ts*) mutant at non-permissive temperatures (Li et al., 2016). With help from two undergraduate students, I have checked the localization of 75 out of the selected 125 proteins in the *sec24 ts* mutant by expressing selected proteins that were fused with mCherry. Each mCherry protein was expressed from a plasmid, either under the control of a strong promoter, *GAL1*, or the endogenous promoter. We then examined the localizations of each protein at both permissive temperature 23°C and non-permissive temperature 37°C. We found that Sec63-mC, Slc1(sphingolipid compensation1) -mC and Lcb1(long-chain base)-mC had a perinuclear ER localization pattern in wt cells but disrupted localization patterns in *sec24 ts* mutant (Figure 6.3). Sec63 is a component of translocon complex involved in post-translational protein translocation across the ER membrane (Young et al., 2001), while Slc1and Lcb1 are involved in sphingolipid metabolism (Buede et al., 1991; Nagiec et al., 1993). These results showed that cellular ER proteins might require Sec24 or possibly the COPII pathway for their perinuclear ER localization in yeast, suggesting a novel function of Sec24 in the perinuclear ER targeting of cellular ER proteins.

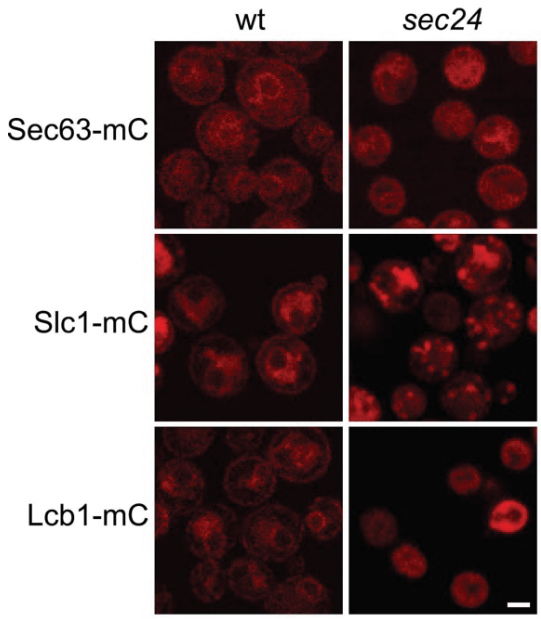


**Figure 6.3. Putative cellular ER proteins that require Sec24 for their perinuclear ER localization in yeast.**

Confocal microscopic images of mC-tagged cellular ER proteins such as Sec63, Slc1 and Lcb1 in wt and *sec24 ts* mutant cells. The ring localization pattern, which indicates the perinuclear ER localization of cellular ER proteins, were observed in wt cells, but disrupted localization patterns were observed in *sec24 ts* mutant cells. Both wt and *sec24 ts* mutant cells were shifted from 23°C to 37°C and cultured for 2 h to inactivate Sec24 before imaging. Scale bar: 2 μm.

*Proposed experiments:*

1. Establish a chromosome-based screening system to identify cellular perinuclear proteins that require Sec24 for targeting

To eliminate false positives due to overexpression of cellular proteins from plasmid, we will examine the localizations of GFP-tagged and chromosome-borne cellular perinuclear ER proteins in *sec24 ts* mutant. To establish the screening system, I propose to create *sec24 ts* mutation in each yeast GFP strain of candidate cellular ER proteins by replacing the wt *SEC24* gene with a *sec24 ts* mutant. By comparing the localization patterns of candidate

proteins in wt and *sec24 ts* mutant cells, cellular ER proteins that require Sec24 for their perinuclear ER localization can be identified. Along with the data from plasmid-borne system, I expect the complementary system will provide accurate information of mis-localization in the *sec24 ts* mutant.

2. Determine the possible roles of COPII components in targeting perinuclear ER of cellular ER proteins

If Sec24 is required for cellular ER protein targeting to the perinuclear ER, it is possible that other COPII components might also be involved in this process. Since the vast majority of COPII *ts* mutants are available, I propose to examine the localization patterns of candidate proteins in other individual COPII *ts* mutants to determine their roles in targeting proteins to the perinuclear ER.

*Potential pitfalls and alternatives:*

Expressing cellular ER proteins from chromosomes, the intensity of GFP signal of fusion proteins may be not strong enough to be detected with our current epifluorescence microscope setting due to low protein expression levels. In this case, I propose to use confocal microscope to detect the GFP signal for those weaker expressers.

All commercialized yeast GFP strains have GFP fused to the C-terminus of cellular proteins. Fusion of GFP at C-terminus may affect the protein localization. For those that we identified as candidate, I propose to check the localization with GFP tagged to the N-terminus of the candidate proteins as well. Dr. Maya Schuldiner, our collaborator in Israel, has created

N-terminal GFP fusion strains (Yofe et al., 2016). We will be able to use the available N-terminally tagged strains for confirmation.

### 6.2.2 The trafficking of BMV 1a to the perinuclear ER membrane in yeast upon its translation

*Rationale and preliminary data:*

BMV 1a localizes to the perinuclear ER membrane to initiate VRC assembly in yeast (Schwartz et al., 2002). I have demonstrated that COPII coat proteins and Erv14 are involved in targeting BMV 1a to the perinuclear ER (Li et al., 2016). However, it is unclear whether COPII components and Erv14 are involved in the stabilization or the trafficking of BMV 1a to the perinuclear ER membrane. To better understand the roles of COPII and Erv14 in targeting BMV 1a to the perinuclear ER, I examined the localizations of BMV 1a in wt and *erv14Δ* cells following a time course upon its expression. My preliminary data showed that BMV 1a initiated its protein expression as dispersed dots in the cytoplasm of wt and *erv14Δ* cells at about 2-3 h post galactose induction (pgi) of its expression, then gradually enriched to the perinuclear ER in wt cells but blocked in the cytoplasm in the majority of *erv14Δ* cells at ~4 h pgi (Figure 6.4A, B). The Western blot data showed that BMV 1a accumulation level increased gradually within 4 h pgi in both wt and *erv14Δ* cells and no significant differences were found between wt and *erv14Δ* cells (Figure 6.4C). Finally, BMV 1a localized to the perinuclear ER in most wt cells, while blocked in the cytoplasm of the majority of *erv14Δ* cells after overnight growth in galactose medium (Figure 6.4A, B). These results suggest that BMV 1a is transported from its initial protein expression site, likely in the cytoplasm, to the

perinuclear ER in yeast, and furthermore, Erv14 is involved in this process.

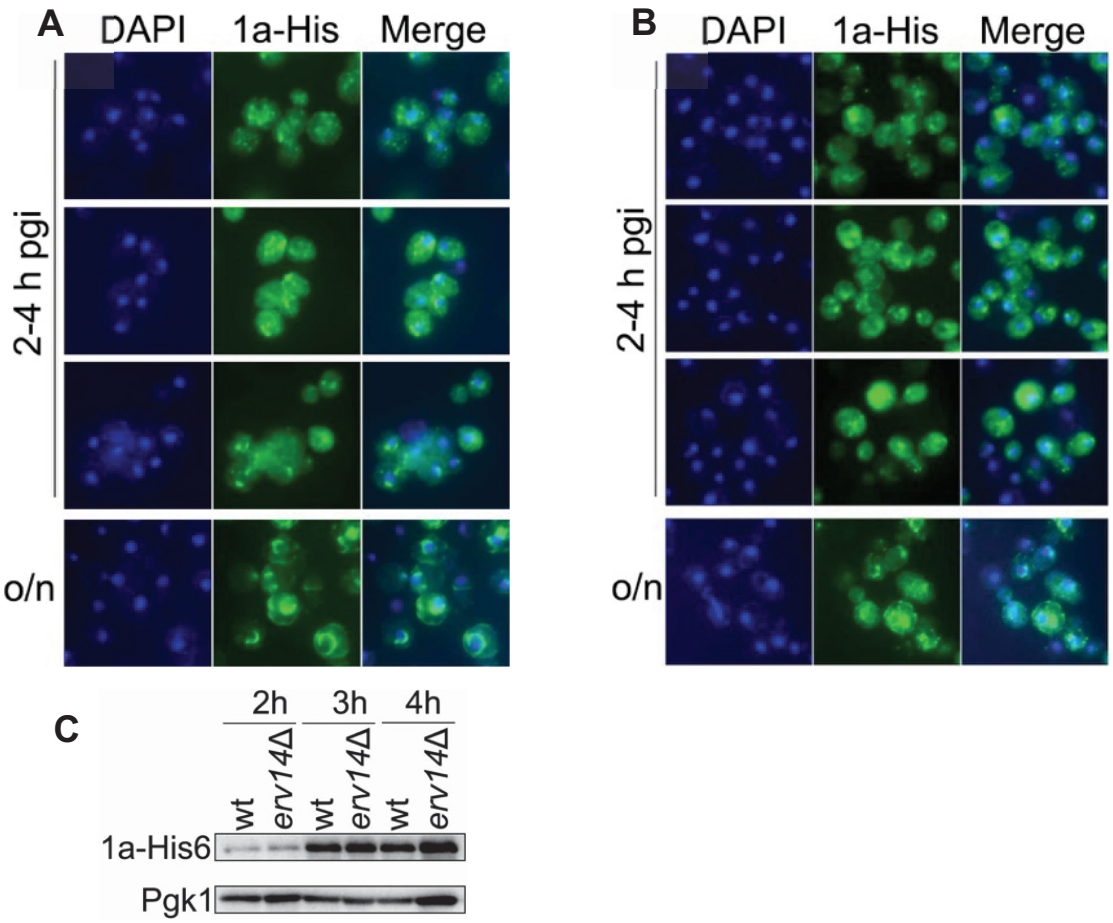


**Figure 6.4. Localization patterns and protein accumulation levels of BMV 1a-His6 in wt and *erv14Δ* cells in a time course experiment.**

**(A, B)** Immunofluorescence images of BMV 1a-His6 distribution in wt (A) and *erv14Δ* cells (B) at different time points pgi. The cells were cultured overnight at 30°C in synthetic medium with raffinose, and then subcultured with galactose to induce BMV 1a-His6 expression. Yeast cells were harvested for immunofluorescence microscopy at 2, 3, 4 h pgi or overnight. BMV 1a-His6 was detected by using an anti-His mAb and anti-mouse secondary antibody conjugated to Alexa Fluor 488. The nuclei were stained with DAPI (blue). **(C)** BMV 1a-His6 protein accumulation level in wt and *erv14Δ* cells at 2, 3, 4 h pgi. Monoclonal anti-His antibody was used to detect BMV 1a-His6. Pgk1 served as a loading control. A representative blot is shown.

Interestingly, the localization pattern of BMV 1a upon expression is very similar to the locations of ERES in yeast (Budnik and Stephens, 2009; Graef et al., 2013; Rossanese et al.,

1999). Based on this observation, I hypothesize that BMV 1a might initiate its protein expression associated with the ERES in the cytoplasmic ER network, and then transported to the perinuclear ER through unidentified cellular machineries, maybe cellular early secretory pathway, microtubules, or simply by diffusion.

Interestingly, I found that another early secretory pathway, COPI, was negatively involved in targeting BMV 1a to the perinuclear ER. COPI is responsible for protein retrograde transport from the Golgi apparatus to the ER membrane. There were more than 80% cells of *sec33-1* and *sec21-1 ts* mutants with BMV 1a localized to the perinuclear ER at 37°C as compared to about 30% at 23°C (Figure 6.5), suggesting that dysfunctional Sec33 and Sec21 facilitate the targeting of BMV 1a to the perinuclear ER. My results were consistent with the involvement of COPI and COPII in another (+)RNA iruse, foot-and-mouth disease virus (FMDV). FMDV infection was inhibited when COPII pathway was blocked but enhanced when COPI pathway was blocked, suggesting that FMDV initiates virus replication on the membranes that are formed at ERES (Midgley et al., 2013).

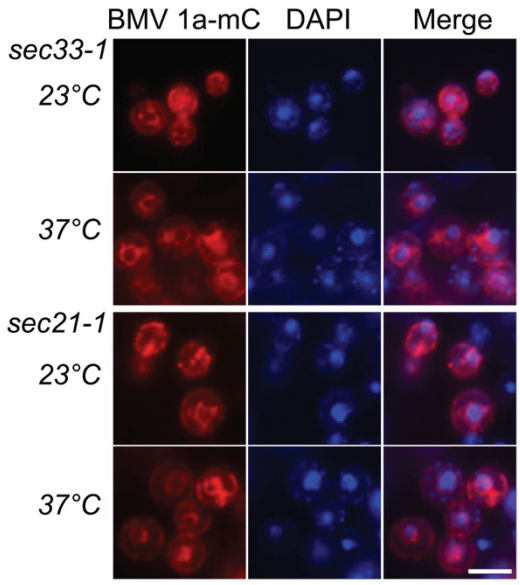


**Figure 6.5. Disruption of COPI coat proteins Sec33 and Sec21 facilitate BMV 1a-mC's association with the perinuclear ER.**

Fluorescence microscopic images of BMV 1a-mC distribution in *sec33-1* and *sec21-1 ts* mutants at 23°C and 37°C. The *ts* mutants were cultured overnight at 23°C in synthetic medium with galactose and subcultured in the same medium at 23°C and 37°C for 2 h. Then harvested the cells and fixed with 4% formaldehyde, removed the cell wall with lyticase and made the cell membrane permissive with Triton X-100 for DAPI staining. The nuclei were stained with DAPI (blue). Scale bar: 5 μm.

*Proposed experiments:*

1. Identify the initial protein expression sites of BMV 1a in yeast

ERES are the sites where COPII vesicles are assembled and appear as scattered puncta throughout cytoplasmic ER membranes (Budnik and Stephens, 2009; Rossanese et al., 1999). To determine the initial protein expression sites of BMV 1a, I propose to check if any COPII coat proteins, including Sec13, Sec31, Sec24 and Sec23 (Okamoto et al., 2012), colocalizes with BMV 1a. If BMV 1a colocalizes with ERES marker protein, it will validate our hypothesis.

We also propose to confirm whether BMV 1a is incorporated into COPII vesicles by performing an *in vitro* COPII vesicle budding assay (Barlowe et al., 1994), in collaboration with Dr. Elizabeth Miller at MRC Laboratory of Molecular Biology, UK. Dr. Miller is an expert on the COPII pathway and a pioneer that established the assay. In this assay, purified COPII components, Sar1, Sec23, 24, 13, and 31 will be incubated with the microsomal fraction isolated from yeast cells expressing BMV 1a for 2-4 hours. If BMV 1a is incorporated into vesicles, it will be recruited away from the microsome into assembled COPII vesicles, which will be separated from the microsome by ultracentrifugation.

2. Determine the role of COPI in BMV 1a trafficking to the perinuclear ER

BMV 1a's perinuclear ER association was promoted in cells with dysfunctional COPI components, *sec21-1* and *sec31-1* at a non-permisive temperature (Figure 6.5). I hypothesize that individual COPI components might antagonize the traffick of BMV 1a to the perinuclear ER. There are seven major components of COPI, consisting of Sec33 (α-COP), Sec27 (β′-COP), and Sec28 (ε-COP) for a cage-like subcomplex, and Sec21 (γ-COP), Ret2 (δ-COP), Ret3 (ζ-COP), Sec26 (β-COP) for an adaptor subcomplex (Brandizzi and Barlowe, 2013; Gomez-Navarro and Miller, 2016). All COPI components are encoded by single essential genes except Sec28. I propose to test the localization pattern of BMV 1a-mC in *ts* mutants of other COPI components, similar to what I did for *sec33-1* and *sec21-1 ts* mutants (Figure 6.5). Because *SEC28* is a non-essential gene, I propose to check BMV 1a localization and viral replication in *sec28Δ* deletion mutant.

3. Determine the possible role of microtubules in BMV 1a trafficking to the perinuclear ER

Microtubules are the largest type of filament, found throughout the cytoplasm, and play important roles in trafficking of COPII and COPI vesicles (Caviston and Holzbaur, 2006). In budding yeast, microtubules are composed of a single β-tubulin (Tub2) (Neff et al., 1983) and two α-tubulin isotypes (Tub1 and Tub3) (Schatz et al., 1986). Besides, there are seven microtubule-based motor proteins in yeast, including the minus-end-directed dynein and plus-end-directed kinesin. Dynein is a large two headed ATPase, composed of heavy chain Dyn1, light chain Dyn2 and intermediate chain Pac11; while kinesin has multicomponent complexes, including six kinesin-related proteins Cin8, Kar3, Kip1, Kip2, Kip3 and Smy1 (Hildebrandt and Hoyt, 2000). Previous study has shown that Sec23 interacted directly with dynactin complex via $p150^{Glued}$ to create a direct link between COPII and dynactin. This interaction could functionally couple cargo protein export from the ERES to microtubules for trafficking to the Golgi apparatus, suggesting that COPII vesicles are associated with motors and microtubules for their organization and movement to the Golgi apparatus (Watson et al., 2005). I hypothesize that microtubules might be involved in BMV 1a trafficking to the perinuclear ER, and propose to check BMV 1a localization as well as viral replication in the available microtubule-related *ts* and deletion mutants.

*Potential pitfalls and alternatives:*

While my data suggest that BMV 1a might be associated with ERES. However, if it is not, I propose to test whether BMV 1a colocalizes with Golgi marker proteins, such as Pmr1 (Antebi and Fink, 1992), because the Golgi apparatus is adjacent to ERES and has a similar dispersed localization pattern in yeast. If BMV 1a co-localizes with the Golgi markers, it may

suggest that BMV 1a is target to the Golgi for further modifications.

### 6.2.3 The biological significance of BMV replication sites at specific ER subdomains in *Nicotiana benthamiana*

*Rationale and preliminary data:*

In Chapter 3, I showed that BMV 1a-mC primarily localized to three-way junctions and ER sheets in addition to the perinuclear ER in *N. benthamiana*, and that BMV infection rearranged specific ER subdomains that mainly colocalized with BMV 1a-mC in *N. benthamiana*. Previous study has shown that BMV replicates in the cytoplasmic ER membrane in *N. benthamiana* (Bamunusinghe et al., 2011), but did not identify any specific ER subdomains for BMV replication. BMV depends on host ER membranes to assemble VRCs, while ER morphology is well maintained by membrane-shaping proteins such as reticulons (RTNs), Lunapark (Lnp), dynamin-like GTPase Sey1 in yeast and atlastin (ATL) in mammals (Hu et al., 2008; Hu et al., 2009; Powers et al., 2017; Wang et al., 2016). Therefore, I hypothesize that BMV remodels ER subdomains at three-way junctions and ER sheets during viral replication in *N. benthamiana*, and that membrane-shaping proteins play important roles in BMV replication through the regulation of these specific ER subdomains.

*Proposed experiments:*

1. Characterize the ER subdomains that colocalize with BMV replication sites in *N. benthamiana*

Although ER membrane is highly dynamic, BMV-induced VRCs in yeast are relatively stable (Schwartz et al., 2002). I propose to examine membrane mobility of BMV-rearranged ER subdomains in *N. benthamiana* by fluorescence recovery after photobleaching (FRAP) analysis. If BMV-rearranged ER subdomains are viral replication sites, I expect that the GFP-HDEL signal of BMV-rearranged ER subdomains will not or inefficiently be recovered after photobleaching. Viral replication intermediate, dsRNA, is well-recognized as the sites of VRCs. A specific monoclonal antibody, J2, has been commonly used to identify dsRNAs (Lukács, 1994; Weber et al., 2006). I propose to detect BMV dsRNA with J2 by immunofluorescence microscopy approach and check if the dsRNA signal colocalizes with the remodeled domain to provide further verification.

2. Determine the roles of Lunapark proteins in BMV replication in *N. benthamiana*

Membrane protein Lnp localizes to the three-way junctions of ER membranes in yeast and mammals. In the absence of *LNP1*, three-way junctions were no longer clearly observable and ER membranes were densely packed (Chen et al, 2012). In yeast, Lnp1 is required for BMV replication (data not shown). It is consistent with my finding that BMV 1a-mC localized to the three-way junctions (Figure 3.1, Chapter 3). I propose to examine whether plant homologs of Lnp1 co-localize with BMV 1a-mC and BMV-remodeled subdomains, and test BMV replication when gene expression of *NbLNP* is knocked down by VIGS approach.

*Potential pitfalls and alternatives:*

Although a single gene in yeast, there are two *LNP* genes (AT2G24330 and AT4G31080) in the *Arabidopsis* (Altschul et al., 1997) and three members in *N. benthamiana* (the draft genome v1.0.1, Sol Genomics Genome). It may need to knock down all three *NbLNP* genes to achieve the expected phenotype. Gene expression of individual or combination of *NbLNPs* will be knocked to test the effect on ER morphology and BMV replication.

### 6.2.4 Identification of cargo proteins of plant CNIHs

*Rationale and preliminary data:*

I have shown that NbCNIH2 and 5 as well as AtCNIH1, 4 and 5 can functionally replace Erv14 in yeast. I hypothesize that plant CNIHs function as cargo receptors and participate in several cellular processes through the trafficking of many cellular protein. Moreover, AtCNIH5 was found to interact with ~500 cellular proteins, including many nutrient transporters, glutamate receptors, plant immune response-related proteins (Jones et al., 2014). These interactors may depend on AtCNIH5 for exiting ER membrane. Previous study has shown that a sodium transporter of rice OsHKT1;3 localized to the Golgi apparatus in wt cells but retained at the ER membrane in *erv14*Δ cells (Rosas-Santiago et al., 2015). My preliminary data showed that AtSWEET1, a sugar transporter of *A. thaliana*, was localized to the plasma membrane in wt cells but retained at the ER membrane in *erv14Δ* cells (Figure 6.6). This result suggests that Erv14 facilitates AtSWEET1 trafficking to the plasma membrane in yeast, and that the yeast *erv14Δ* mutant can be used to determine the dependence of individual candidates of plant cargo proteins on Erv14 for their ER exit.

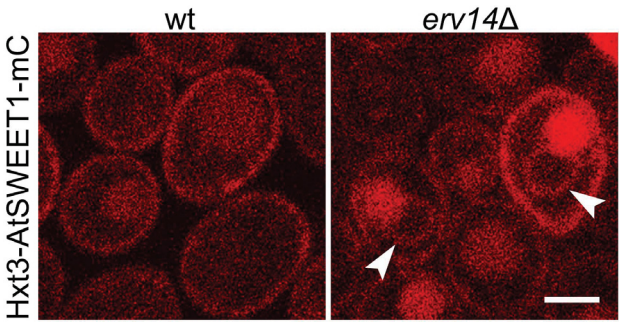


**Figure 6.6. Erv14 facilitates the trafficking of AtSWEET1 to the plasma membrane in yeast.** Confocal microscopic images of the distribution of mC-tagged AtSWEET1 in wt and *erv14Δ* cells. The expression of AtSWEET1 is driven by the promoter of *HXT3*. Hxt3 is a sugar transporter and Erv14-dependent cargo in yeast. AtSWEET1 localized to the plasma membrane in wt cells whereas retained at the ER membrane in *erv14Δ* cells. Arrowheads point to the perinuclear ER membrane in *erv14Δ* cells. Scale bar: 2 μm.

*Proposed experiments:*

1. Identify plant membrane proteins that interact with CNIHs

The split ubiquitin system (SUS) is a well-established system to examine protein-protein interactions (Obrdlik et al., 2004) and has been used to examine the interactions between Erv14 and its client cargos (Pagant et al., 2015), including the interaction between BMV 1a and Erv14 (Li et al., 2016). In a previous large-scale protein-protein assay, 3289 Arabidopsis membrane and signaling proteins were cloned into SUS bait and prey vectors. Among the five AtCNIHs, AtCNIH5 was analyzed and it interacted with ~500 proteins, with 96% are membrane proteins. Some of these interactors might be cargo proteins that depend on AtCNIH5 for trafficking to the final destinations. I propose to screen the library with AtCNIH1-4 to identify interacting partners. The Gateway donor vectors harboring ~3289 proteins that used in the Associomics project are available in Dr. Guillaume Pilot lab at

PPWS (Jones et al., 2014). I propose to identify the clones expressing membrane proteins. Furthermore, all the interactions and the sites where interactions occur can be further verified in plant by bimolecular fluorescence complementation (BiFC) approach (Miller et al., 2015).

2. Verify that AtCNIH interactors are possible cargo proteins in yeast

I have shown that AtSWEET1 localized at the plasma membrane and Erv14 facilitated the trafficking of AtSWEET1, indicating that plant cargo proteins can be studied in yeast. To verify that interactors of AtCNIHs are cargo proteins of AtCNIHs, I propose to examine the localization of each of AtCNIH-interactors in wt and *erv14*Δ cells. For those whose distribution is affected in *erv14*Δ cells, and each of plant CNIHs will be tested whether the defective distribution of the interactors can be complemented in *erv14Δ* cells. If the defective distribution can be complemented, it can be concluded that the interactor is a putative cargo protein of specific AtCNIHs.

*Potential pitfalls and alternatives:*

I recognize that this study will analyze plant cargos in yeast, leading to possible false positives or negatives and should treat results with caution. Given enough time, all of putative cargo proteins verified in the yeast system can be tested in *N. benthamiana* in untreated and *NbCNIH* knockdown plants in the presence and absence of AtCNIHs. It needs to be noted that there are ~500 putative cargo proteins of AtCNIH5, it is not realistic to analyze them directly in plants, supporting our plan in yeast for initial verification.

### 6.2.5 Determine the roles of CNIHs in ER morphology maintenance and pollen development

*Rationale and preliminary data:*

My preliminary data showed that NbCNIH5 and Erv14/Erv15 are involved in ER tubule maintenance. Erv14 is an integral ER membrane protein and self-interacts to form protein oligomers (Li et al., 2016). These are also basic features shared among ER membrane-shaping proteins, such as Rtn1 and Yop1 (Hu et al., 2008). Previous studies have shown that HsCNIH2 and HsCNIH3 function as accessary components of glutamate receptors involved in neuron cell signal transmission (Herring et al., 2013; Schwenk et al., 2009). Glutamate receptor–like genes in plants are mainly involved in calcium influx across the plasma membrane (Kwaaitaal et al., 2011; Li et al., 2013; Michard et al., 2011). Therefore, the activity of glutamate receptor would subsequently affect the cytoplasmic calcium concentration in plant, and potentially cause ER stress to affect ER morphology. I hypothesize that NbCNIH5 functions as a cargo receptor involved in the regulation of glutamate receptor activity in plant.

In addition, *atcnih1* and *atcnih4* mutants showed abnormal pollen development with reduced starch accumulation in pollen and aberrant pollen morphology. Previous studies have demonstrated that many protein families play crucial roles in pollen development. For instance, arabinogalactan proteins (AGPs) are important for pollen development, pollen germination and pollen tube growth, such as AtAGP6 and AtAGP11 (Coimbra et al., 2009; Coimbra et al., 2010; Levitin et al., 2008). SWEETs are sugar transporters and important for

pollen wall development and pollen viability by affecting glucose efflux from the tapetum for pollen nutrients, such as AtSWEET1, 5, 8 and 13 (Chandran, 2015; Engel et al., 2005; Guan et al., 2008; Song et al., 2009). Pectin lyase-like superfamily proteins are involved in pectin degradation and important for microspore separation during pollen development (Cao, 2012). Therefore, I hypothesize that AtCNIH1 and AtCNIH4 function as cargo receptors involved in pollen development by affecting the distribution and trafficking of cellular protein families that are required for pollen development.

*Proposed experiments:*

1. Determine the roles of NbCNIH5 in tubular ER maintenance in *N. benthamiana*

Aequorin is a calcium-sensitive luminescent protein that was isolated from the hydrozoan *Aequorea victoria* and used to report the changes of intracellular calcium levels in plant (Knight et al., 1996; Knight et al., 1991). I propose to check the intracellular calcium concentration in leaf tissues of *NbCNIH5* knockdown plant by *aequorin* approach (Hann and Rathjen, 2007; Knight et al., 1996), and also examine the subcellular localization of NbCNIH5 to determine how NbCNIH5 regulate glutamate receptor activity, such as direct regulation if NbCNIH5 localizes to the plasma membrane or indirect if localizes to the ER membrane.

2. Determine the roles of AtCNIH1 and AtCNIH4 in pollen development of *A. thaliana*

I propose to determine which anther and pollen developmental stages have been affected in *atcnih1* and *atcnih4* mutants by scanning EM approach (Gómez et al., 2015; Sanders et al.,

1999), and examine pollen viability in *atcnih1* and *atcnih4* mutants by Alexander's staining, fluorescein diacetate staining and DAPI staining approaches (Zhao et al., 2016). Since *in vitro* pollen germination has been affected in *atcnih1* and *atcnih4* mutants, I propose to check *in vivo* pollen germination by aniline blue staining approach (Ishiguro et al., 2001). I also propose to check if any plant cargo proteins of AtCNIH1 or AtCNIH4 are relevant to the protein families of AGPs, SWEETs, or pectin lyase-like protein. If so, we will validate their interactions by SUS in yeast and BiFC in plant.

*Potential pitfalls and alternatives:*

If NbCNIH5 does not function as a cargo receptor, it is possible that NbCNIH5 might function as a novel membrane-shaping protein directly involved in ER morphology maintenance. If so, I propose to perform *in vivo* tubule formation analysis by expressing NbCNIH5 in *erv14/15Δ* double deletion mutant and *rtn1/rtn2/yop1Δ* triple deletion mutant to test whether NbCNIH5 can rescue ER tubule formation in yeast. If so, we then will perform *in vitro* tubule formation analysis to check whether NbCNIH5 can generate membrane tubules when reconstitutes with lipids into proteoliposomes, similar to what has been done for Rtn and Yop1 (Hu et al., 2008).

### 6.2.6 Determine the roles of CNIHs in plant pathogen infection

*Rationale and preliminary data:*

Bacterial growth is well supported by the nutrients in plant apoplastic fluids (O'Leary et al., 2016). SWEETs play important roles in sugar efflux to the apoplast for supporting

bacterial pathogen growth (Chen et al., 2010). If AtCNIHs are involved in the trafficking and distribution of nutrient transporters such as SWEETs to the plasma membrane, absence of AtCNIHs would subsequently inhibit bacterial growth. Interestingly, *Pst* DC300 infection significantly increased gene expression level of *AtCNIH2* and *AtCNIH3*, suggesting that bacterial pathogen might regulate putative cargo receptors such as AtCNIH2 and AtCNIH3 to facilitate the distribution and function of their cargo proteins. We hypothesize that AtCNIH2, AtCNIH3 and AtCNIH5 function as cargo receptors involved in bacterial pathogen infection through the regulation of nutrient transporters.

As compared to bacterial pathogen infection in plants, oomycetes also take advantages of nutrients in plant apoplastic fluids during infection. A specialized feeding structure of oomycetes called haustorium can be observed in most obligate biotrophs during colonization, and this feeding structure plays an important role in nutrient uptake (Hardham, 2007). Haustoria are not only important for fungal pathogen to import sugars such as by the hexose transporter on haustorial plasma membrane (Voegele et al., 2001), but also important for oomycete pathogen to access essential nutrients from plant apoplastic fluids through the nutrient transporters on haustorial plasma membrane (Abrahamian et al., 2016). I hypothesize that oomycetes might adopt a similar strategy as bacterial pathogens, in terms of regulating plant nutrient transporters such as SWEETs, to affect nutrient contents in plant apoplastic fluids during oomycete infection.

*Proposed experiments:*

1. Determine the roles of CNIHs in plant bacterial pathogen infection

I propose to first check at which phase of *Pst* DC3000 life cycle, either the epiphytic phase on plant surface or a subsequent endophytic phase in the apoplast, that AtCNIH2, AtCNIH3 and AtCNIH5 are involved. Previous studies have shown that stomata play an important role in limiting bacterial invasion by interrupting the transition from epiphytic phase to endophytic phase (Melotto et al., 2008). On the contrary, *Pst* DC3000 uses its virulence factor such as coronatine to open stomata for entering plant epidermal cells to start the epiphytic phase (Melotto et al., 2006). Therefore, I propose to measure stomatal aperture in wt, *atcnih2*, *atcnih3* and *atcnih5* mutants under various conditions to determine: 1) whether the lack of AtCNIH2, 3, or 5 will affect stomatal opening in the absence of *Pst* DC3000 infection; 2) whether these mutants affect bacteria-mediated signaling pathway that regulates stomatal opening upon *Pst* DC3000 infection.

I also propose to analyze metabolite contents in the apoplastic fluids of wt, *atcnih2*, *atcnih3* and *atcnih5* mutants with and without bacterial infection. These can be done by collecting the apoplastic fluids from leaf tissues of wt, *atcnih2*, *atcnih3* and *atcnih5* mutants by vacuum infiltration and centrifugation approach (Madsen et al., 2016) and checking their metabolite levels such as organic acids, sugars and amino acids by gas chromatography mass spectrometry (Lisec et al., 2006). Therefore, we would determine the roles of AtCNIH2, AtCNIH3 and AtCNIH5 in plant bacterial pathogen infection. In addition, I propose to check *Pst* DC3000 growth in *N. benthamiana* plants with *NbCNIH2* and/or *NbCNIH5* knocked down by blunt syringe inoculation approach (Wei et al., 2007) and determine whether plant CNIHs play a conserved role in bacterial pathogen infection.

2. The potential roles of CNIHs in plant oomycete and viral pathogen infections

I propose to inoculate wt and *atcnih* mutants with the biotrophic oomycete *Hyaloperonospora arabidopsis* (*Hpa*), which is a natural pathogen of *A. thaliana* and causes downy mildew disease (McDowell, 2014). Based on the resistance/susceptibility of Arabidopsis *atcnih* mutants to Hpa to determine the roles of AtCNIHs in *Hpa* infection. Additionally, I propose to inoculate wt and *atcnih* mutants with the hemibiotrophic oomycete *Phytophthora infestans* (*Pi*), which is a non-host pathogen to *A. thaliana*, but causes serious potato and tomato diseases such as late blight disease (Huitema et al., 2003; Kamoun, 2001), to test whether knockout of *AtCNIHs* can increase *A. thaliana* susceptibility to *Pi*.

I additionally propose to explore the roles of NbCNIHs in plant (+)RNA virus infection. *N. benthamiana* is the most widely used model plant for studying plant virus-host interactions (Goodin et al., 2008). In addition to BMV, we will inoculate *NbCNIHs* knockdown plants with *cucumber mosaic virus* (CMV) (Pagán et al., 2010), *turnip mosaic virus* (TuMV) (Garcia-Ruiz et al., 2010) and *spring beauty latent virus* (SBLV) (Fujisaki et al., 2009), and test viral replication. SBLV is in the same genus with BMV and replicates in ER membranes. CMV and BMV are in the same family but CMV replicates in tonoplasts (or vacuole membranes). TuMV is in potyvirus but replicate in both ER and chloroplasts. The replication results of these 3 viruses should provide information on whether CNIHs are broadly involved in replication of other plant (+)RNA viruses.

*Potential pitfalls and alternatives:*

Due to the functional redundancy of AtCNIHs, it is possible that each of AtCNIHs might not play a dramatic role in oomycete infection. Alternatively, I propose to test oomycete infection in the high order *atcnih* mutants, such as double or triple knockout mutants that I am in the process to generate.

In addition, I found that BMV replication in VIGS-mediated knockdown plants showed a lot of variance due to plant growth stage, gene knockdown effect, and BMV infiltration time. I thus propose to infect *atcnih* knockout Arabidopsis mutants, which have stable and consistent gene knockout phenotype, with various plant (+)RNA viruses such as CMV, GFP-TuMV and SBLV by the sap of virus infected leaf tissues, and then test viral replication.

In summary, the cargo receptor Erv14 and several COPII components, Sec13, Sec24 and Sec31, are involved in targeting BMV 1a to the perinuclear ER membrane in yeast, suggesting a novel function of COPII vesicles in protein perinuclear ER targeting and revealing an important role of CNI protein family in BMV replication. CNI proteins are unexpectedly involved in maintaining ER tubules in yeast and plant, and also play a crucial role in pollen development and plant bacterial pathogen *Pst* DC3000 infection in Arabidopsis. Based on my data, it is possible to develop an alternative strategy to make plants resistant to viruses and/or bacterial pathogens by manipulating plant CNIHs.

## 6.3 References

**Abrahamian, M., Ah-Fong, A. M. V., Davis, C., Andreeva, K. and Judelson, H. S.** (2016). Gene expression and silencing studies in Phytophthora infestans reveal infection-specific nutrient transporters and a role for the nitrate reductase pathway in plant pathogenesis. *PLoS Pathog* **12**, e1006097.

**Altschul, S. F., Madden, T. L., Schäffer, A. A., Zhang, J., Zhang, Z., Miller, W. and Lipman, D. J.** (1997). Gapped BLAST and PSI-BLAST: a new generation of protein database search programs. *Nucleic Acids Res* **25**, 3389-3402.

**Annamalai, P. and Rao, A. L. N.** (2005). Replication-independent expression of genome components and capsid protein of brome mosaic virus in planta: A functional role for viral replicase in RNA packaging. *Virology* **338**, 96-111.

**Antebi, A. and Fink, G. R.** (1992). The yeast Ca(2+)-ATPase homologue, PMR1, is required for normal Golgi function and localizes in a novel Golgi-like distribution. *Mol Biol Cell* **3**, 633-654.

**Bamunusinghe, D., Seo, J.-K. and Rao, A. L. N.** (2011). Subcellular localization and rearrangement of endoplasmic reticulum by brome mosaic virus capsid protein. *J Virol* **85**, 2953-2963.

**Barlowe, C., Orci, L., Yeung, T., Hosobuchi, M., Hamamoto, S., Salama, N., Rexach, M. F., Ravazzola, M., Amherdt, M. and Schekman, R.** (1994). COPII: A membrane coat formed by Sec proteins that drive vesicle budding from the endoplasmic reticulum. *Cell* **77**, 895-907.

**Brandizzi, F. and Barlowe, C.** (2013). Organization of the ER-Golgi interface for membrane traffic control. *Nat Rev Mol Cell Biol* **14**, 382-392.

**Budnik, A. and Stephens, D. J.** (2009). ER exit sites – localization and control of COPII vesicle formation. *FEBS Lett* **583**, 3796-3803.

**Buede, R., Rinker-Schaffer, C., Pinto, W. J., Lester, R. L. and Dickson, R. C.** (1991). Cloning and characterization of LCB1, a Saccharomyces gene required for biosynthesis of the long-chain base component of sphingolipids. *J Bacteriol* **173**, 4325-4332.

**Cao, J.** (2012). The pectin lyases in Arabidopsis thaliana: evolution, selection and expression profiles. *PLoS ONE* **7**, e46944.

**Caviston, J. P. and Holzbaur, E. L. F.** (2006). Microtubule motors at the intersection of trafficking and transport. *Trends Cell Biol* **16**, 530-537.

**Chandran, D.** (2015). Co-option of developmentally regulated plant SWEET transporters for pathogen nutrition and abiotic stress tolerance. *IUBMB Life* **67**, 461-471.

**Chen, L.-Q., Hou, B.-H., Lalonde, S., Takanaga, H., Hartung, M. L., Qu, X.-Q., Guo, W.-J., Kim, J.-G., Underwood, W., Chaudhuri, B. et al.** (2010). Sugar transporters for intercellular exchange and nutrition of pathogens. *Nature* **468**, 527-532.

**Coimbra, S., Costa, M., Jones, B., Mendes, M. A. and Pereira, L. G.** (2009). Pollen grain development is compromised in Arabidopsis agp6 agp11 null mutants. *J Exp Bot* **60**, 3133-3142.

**Coimbra, S., Costa, M., Mendes, M. A., Pereira, A. M., Pinto, J. and Pereira, L. G.** (2010). Early germination of Arabidopsis pollen in a double null mutant for the arabinogalactan protein genes AGP6 and AGP11. *Sex Plant Reprod* **23**, 199-205.

**D'Arcangelo, J. G., Stahmer, K. R. and Miller, E. A.** (2013). Vesicle-mediated export from the ER: COPII coat function and regulation. *Biochim Biophys Acta* **1833**, 2464-2472.

**Diaz, A., Zhang, J., Ollwerther, A., Wang, X. and Ahlquist, P.** (2015). Host ESCRT proteins are required for bromovirus RNA replication compartment assembly and function. *PLoS Pathog* **11**, e1004742.

**Engel, M. L., Holmes-Davis, R. and McCormick, S.** (2005). Green sperm. Identification of male gamete promoters in Arabidopsis. *Plant Physiol* **138**, 2124-2133.

**Fujisaki, K., Iwahashi, F., Kaido, M., Okuno, T. and Mise, K.** (2009). Genetic analysis of a host determination mechanism of bromoviruses in Arabidopsis thaliana. *Virus Res* **140**, 103-111.

**Garcia-Ruiz, H., Takeda, A., Chapman, E. J., Sullivan, C. M., Fahlgren, N., Brempelis, K. J. and Carrington, J. C.** (2010). Arabidopsis RNA-dependent RNA polymerases and dicer-like proteins in antiviral defense and small interfering RNA biogenesis during Turnip Mosaic Virus infection. *Plant Cell* **22**, 481-496.

**Gómez, J. F., Talle, B. and Wilson, Z. A.** (2015). Anther and pollen development: A conserved developmental pathway. *J Integr Plant Biol* **57**, 876-891.

**Gomez-Navarro, N. and Miller, E. A.** (2016). COP-coated vesicles. *Curr Biol* **26**, R54-R57.

**Goodin, M. M., Zaitlin, D., Naidu, R. A. and Lommel, S. A.** (2008). Nicotiana benthamiana: Its history and future as a model for plant–pathogen interactions. *Mol Plant Microbe In* **21**, 1015-1026.

**Gopinath, K., Dragnea, B. and Kao, C.** (2005). Interaction between brome mosaic virus proteins and RNAs: effects on RNA replication, protein expression, and RNA stability. *J Virol* **79**, 14222-14234.

**Graef, M., Friedman, J. R., Graham, C., Babu, M. and Nunnari, J.** (2013). ER exit sites are physical and functional core autophagosome biogenesis components. *Mol Biol Cell* **24**, 2918-2931.

**Guan, Y.-F., Huang, X.-Y., Zhu, J., Gao, J.-F., Zhang, H.-X. and Yang, Z.-N.** (2008). RUPTURED POLLEN GRAIN1, a member of the MtN3/saliva gene family, is crucial for exine pattern formation and cell integrity of microspores in Arabidopsis. *Plant Physiol* **147**, 852-863.

**Hann, D. R. and Rathjen, J. P.** (2007). Early events in the pathogenicity of Pseudomonas syringae on Nicotiana benthamiana. *Plant J* **49**, 607-618.

**Hardham, A. R.** (2007). Cell biology of plant–oomycete interactions. *Cell Microbiol* **9**, 31-39.

**Herring, Bruce E., Shi, Y., Suh, Young H., Zheng, C.-Y., Blankenship, Sabine M., Roche, Katherine W. and Nicoll, Roger A.** (2013). Cornichon proteins determine the subunit composition of synaptic AMPA receptors. *Neuron* **77**, 1083-1096.

**Hildebrandt, E. R. and Hoyt, M. A.** (2000). Mitotic motors in Saccharomyces cerevisiae. *BBA-Mol Cell Res* **1496**, 99-116.

**Hu, J., Shibata, Y., Voss, C., Shemesh, T., Li, Z., Coughlin, M., Kozlov, M. M., Rapoport, T. A. and Prinz, W. A.** (2008). Membrane proteins of the Endoplasmic Reticulum induce high-curvature tubules. *Science* **319**, 1247-1250.

**Hu, J., Shibata, Y., Zhu, P.-P., Voss, C., Rismanchi, N., Prinz, W. A., Rapoport, T. A. and Blackstone, C.** (2009). A class of dynamin-like GTPases involved in the generation of the tubular ER network. *Cell* **138**, 549-561.

**Huh, W.-K., Falvo, J. V., Gerke, L. C., Carroll, A. S., Howson, R. W., Weissman, J. S. and O'Shea, E. K.** (2003). Global analysis of protein localization in budding yeast. *Nature* **425**, 686-691.

**Huitema, E., Vleeshouwers, V. G. A. A., Francis, D. M. and Kamoun, S.** (2003). Active defence responses associated with non-host resistance of Arabidopsis thaliana to the oomycete pathogen Phytophthora infestans. *Mol Plant Pathol* **4**, 487-500.

**Ishiguro, S., Kawai-Oda, A., Ueda, J., Nishida, I. and Okada, K.** (2001). The DEFECTIVE IN ANTHER DEHISCENCE1 gene encodes a novel phospholipase A1 catalyzing the initial step of jasmonic acid biosynthesis, which synchronizes pollen maturation, anther dehiscence, and flower opening in Arabidopsis. *Plant Cell* **13**, 2191-2209.

**Jones, A. M., Xuan, Y., Xu, M., Wang, R.-S., Ho, C.-H., Lalonde, S., You, C. H., Sardi, M. I., Parsa, S. A., Smith-Valle, E. et al.** (2014). Border control-a membrane-linked interactome of Arabidopsis. *Science* **344**, 711-716.

**Kamoun, S.** (2001). Nonhost resistance to Phytophthora: novel prospects for a classical problem. *Curr Opin Plant Biol* **4**, 295-300.

**Knight, H., Trewavas, A. J. and Knight, M. R.** (1996). Cold calcium signaling in Arabidopsis involves two cellular pools and a change in calcium signature after acclimation. *Plant Cell* **8**, 489-503.

**Knight, M. R., Campbell, A. K., Smith, S. M. and Trewavas, A. J.** (1991). Transgenic plant aequorin reports the effects of touch and cold-shock and elicitors on cytoplasmic calcium. *Nature* **352**, 524-526.

**Kwaaitaal, M., Huisman, R., Maintz, J., Reinstädler, A. and Panstruga, R.** (2011). Ionotropic glutamate receptor (iGluR)-like channels mediate MAMP-induced calcium influx in Arabidopsis thaliana. *Biochem J* **440**, 355-373.

**Levitin, B., Richter, D., Markovich, I. and Zik, M.** (2008). Arabinogalactan proteins 6 and 11 are required for stamen and pollen function in Arabidopsis. *Plant J* **56**, 351-363.

**Li, F., Wang, J., Ma, C., Zhao, Y., Wang, Y., Hasi, A. and Qi, Z.** (2013). Glutamate receptor-like channel3.3 is involved in mediating glutathione-triggered cytosolic calcium transients, transcriptional changes, and innate immunity responses in Arabidopsis. *Plant Physiol* **162**, 1497-1509.

**Li, J., Fuchs, S., Zhang, J., Wellford, S., Schuldiner, M. and Wang, X.** (2016). An unrecognized function for COPII components in recruiting the viral replication protein BMV 1a to the perinuclear ER. *J Cell Sci* **129**, 3597-3608.

**Lisec, J., Schauer, N., Kopka, J., Willmitzer, L. and Fernie, A. R.** (2006). Gas chromatography mass spectrometry-based metabolite profiling in plants. *Nat Protoc* **1**, 387-396.

**Lukács, N.** (1994). Detection of virus infection in plants and differentiation between coexisting viruses by monoclonal antibodies to double-stranded RNA. *J Virol Methods* **47**, 255-272.

**Madsen, S. R., Nour-Eldin, H. H. and Halkier, B. A.** (2016). Collection of apoplastic fluids from Arabidopsis thaliana leaves. In *Biotechnology of Plant Secondary Metabolism: Methods and Protocols*, (ed. A. G. Fett-Neto), pp. 35-42. New York, NY: Springer New York.

**McDowell, J. M.** (2014). Hyaloperonospora arabidopsidis: A model pathogen of Arabidopsis. In *Genomics of Plant-Associated Fungi and Oomycetes: Dicot Pathogens*, (eds R. A. Dean A. Lichens-Park and C. Kole), pp. 209-234. Berlin, Heidelberg: Springer Berlin Heidelberg.

**Melotto, M., Underwood, W. and He, S. Y.** (2008). Role of stomata in plant innate immunity and foliar bacterial diseases. *Annu Rev Phytopathol* **46**, 101-122.

**Melotto, M., Underwood, W., Koczan, J., Nomura, K. and He, S. Y.** (2006). Plant stomata function in innate immunity against bacterial invasion. *Cell* **126**, 969-980.

**Michard, E., Lima, P. T., Borges, F., Silva, A. C., Portes, M. T., Carvalho, J. E.,**

**Gilliham, M., Liu, L.-H., Obermeyer, G. and Feijó, J. A.** (2011). Glutamate receptor–like genes form Ca2+ channels in pollen tubes and are regulated by pistil D-serine. *Science* **332**, 434-437.

**Midgley, R., Moffat, K., Berryman, S., Hawes, P., Simpson, J., Fullen, D., Stephens, D. J., Burman, A. and Jackson, T.** (2013). A role for endoplasmic reticulum exit sites in foot-and-mouth disease virus infection. *J Gen Virol* **94**, 2636-2646.

**Miller, E. A., Beilharz, T. H., Malkus, P. N., Lee, M. C. S., Hamamoto, S., Orci, L. and Schekman, R.** (2003). Multiple cargo binding sites on the COPII subunit Sec24p ensure capture of diverse membrane proteins into transport vesicles. *Cell* **114**, 497-509.

**Miller, K. E., Kim, Y., Huh, W.-K. and Park, H.-O.** (2015). Bimolecular fluorescence complementation (BiFC) analysis: advances and recent applications for genome-wide interaction studies. *J Mol Biol* **427**, 2039-2055.

**Nagiec, M. M., Wells, G. B., Lester, R. L. and Dickson, R. C.** (1993). A suppressor gene that enables Saccharomyces cerevisiae to grow without making sphingolipids encodes a protein that resembles an Escherichia coli fatty acyltransferase. *J Biol Chem* **268**, 22156-22163.

**Neff, N. F., Thomas, J. H., Grisafi, P. and Botstein, D.** (1983). Isolation of the β-tubulin gene from yeast and demonstration of its essential function in vivo. *Cell* **33**, 211-219.

**O'Leary, B. M., Neale, H. C., Geilfus, C. M., Jackson, R. W., Arnold, D. L. and Preston, G. M.** (2016). Early changes in apoplast composition associated with defence and disease in interactions between Phaseolus vulgaris and the halo blight pathogen Pseudomonas syringae Pv. phaseolicola. *Plant Cell Environ* **39**, 2172-2184.

**Obrdlik, P., El-Bakkoury, M., Hamacher, T., Cappellaro, C., Vilarino, C., Fleischer, C., Ellerbrok, H., Kamuzinzi, R., Ledent, V., Blaudez, D. et al.** (2004). K+ channel interactions detected by a genetic system optimized for systematic studies of membrane protein interactions. *Proc Natl Acad Sci USA* **101**, 12242-12247.

**Okamoto, M., Kurokawa, K., Matsuura-Tokita, K., Saito, C., Hirata, R. and Nakano, A.** (2012). High-curvature domains of the ER are important for the organization of ER exit sites in Saccharomyces cerevisiae. *J Cell Sci* **125**, 3412-3420.

**Pagán, I., Fraile, A., Fernandez-Fueyo, E., Montes, N., Alonso-Blanco, C. and García-Arenal, F.** (2010). Arabidopsis thaliana as a model for the study of plant–virus co-evolution. *Philos T R Soc B* **365**, 1983-1995.

**Pagant, S., Wu, A., Edwards, S., Diehl, F. and Miller, Elizabeth A.** (2015). Sec24 is a coincidence detector that simultaneously binds two signals to drive ER export. *Curr Biol* **25**, 403-412.

**Powers, R. E., Wang, S., Liu, T. Y. and Rapoport, T. A.** (2017). Reconstitution of the

tubular endoplasmic reticulum network with purified components. *Nature* **543**, 257-260.

**Rosas-Santiago, P., Lagunas-Gómez, D., Barkla, B. J., Vera-Estrella, R., Lalonde, S., Jones, A., Frommer, W. B., Zimmermannova, O., Sychrová, H. and Pantoja, O.** (2015). Identification of rice cornichon as a possible cargo receptor for the Golgi-localized sodium transporter OsHKT1;3. *J Exp Bot* **66**, 2733-2748.

**Rossanese, O. W., Soderholm, J., Bevis, B. J., Sears, I. B., O'Connor, J., Williamson, E. K. and Glick, B. S.** (1999). Golgi structure correlates with transitional Endoplasmic Reticulum organization in Pichia pastoris and Saccharomyces cerevisiae. *J Cell Biol* **145**, 69-81.

**Sanders, P. M., Bui, A. Q., Weterings, K., McIntire, K. N., Hsu, Y.-C., Lee, P. Y., Truong, M. T., Beals, T. P. and Goldberg, R. B.** (1999). Anther developmental defects in Arabidopsis thaliana male-sterile mutants. *Sex Plant Reprod* **11**, 297-322.

**Schatz, P. J., Pillus, L., Grisafi, P., Solomon, F. and Botstein, D.** (1986). Two functional alpha-tubulin genes of the yeast Saccharomyces cerevisiae encode divergent proteins. *Mol Cell Biol* **6**, 3711-3721.

**Schwartz, M., Chen, J., Janda, M., Sullivan, M., den Boon, J. and Ahlquist, P.** (2002). A positive-strand RNA virus replication complex parallels form and function of retrovirus capsids. *Mol Cell* **9**, 505-514.

**Schwenk, J., Harmel, N., Zolles, G., Bildl, W., Kulik, A., Heimrich, B., Chisaka, O., Jonas, P., Schulte, U., Fakler, B. et al.** (2009). Functional proteomics identify cornichon proteins as auxiliary subunits of AMPA receptors. *Science* **323**, 1313-1319.

**Senthil-Kumar, M. and Mysore, K. S.** (2014). Tobacco rattle virus–based virus-induced gene silencing in Nicotiana benthamiana. *Nat Protoc* **9**, 1549-1562.

**Song, L.-F., Zou, J.-J., Zhang, W.-Z., Wu, W.-H. and Wang, Y.** (2009). Ion transporters involved in pollen germination and pollen tube tip-growth. *Plant Signal Behav* **4**, 1193-1195.

**Venditti, R., Wilson, C. and De Matteis, M. A.** (2014). Exiting the ER: what we know and what we don't. *Trends Cell Biol* **24**, 9-18.

**Voegele, R. T., Struck, C., Hahn, M. and Mendgen, K.** (2001). The role of haustoria in sugar supply during infection of broad bean by the rust fungus Uromyces fabae. *Proc Natl Acad Sci USA* **98**, 8133-8138.

**Wang, S., Tukachinsky, H., Romano, F. B. and Rapoport, T. A.** (2016). Cooperation of the ER-shaping proteins atlastin, lunapark, and reticulons to generate a tubular membrane network. *eLife* **5**, e18605.

**Watson, P., Forster, R., Palmer, K. J., Pepperkok, R. and Stephens, D. J.** (2005).

Coupling of ER exit to microtubules through direct interaction of COPII with dynactin. *Nat Cell Biol* **7**, 48-55.

**Weber, F., Wagner, V., Rasmussen, S. B., Hartmann, R. and Paludan, S. R.** (2006). Double-stranded RNA is produced by positive-strand RNA viruses and DNA viruses but not in detectable amounts by negative-strand RNA viruses. *J Virol* **80**, 5059-5064.

**Wei, C.-F., Kvitko, B. H., Shimizu, R., Crabill, E., Alfano, J. R., Lin, N.-C., Martin, G. B., Huang, H.-C. and Collmer, A.** (2007). A Pseudomonas syringae pv. tomato DC3000 mutant lacking the type III effector HopQ1-1 is able to cause disease in the model plant Nicotiana benthamiana. *Plant J* **51**, 32-46.

**Yofe, I., Weill, U., Meurer, M., Chuartzman, S., Zalckvar, E., Goldman, O., Ben-Dor, S., Schütze, C., Wiedemann, N., Knop, M. et al.** (2016). One library to make them all: Streamlining yeast library creation by a SWAp-Tag (SWAT) strategy. *Nat Methods* **13**, 371-378.

**Young, B. P., Craven, R. A., Reid, P. J., Willer, M. and Stirling, C. J.** (2001). Sec63p and Kar2p are required for the translocation of SRP-dependent precursors into the yeast endoplasmic reticulum in vivo. *Embo J* **20**, 262-271.

**Zhao, B., Shi, H., Wang, W., Liu, X., Gao, H., Wang, X., Zhang, Y., Yang, M., Li, R. and Guo, Y.** (2016). Secretory COPII protein SEC31B is required for pollen wall development. *Plant Physiol* **172**, 1625-1642.